DETERMINATION OF SALINITY AND ITS EXTENT USING DIGITAL REMOTELY SENSED DATA IN INDO-GANGETIC ALLUVIAL PLAINS NEAR KANPUR

A Thesis Submitted
in Partial Fulfilment of the Requirements
for the Degree of
MASTER OF TECHNOLOGY

by

PRAVEEN DWIVEDI

to the

DEPARTMENT OF CIVIL ENGINEERING
INDIAN INSTITUTE OF TECHNOLOGY KANPUR
May, 1995

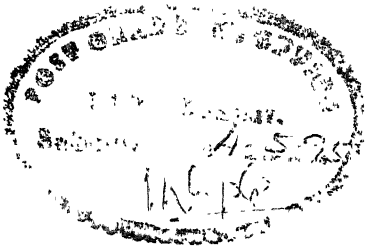

CERTIFICATE

Certified that the work presented in this thesis entitled *"Determination of Salinity and its Extent using Digital Remotely Sensed Data in Indo-Gangetic Alluvial Plains near Kanpur"* by **Mr. Praveen Dwivedi** has been carried out under my supervision and has not been submitted elsewhere for any degree.

May, 1995

Nitin Tripathi 04.5.95

(Nitin Kumar Tripathi)
Department of Civil Engineering
Indian Institute of Technology
Kanpur

ACKNOWLEDGEMENT

I have no words to express my sincere gratitude to Dr. K.V.G.K. Gokhale and Mr. Nitin Kr. Tripathi for their deep involvement and constant encouragement throughout the course of this work and for their being continuous source of inspiration for me.

I express my profound sense of reverence to Mr. Nitin Tripathi for his painstaking effort to get this work into final framework in the absence of Dr. Gokhale. The help of Dr. Gokhale at the initial stages of this study and especially in recognising a potential area is beyond appreciation.

I am grateful to Dr. B.C. Raymahashay, Dr. Onkar Dikshit and other faculty members, whose lectures and guidance developed some capabilities in me to take this work.

I am very much grateful to Mr. Ajay Diwakar and Mr. Ramkishen for their help during field visits.

I am grateful to Dr. C. Venkobachar and his students, Mr. M.G. Gracius and Ms. Ligy Philip for allowing and helping me during the experiment in environment laboratory. I am also thankful to Mr R. Awasthi and Mr. S.N. Mishra for their co-operation during experiments..

I am grateful to Mr. Umakant, Mr. Paul and Mr. Vishwanath for their help in Material Science laboratories during X-ray and SEM analysis. I am also grateful to Mr. Trivedi and Mr. Srivastava of Geotechnical laboratory. Thanks are due to J.C. Verma to make so good drawings.

Thanks are due to Mr. G.P.Mishra and Ramkishen for their support and help at various stages of this work. I thanks to all my colleages of Survey and Remote Sensing Lab for their sharing memorable moments in the course of this work.

I am thankful to Tyagi (Gillu), Gulla, Ashish (Geela), Sud, Chauhan Mama, Deepam, Rajkumar, Suresh, Rajeev, Meena, Sudhir, Anand, Ravi, Brijesh,Thakur, Raman, Ajay, Pandeyji, Chanduka, Panda, Naveen, Diwakar, Akshay, Mohit, Bhim, SP, Jha and many others for their constant assistance and encouragement. All these deserves a special mention here to record my heartiest gratitude for making my stay at IIT Kanpur memorable and pleasant.

The cooperation extended by Mr. and Mrs. Nitin Tripathi at critical stage of this work is beyond thanking words. I can never forget the pain they have taken at final stage of the work.

Hardly any word suffice me to pay my gratitudes to my family members for their infallible support and inspiration throughout my academic career. This work could not have been completed without the blessing of my parents and other family members.

Praveen

PRAVEEN DWIVEDI

To my
Parents, Brothers
and
Shashank

CONTENTS

LIST OF TABLES

LIST OF FIGURES

LIST OF PLATES

ABSTRACT

The present work is dedicated to investigate soil salinity in alluvial plains near Kanpur. The thrust is to evolve the tools of digital image processing for visual identification of salt affected regions and also to estimate concentration of salt quantitatively. A detailed investigation to understand the spectral reflectance characteristics of soil and the effect of salinity on it has been carried out. This is of immense importance in future applications on soil salinity studies. Based on MGTR observations and laboratory studies, suitable band or a set of bands can be selected.

Several field visits have been conducted to perform in-situ MGTR experiments and collect soil samples. These are analyzed gravimetrically, chemically, using X-ray and also Scanning Electron Microscopy. These tests and analysis has confirmed the presence of various salts/minerals and their concentrations. These results have been utilized extensively for modeling.

Empirical relationships between spectral reflectance and various parameters like moisture content, pH and alkalinity are developed. Salinity is quantified in terms of alkalinity and pH. Non linear empirical relationships are found particularly suitable. This approach is extended to satellite sensing and the relations for it are also obtained. The proposed models are verified using Chi-square test. Quantitative analysis is carried out and results of both, MGTR and satellite data are compared. The models prove to be useful for quantitative estimation of moisture content and salinity in the soil.

Two new indices namely, salinity index (SI) and normalized difference salinity index (NDSI) are proposed. These are suitable to enhance saline zones of the soil. Empirical relationship of these with soil properties are also developed on similar lines.

Various digital image processing techniques are applied on satellite data to enhance the image for better identification and delineation of saline zones. SI and

NDSI images are also prepared and found suitable for better understanding of saline zones. Optimum index factor (OIF) is calculated to determine the best band combinations for creating FCC's. Color composites are developed using original data as well as principal components. These prove to be very useful for visual interpretation of different features including saline zones of different concentrations. The area has been divided into three levels of salinity and an image to this effect is generated. The predictions made are verified by limited field checks.

CHAPTER 1

INTRODUCTION

1.1 General

The civil engineer has many diverse and important encounters with soil. All civil engineering structures such as building, bridge, highway, canal, dam are founded in or on the earth. It is, therefore, very necessary to know various properties (both, physical and chemical) of soils and the factors affecting them. The effect of ground water on the behavior of soil is an important aspects which governs design and usefulness of structure. A knowledge of shrinkage and swelling character of soil, which is mainly dependent on groundwater and its movement, is also very essential. Chemical properties of soil and ground water have a significant relationship with the performance of the foundation and hence overall structure. The presence of salts reduces the life and strength of structure considerably. In particular, the study of soil is important for civil engineer on many accounts like:

- Economic development,
- Environmental hazard due to groundwater,
- Soil erosion and salinity, land slides etc.,
- Regional planning like highway, urban and industrial development,
- Land cover and land use including agricultural use,
- Siting of any engineering structure.

An adequate knowledge of the soil properties like soil moisture and their variation with time and space is fundamental to the proper understanding of hydrological cycle. Quantitative knowledge of the soil moisture is needed in order to construct water balance model for water resource projects, vegetation studies, crop management and for surface and subsurface flow predictions.

Soil salinity is one of the major problem frequently observed on fields. It

hampers the land use for both, agricultural purposes as well as for many Civil Engineering use. Identification of salt affected area and its extent is very important for planning any structure or land use of that area. Salt affected soils cover an estimated seven million hectare of India's total geographical area of 328 million hectares (Rao et. al. 1991, Dwivedi, 1992). It also poses a threat to crop production as most of them are lying barren. Salt present in soil reacts with construction materials and reduces their strength and life. To reclaim such soils for agriculture or any other purpose, the information on the nature, extent and spatial distribution of these soils is essential.

Salinization is a continuous process and operates whenever conditions are favorable. Consequently, in due course of time, new areas get affected while some other affected areas are reclaimed using remedial and other advanced agronomic practices. As a result, there is shrinkage in the area under salt affected zones of a region. It is in this context that the spread or shrinkage of salinity over a given period of time and the assessment of the efficacy of reclamation of salt affected lands assume greater importance. Until recently, systematic monitoring of salt affected soils was lacking partly due to the time lag between the survey carried out and the information provided to the planner. With the development and advancement in remote sensing techniques, this aspect can be easily dealt with.

Ground based surveys and field measurements, though much accurate, can not provide global coverage economically and efficiently. It is also time consuming and information is generally available to the planner/management only after a large time-lag. Remote sensing, providing real time information with global coverage, can be a very effective tool to these applications. One of the fundamental advantage of advanced remote sensing data is spatial resolution. With the aid of remote sensing techniques, it is possible to get information over large areas in no time. Both, temporal and spatial variations can be easily followed. The data provided by the remote sensing satellites may be analyzed both for qualitative and quantitative estimation of various soil parameters.

The use of remote sensing for surveying and mapping of salt affected soils begins with black and white aerial photography. The surface can reveal presence of salts in two different ways: one, directly on bare soils with efflorescence and salt crusts or indirectly by affecting type of vegetation or moisture condition. Well developed saline efflorescence and crusts are always associated with high reflectance in visible wavelength compared to non saline soil. Moreover, crusted saline surfaces are smoother than non saline surfaces. The spectral reflectance of a typical soilscape, though specific, may vary according to the surface conditions modified by factors like ploughing, erosion, and salinity. Extent of salinity may vary with seasons and it's response also varies accordingly. Hence in present study, satellite data is obtained for two periods namely, November 1992 and April 1993. Several computer programs are written to analyze and manipulate digital data. Help of standard packages like, IDRISI and ILWIS, is also taken at various stages of this study. Soil moisture and soil salinity are two major and to an extent, related concepts. Higher the moisture in the area higher is the probability of salinization in long terms. Chemical and mineralogical composition is determined using appropriate techniques. Modeling of variation in the spectral reflectance of the soil with moisture and salinity is attempted.

1.2 Aim of the Present Work

The broad objective of present study is to utilize remote sensing for delineating saline zones and to model the spectral behavior of soil salinity taking into account both, ground field data and IRS-1B data. In this study, the effect of soil moisture and salinity on the nature of soil reflectance is investigated. Digital image processing is used to enhance the raw satellite image for better delineation of soil salinity and establish the potentials of remotely sensed data to soil salinity application. In particular, the aim of the present work is attained by:

- investigating the spectral behavior of normal soil, saline soil and vegetation cover,
- studying and analyzing the effect of moisture and salinity in soil and also developing a model to predict them using Multiband Ground truth Radiometer and IRS - 1B data.
- estimating the change in salt affected area coverage between two seasons using satellite digital data.

1.3 Organization of the present work

The present work is divided into seven chapters. Chapter 1 deals with the brief introduction of the problem and various aspects associated with it. It also includes aim of the present work and the way it is organized in subsequent chapters. Chapter 2 includes literature review. It gives a brief introduction to remote sensing principles, techniques, and discusses about the work done in the past related to salinity and moisture in the soil. The scope of the study is presented in Chapter 3. In chapter 4, Data acquisition and laboratory analysis techniques including details of MGTR and field work are discussed. Chapter 5 is concerned with details of digital satellite images and processing techniques . Chapter 6 is related to quantitative analysis of soil moisture and salinity parameters with MGTR and satellite data. Finally, Chapter 7 concludes the present work and briefs the future recommendations.

CHAPTER 2

LITERATURE REVIEW

2.1 BASIC PRINCIPLES OF REMOTE SENSING

Remote sensing is defined as the science and art of obtaining information about an object, area, or phenomenon through the analysis of data acquired by a device that is not in contact with the object, area or phenomenon under investigations (Lillesand, and kiefer, 1994). Briefly, it is collection of information without being in physical contact with the object. The simplest example of remote sensing is the sighting of objects by human eye. The prime objective of remote sensing is to obtain environmental and natural resources data related to our earth for application in civil engineering, geology, geography forestry, agriculture, and so many other areas.

The analysis and interpretation of a remotely sensed data requires an understanding of the interaction of electromagnetic radiation with the object and its parameters. A remote sensing system using electromagnetic radiation has four components (Curran, 1985) which are as follows:

(i) Source:

The source of electromagnetic radiation may be natural like the Sun's reflected light or the Earth's emitted heat, or man made, like microwave radar.

(ii) Earth's surface interaction:

The amount and characteristics of radiation emitted or reflected from the earth's surface is dependent upon the characteristics of the objects on the earth's surface.

(iii) Atmospheric Interaction:

Electromagnetic energy passing through the atmosphere is distorted and scattered.

(iv) Sensor:

The electromagnetic radiation that has interacted with the surface of the Earth and the atmosphere is recorded by a sensor, for example a radiometer camera.

2.1.1 Active and Passive Systems

Remote sensing system can be of two kinds: active and passive. In active systems, sensor has its own source of EM energy, sends signals to the concerned objects and measures the reflected energy. A passive remote sensing system records the energy naturally radiated or refracted from an object (Kennie and Matthews,1985).

2.1.2 Electromagnetic Spectrum

The link between the components of remote sensing system is electromagnetic energy. The source of most commonly used energy for remote sensing is sun. Electromagnetic spectrum extends from cosmic rays at extremely short wavelengths to long frequency radio waves at long wavelengths end.(Fig 2.1). Although names are generally assigned to regions of electromagnetic spectrum for convenience, there is no clear cut dividing line between one nominal spectral region and other. These radiation travel in harmonic, sinusoidal fashion with the velocity of light. Several regions of the

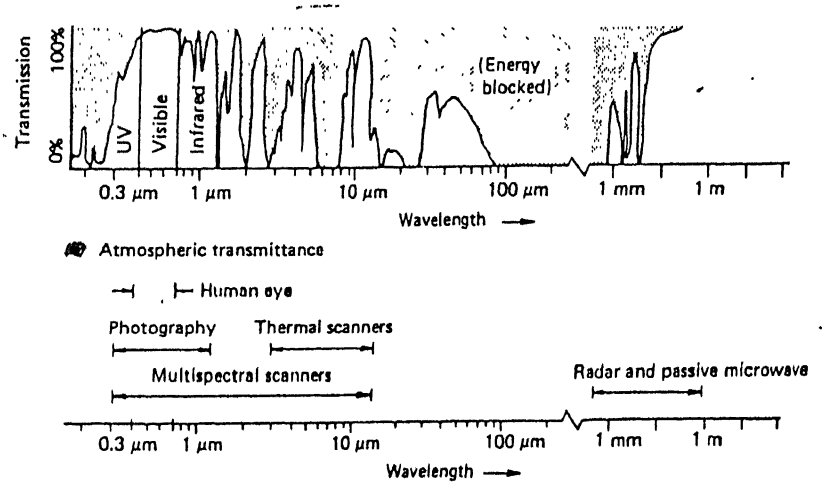

Figure 2.1: Spectral Characteristics of (a) Energy Source (b) Atmospheric Windows (c) Electromagnetic Spectrum (Lillesand and Kiefer, 1994)

electromagnetic spectrum are of particular interest for remote sensing, the most important ones being visible (400-700 nm),near infrared (700-1000 nm).

Electromagnetic radiation are composed of photons, whose energy is given by equation (2.1)

$$E = h c / \lambda \qquad (2.1)$$

where

E is the energy of photon in joules,

h is Planck's constant in Joules-sec,

c is the velocity of light in m/sec and,

λ is the wavelength of electromagnetic radiation in meter.

It is clear that longer the wavelength, the lower its energy content. This has important implication in remote sensing from the stand point that naturally emitted long wavelength radiation, such as microwave emission, from terrain features, is more difficult to be sensed than radiation of shorter wavelength, such as thermal infrared (IR). The low energy content of long wavelength means that system operating at long wavelengths must view larger areas of the earth in order to obtain a detectable energy signal.

2.1.3 Spectral Signature

Different objects or materials give different response after interacting with the electromagnetic energy, depending primarily upon its surface properties, and its atomic and molecular structure. Wavelength dependent component of this is termed as spectral response. Spectral response measured by remote sensors over various features often permit an assessment of the type and condition of the objects. These responses are generally known as "spectral signatures". Spectral signature implies a pattern which is unique and absolute, whereas, spectral response implies a pattern which is distinctive but not unique (Lillesand and Keifer, 1994).

2.1.4 Reflectance and Radiance

Reflectance and radiance are two important but often misused terms in remote sensing, and generally, one is used in place of other. The radiance (L) refer to radiation within a given angle of observation. Its unit is watt per square meter per steradian and if it is observed within a particular wavelength range, it is termed as spectral radiance. Reflectance (ρ), a unitless quantity, is the ratio of reflected (ϕ_R) to incident (ϕ_I) radiant flux, Where radiant flux (ϕ_R) is the total energy radiated in all directions for a unit of time. If it is observed within a particular wavelength range, it is termed as spectral reflectance $\rho(\lambda)$. Spectral reflectance $\rho(\lambda)$ of an feature is defined as the ratio of the reflectance energy $E_R(\lambda)$ from the feature to the incident energy $E_I(\lambda)$ on the feature at a particular wavelength (λ) (Lillesand,T.M., and Keifer,R.W.,1994). Spectral signatures of earth features may be quantified in terms of spectral reflectance. It is given as

$$\rho(\lambda) = E_R(\lambda) / E_I(\lambda) \qquad (2.2)$$

where

$\rho(\lambda)$ = Spectral reflectance

$E_R(\lambda)$ = Reflected energy

$E_I(\lambda)$ = Incident energy

2.2 INTERACTION OF ELECTROMAGNETIC RADIATIONS

Electromagnetic radiations interacts with the Atmosphere and Earth surface features and produces a particular response which is characteristics of it. These are discussed here briefly.

2.2.1 Interaction with Atmosphere

Irrespective of its source, all radiations detected by remote sensors passes through some distance, or a path length, of atmosphere. The energy recorded by a sensor is always modified to some extent by the atmosphere between the sensor and the ground. Atmosphere has varied effects on these radiations through the mechanism of atmospheric scattering and absorption. It affects radiance in two contradictory ways: One, it attenuates energy illuminating a ground object and other, acting as a reflector and thus adding a scattered signal component.

Atmospheric Windows

The transmittance of atmosphere for radiations of different wavelengths varies significantly as shown in previous figure (2.1). For some regions of electromagnetic spectrum, the atmosphere is highly transmittive and very small absorption takes place. The radiations in this range are nearly free from the effects of absorption. These regions of high transmittance are generally referred as "atmospheric windows" (Kennie and Matthews, 1985). These windows are utilized maximum in remote sensing.

2.2.2 Interaction with Earth Surface Features

The interaction of incident electromagnetic radiation with any object on the surface of the earth can produce number of changes in it like, change of magnitude, direction, wavelength, polarization and phase (Janza et. al., 1975). The remote sensor detect and record these changes. The resulting data is analyzed and interpreted to identify the characteristics of the object that produced these changes in the incident radiation.

2.2.2.1 Energy Equation

When electromagnetic energy is incident on any given earth surface feature, three fundamental energy interactions namely, reflection, absorption, and transmission, are possible. The extent to which each of these is present, is characteristics of the feature concerned. The interrelationship between these components can be given as, using principle of conservation of energy,

$$E(\lambda) = E_A(\lambda) + E_R(\lambda) + E_T(\lambda) \quad (2.3)$$

where,

$E(\lambda)$ = Incident energy

$E_A(\lambda)$ = Absorbed energy

$E_R(\lambda)$ = Reflected energy

$E_T(\lambda)$ = Transmitted energy

All energy components being a function of wavelength (λ).

2.2.2.2 Specular and Diffuse Reflection

Incident energy on an object is reflected primarily in two manners: specular and diffuse, depending on the nature of surface. Specular reflection is that kind of reflection in which energy leaves the reflecting surface without being scattered, with the angle of incidence being equal to the angle of reflectance. In diffuse reflection, the incident energy is scattered in all directions. Surfaces, which reflects specularly, are generally smooth relative to the wavelength of the incident energy while rough surfaces reflects diffusively (Mather,1987).

Most of the remote sensing system operates in the wavelength region in which reflected energy predominates. In remote sensing system, we are most often

interested in measuring the diffused reflectance properties of terrain features. Diffused reflectance contains the information on the nature of the reflecting surface, whereas, specular reflection does not (Lillesand, and Keifer, 1994).

2.2.2.3 Spectral Reflectance Curve

Many Earth surface features of interest can be identified, mapped and studied on the basis of their spectral characteristics. To utilize remote sensing data effectively, one must know and understand the spectral characteristics of the particular feature and the factors influencing them. A graph of spectral reflectance of an object as a function of wavelength is termed a spectral reflectance curve ((Lillesand, and Keifer, 1994). The configuration of spectral reflectance curve gives us insight into the spectral characteristics of an object and has a strong influence on the choice of wavelength region(s). This is because, the two features may be showing similar response in a particular spectral range but in some other spectral range, their response may be significantly different.

2.2.2.4 Spectral Reflectance of Vegetation, Soil, and Water

The majority of the flux incident on a soil surface is either reflected or absorbed and little is transmitted. Fig. 2.2 shows typical reflectance curves for four basic earth surface features namely, Healthy green vegetation, dead grass, dry bare soil and clear lake water. The lines in this figure represents average reflectance curves compiled by measuring upon a large samples of features. Although the reflectance of individual features may vary considerably above and below the average, these curves demonstrates some fundamental points concerning spectral reflectance of these features.

Spectral signature of vegetation shows marked difference from visible to

near infrared portion of the electromagnetic spectrum. Healthy green vegetation generally reflects 40 to 50 percent of the incident near infrared energy (0.7-1.1 μm), with the chlorophyll in the plants absorbing approximately 80 to 90 percent of the incident energy in the visible (0.4-0.7 μm) part of the spectrum (Jensen,1986). At about 0.7 μm, reflectance increases dramatically. Plant reflectance in the range 0.7 to 1.3 μm results primarily from the internal structure of the plant leaves.(Mather, 1987)

The most distinctive characteristics of the spectral reflectance pattern of water is the energy absorption at near infrared wavelengths. Unlike vegetation or soil, the majority of the radiant flux incident upon water is not reflected but is either absorbed or transmitted. In visible wavelength region of electromagnetic radiation, little light is absorbed, a small amount, usually under 5 percent is reflected and the majority is transmitted. Water absorbs near infrared and middle infrared wavelength strongly as it is clear from figure 2.2 (Curran,P.J.,1988). Identifying and delineating water bodies with remote sensing data is done most easily and accurately in near infrared wavelengths because

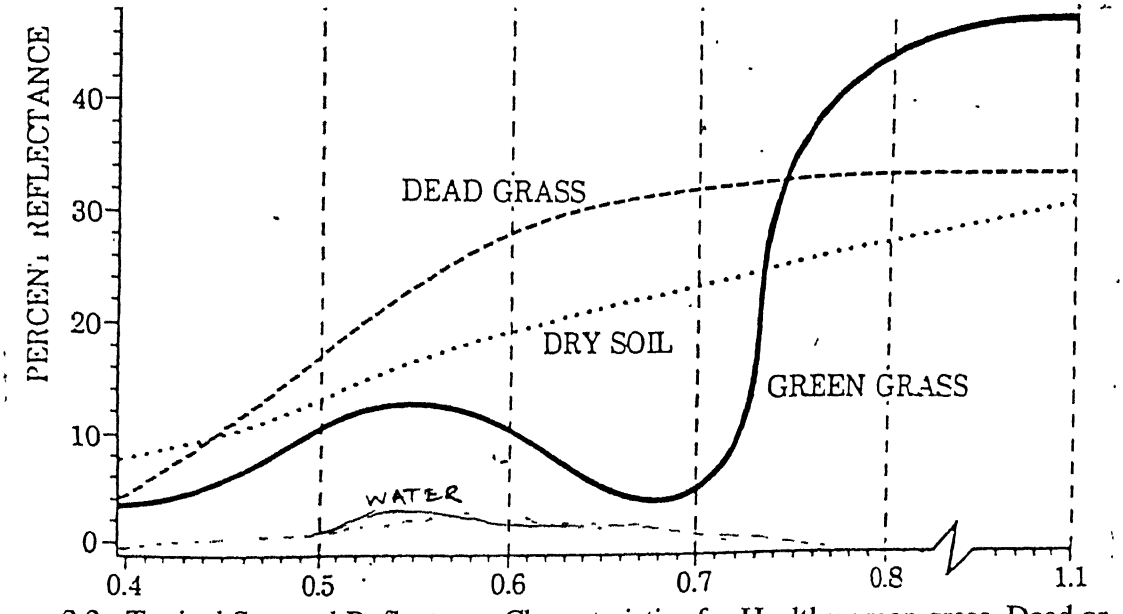

Figure 2.2: Typical Spectral Reflectance Characteristics for Healthy green grass, Dead or senescing grass, Bare dry soil, and Water surface for the wavelength interval from 0.4 to 1.1 μm. (Source: Jensen, 1986)

themselves primarily in visible wavelengths (Lillesand and Kiefer,1994).

Soil and dead grass show a continuous positive relationship in above discussed wavelength regions. Spectral response of soil is generally influenced by the factors like moisture content, soil texture (proportion of sand, silt and clay), surface roughness, presence of iron oxide, organic matter content and salt. The effect of these factors is complex, variable, and interrelated (Lillesand and Keifer, 1994). In visible wavelengths, the presence of soil moisture considerably reduces the surface reflectance of soil. Reflectance in near and middle infrared wavelengths is also negatively related to soil moisture (Jensen,1986).

Soil moisture content is strongly related to the soil texture; coarse sandy soils are usually well drained, resulting in lower moisture content and relatively high reflectance, poorly drained fine textured soils will generally have lower reflectance. In the absence of water, however, the soil itself will exhibit the reverse tendency; coarse textured soil will appear darker than fine textured soils. Thus the reflectance properties of a soilscape is consistent only within particular ranges of conditions (Lillesand and Keifer, 1994).

Dry soil generally has higher reflectance than green vegetation and lower reflectance than dead vegetation in the visible region. In near infrared, reverse is true. Dead or senescent vegetation reflects a greater amount of energy than healthy green vegetation throughout the visible spectrum (0.4-0.7 μm), Conversely, it reflects less than green vegetation in the reflective infrared region (0.7-1.1 μm) (Jensen,1986, Lillesand and Keifer, 1994, Curran,1985).

2.3 REMOTE SENSING TECHNIQUES

In order to detect the electromagnetic energy which exists in a wide range of wavelength and frequency, different remote sensing techniques are used. Remotely

collected data can be in many forms. It generally utilizes various kind of sensors, which acquire reflectance data of earth surface features and other objects, emitting and reflecting electromagnetic energy. These data are analyzed using computer or visual means. The major source of data is provided by aerial photograph, Thermal Infrared scanners, microwave imagers, satellites and ground truth radiometers.

2.3.1 Aerial Photography

Aerial photography was the first method of remote sensing, and even today, in the age of satellite and electronic scanner, it still remain the most widely used approach in having remotely sensed information. It is one of the most common and versatile form of remote sensing . Photograph are generally taken by a camera mounted in an aircraft. The basic advantage aerial photography affords over on-the-ground observation include availability, economy, synoptic view point, time frequency ability, spectral and spatial resolution, permanent recording, broadened spectral sensitivity and three dimensional perspective.

Limitations

1. Ground coverage of an aerial photograph is quite large so, it is not easy to study the minute details.
2. Cost of data collection and information retrieval, in aerial photogrammetry, is very high.
3. Air photographs are often difficult to obtain, handle, store, calibrate and interpret.
4. The delineation of soil units in air photograph requires extensive ground truth information.

2.3.2 Thermal Infrared Scanners

The Thermal infrared scanners are developed for imaging outside the visible region of the photographic film. Due to atmospheric effects, These systems are restricted to operation in 3 to 5 μm or 8 to 14 μm range of wavelength. The spatial resolution of thermal imagery is determined by the instantaneous field of view (IFOV), the platform height and the scan angle (θ) of the scanner.

Limitations

1. Thermal imagery exhibits scale distortion.
2. Variation in altitude (tilt and rotation) of the sensor platform causes gaps in the scan coverage.
3. Thermal resolution is highly dependent on the sensitivity of the detector element.
4. Estimation of reference temperature is cumbersome.

2.3.3 Microwave Imagers

Microwave imagers make use of antenna to collect radiation in the microwave regions (100 cm to 0.1 cm wavelengths) or (0.3 to 300 Ghz in frequency) from the ground features. There are two types of imagers, Passive and Active. Passive microwave sensing collects thermal emissions from the Earths' surface in the microwave spectrum. The strength of the passive radiation largely depends on the temperature and dielectric properties of the material rather than on the surface roughness. Active microwave remote sensing involves the sending out of a pulse microwave energy to target and measuring the return or reflected signal. This method is most commonly known

as Radar (Radio detection and ranging).

Limitations

1. The spatial resolution of imagery is dependent on the antenna size (beamwidth). High spatial resolution requires a fast scan rate which is detrimental to temporal resolution.
2. It shows panchromatic distortion.
3. It shows topographic effects like cover reflection, long shadows, terrain layover and foreshortening.

2.3.4 Satellite Remote Sensing

The Earth satellites are man made objects in space revolving around the Earth in their specific orbit. It provides an ideal platform, in space, for remote sensors. According to their orbital characteristics earth satellite can be classified into three types, sun-synchronous, Geo.-synchronous and general orbit.

2.3.4.1 Sun-synchronous Satellites

These are designed in such a way that the ascending node of each orbit of the satellite will begin at the same local time. In the angular relationship between sun satellite orbital plane is kept constant. Thus the angle of sun's illumination remains constant for a given latitude over a short period. The orbital inclination of the satellite is kept near 90°, or near polar, to cover as large an area of the earth as possible. Such satellites are about 1000 km above the earth's surface. IRS series of satellites generally revolves around the earth at an altitude 900 km or so. Sensor receive the signal from the ground features which are transmitted to earth station for recording in digital form on

computer tapes. The output is then converted into the image form using computer assisted techniques. The imaging system on board, on these satellites, generally consists of multispectral scanner (MSS), return beam vidicon (RBV) cameras, thematic mapper (TM) or pushbroom scanners. Spectral characteristics of different satellites is given in Table 2.1. The ground resolution of different satellites is given in Table 2.2.

2.3.4.2 Geo-synchronous Satellites

Geo-synchronous satellites are those that remain directly above a specific point on the Earths' surface, i.e., their orbiting period is equal to the Earth's rotation. This is achieved by placing these satellites at a height of about 35,800 Km (about 5-6 times the earth's radius). Communication and Meteorological satellite come under this category.

2.3.4.3 General Satellites

General satellites refers to those which have neither a sun-synchronous nor a Geo-synchronous orbit. SEASAT of NASA is of this kind and had a nearly circular orbit with an inclination angle of 100° and an altitude of 800 Km. This was designed to observe the Earths' oceans with microwave sensors.

Advantages

1. Photographic systems are linked to the spectral range 0.6 to 0.9 μm in relatively wide wavelength bands. MSS have range of sensing (visible to thermal infrared) from 0.3 to approx. 14 μm in very narrow spectral bands.
2. MSS systems use the same optical system to collect data in all spectral bands simultaneously thus the problems of spatial and radiometric compatibility as observed

*T*able 2.1: Spectral Characteristics of Various Wavebands of Different Satellites*

Satellite	Wavelength (nm)	Band No.	Spectral Location	Principal applications
IRS	450 - 520	1	Blue	Sensitivity to sedimentation, deciduous/ coniferous forest cover discrimination
IRS	520 - 590	2	Green	Green reflectance of healthy vegetation
IRS	620 - 680	3	Red	Sensitivity to chlorophyll absorption by vegetation, differentiation of soil and geographical boundaries
IRS	770 - 860	4	Near Infrared	Sensitivity to green biomass and moisture in vegetation
Landsat TM	450 - 520	1	Blue	Good water penetration, Strong vegetation absorbance, Forest type mapping, Cultural feature identification
Landsat TM	520 - 600	2	Green	Strong vegetation reflectance, vigor assessment,
Landsat TM	630 - 690	3	Red	Chlorophyll absorption region, Plant species differentiation, Very strong vegetation absorbance
Landsat TM	760 - 900	4	Near Infrared	Very strong vegetation reflectance, Delineating water bodies, High land / water contrasts, Soil moisture sensitive
SPOT	500 - 590	1	Green	Vegetation discrimination
SPOT	610 - 680	2	Red	Differentiation in soil geological boundaries, Plant species identification
SPOT	790 - 890	3	Near Infrared	Soil moisture discrimination, Sensitivity to green biomass and moisture in vegetation

*Table 2.2: Resolution Of different Satellites**

Serial No.	Satellite	Spatial Resolution
1	Landsat MSS	79 m X 79 m
2	Landsat TM	30 m X 30 m
3	IRS LISS 1	72.5 m X 72.5 m
4	IRS LISS 2	36.25 m X 36.25 m
5	SPOT (Multispectral)	20.0 m X 20.0 m
6	SPOT (Panchromatic)	10.0 m X 10.0 m

* (Sources: IRS Data Users Handbook, Lillesand & Kiefer,1994, Mather 1987)

in multiband photography is overcome.

3. MSS data are generated electronically and are easy to calibrate
4. Problem of on-board supply of film for photographic system is easily overcome ~~representation of original scene~~.because MSS data may be electronically transmitted to ground receiving station. This is particularly important for real time receiving of a ground scene.
5. In satellite imagery, it is possible to restore distorted image data as a more faithful representation of original scene .
6. There are few operations like weather forecasting, mineral exploration etc. which are possible by satellite remote sensing systems only.

Limitations

1. The ground resolution of any satellite is much poorer hence it is very difficult to get information for minor and small features.
2. The huge amount of data has to be handled at a time because of large aerial coverage in a scene. This leads to unnecessary data handling, storage and retrieval operation.
3. Analysis of data requires good knowledge on computer.

2.3.5 Multiband Ground Truth Radiometer (MGTR)

The ground truth information is useful in understanding and identifying various features present on Earths' surface, using remote sensing data. The reference information used in the analysis and interpretation of remote sensing data are often referred to by the term ground truth. There are various techniques available to collect the ground truth data. One way of obtaining it is the ground based measurements of the reflectance of the surface materials, and to determine their spectral response characteristics using spectroradiometers. These spectroradiometers permit non-destructive *in-situ* measurements of reflectance data from a desired target, and have been widely used.

MGTR is one of this kind used in present study. It measures the satellite simulated in situ spectral reflectance data of various objects in a series of discrete spectral band rather than over a continuous spectral range.

Advantages

1. It can be used to study minute details with higher accuracy in interpreting which is not possible by satellite remote sensing and high altitude aerial photography.
2. Handling of MGTR data is not a problem as it can be analyzed even on a personal computer.
3. Data collected on this scale can be easily utilized to model the ground features and their spectral response in varying conditions.
4. Remote sensing by MGTR is cheapest as compared to satellite or aerial remote sensing.
5. MGTR measurement of spectral reflectance is most authentic as its resolution is 0.25 x 0.25 m.
6. MGTR data is also free from atmospheric effects which are prevalent in other methods of remote sensing.

Limitations

1. MGTR can not be operated in inaccessible conditions.
2. It can be operated only when sun angle is not greater than 45° and weather is stable.

2.4 APPLICATIONS OF REMOTE SENSING

Study of various natural phenomena and their spatial variation is a difficult task performed by ground surveys and field experiments. Remote sensing offers a practical means for frequent and accurate monitoring of the Earths' natural resources and determining the impact of man's activity on the air, water and land. Data obtained from remote sensors have provided information necessary for making sound decision and policy regarding resource development and land use, specially, in places where field check can not be made. It is always advisable to collect ground truth information, wherever possible, to assist and correlate remote sensing results. Major areas, where remote sensing can be advantageously applied, are as follows:

1. Atmospheric applications
2. Lithosphere applications
3. Biosphere applications
4. Hydrosphere applications

2.4.1 Atmospheric Applications

The atmosphere or the gaseous realm, which surrounds our earth, exercise a great impact on the activities of mankind. Development in meteorological satellites provides ideal platform for remote sensing of meteorological phenomenon in both the

lower and upper atmosphere of the earth. These platforms make regular monitoring of a large part of Earth's atmospheric environment possible with suitably designed instruments. The availability of Geostationary satellite data permit determination of the radiation budget of the earth atmosphere system with greater accuracy. It has been successfully applied in cloud classification, rainfall estimation, wind field analysis and weather forecast.

2.4.2 Lithosphere Applications

Lithosphere, the solid realm called Earth, is the source of chemical elements and compounds vital to life. The application of remote sensing has focused on crust with a view to extract geologic, geomorphologic and hydrologic information which is vital for mineral exploration. It is particularly useful in studying the dynamic aspect of the terrain features, particularly the genetic origin of landforms in geomorphological applications.

2.4.3 Biosphere Applications

The biologically inhabited part of the lithosphere, atmosphere, and hydrosphere is generally known as Biosphere. Remote sensing has been utilized in recent years to obtain maximum information on these aspects. Both temporal and spatial variation of these features can be monitored easily. The application of remote sensing to the study of biosphere has particular economic significance in view of our increasing concern about detailed information on natural resources.

The information on spatial distribution, structure and type of vegetation, crop, and soil is indispensable for the purpose of management in agriculture and forestry, for planning, for feasibility studies in land development projects and many engineering works. Color infrared photography can reveal crop conditions that are not visible to the

human eyes. Thermal infrared sensors are specifically applied to measure soil moisture. Aerial photographs are generally used to locate changes in the land surface pattern that may relate to different soil properties. photographic tone of a soil is largely determined by its water content and organic matter content. Multispectral remote sensing have focused on the estimation of the amount and distribution of vegetation. MSS data have been found to be particularly suitable for the delineation of soil boundaries caused by climatic and vegetative differences which otherwise not observable on conventional aerial photographs. Advanced techniques like leaf area index and normalized difference vegetation index estimation are found particularly useful in estimating vegetation and thus delineating soil boundaries in different applications.

The mapping of land use and land cover is closely related to the study of biosphere. Land is a raw material of a site defined in terms of natural characteristics namely climatic geology, soil topology, hydrology and biology. Land use is man's activities on and in relation to land. Land cover describes the vegetational and artificial constructions covering the land surface (Lo, C.P., 1986). The use of remotely sensed data is particularly appropriate for planners to make decisions concerning land resources management economically. It is the quickest and the best mean to obtain reliable land use and land cover data.

2.4.4 Hydrosphere Applications

The hydrosphere is a liquid water realm characterized by free flows in response to unequal stresses. Remote sensing can be efficiently applied to study physical, chemical, biological, and geological features of hydrosphere. Satellite borne sensors make a good coverage of oceans twice the same day and thus relieve the problem of collecting sea truth data using research vessels.

2.5 Soil Properties and Earlier Works on Soil Salinity

Soil do not behave in a definite manner all the times. Its behavior is governed by conditions in which it is. Its spectral response is dependent on the various ingradients and its physical state. Some of the important factors affecting its response are discussed below.

2.5.1 Soil Properties

Soil as referred by engineers is a complex material produced by the weathering of the solid rock. The soil properties are not unique and are dependent on many factors. Soil in the Indo-Gangetic plains is water formed and transported, called alluvial, and it is sandy silt in nature. Important soil properties of interest are unit weight, porosity, permeability, water content, grain size distribution and consistency of soils.

Unit weight and porosity are an indicator to the compactness of soil. Unit weight is defined, in crude terms, as weight of soil per unit volume, while porosity is the ratio of volume of voids to the total volume of soil sample.

Permeability defines the capability of soil to allow passage of a fluid through it. It is highly dependent on the presence of continuous voids in the soils. The water content or moisture content is defined as the ratio of weight of water to the weight of soils in a given mass of soil. This is an important property which has significant effect on other parameters of soils as well.

The percentages of particles of various size in a given soil sample determines the strength and stability of soil. By consistency of soils we mean the relative ease with which the soil can be deformed. It denotes the degree of firmness of the soil. This is also related to the percentage moisture in the soil.

2.5.2 Soil Salinity

Sailnity in the soil is due to the presence of higher concentration of salts in the soil. When this concentration increases significantly, it can be easily identified on the soil surface as white patches. A large region becomes useless for civil engineers as well as for farmers if it is severely affected by salinity. This salt reacts with the construction materials and reduces the life and strength of the structure built on such grounds. Production and yield of crops is severely affected due to the presence of it. It interferes with the growing of certain crops. Many crops can not be sown in the salt affected areas. It also interferes with the daily life of nearby peoples.

The cause of salinity in a region varies from geomorphic in nature and unprecedented rise in water table. The region under study having alluvial soil and being in the Indo-Gangetic plains of north India have this problem probably due to over irrigation as a result of mismanagement for past many years. The salt minerals come into the water by its interaction with different rocks and subgrade soil then carried by the rivers and canals and consequently deposited during irrigation and subsequent evaporation.

2.5.3 Conventional Methods to Monitor Salinity

Soil salinity is in direct relation to the moisture content of the area. Higher the moisture content and evaporation rate in the area, higher the probability of salinity in the area. Thus to monitor soil salinity in an area, one way is, to know about moisture content of the soil. Conventional methods of assessing moisture in soil is dependent on tonal variations in the soil surface and the presence or absence of particular plant species. Various methods to determine water content in the soil includes gravimetry method, sand bath method, alcohol method, calcium chloride method, and pycnometer method.

Gravimetric method is the most accurate one, though time consuming. Pycnometer method is quicker but it requires specific gravity of the soil sample to be precisely known. Other methods are field methods for crude estimation of moisture. Gravimetry method is adopted in the present study to measure soil moisture content.

2.5.4 Remote Sensing Methods

Remote sensing methods of monitoring soil salinity is dependent on the difference in spectral response as caused by moisture and presence of salt in the soil. Successful application of remote sensing in the study of soil salinity has been made by several peoples. It has provided an easy tool to monitor large area with much less cost and time.

2.5.5 Review of Earlier Works

Enough literature is available on the monitoring of soil moisture and salinity using remote sensing. These works are mainly based on visual interpretation of imagery acquired in appropriate bands to characterize the salinity status of the soil. The effect of image scale is also studied. Chemical analysis is undertaken to find the nature of soil salinity. Earlier attempts on studying the effects of moisture and salt on soil using remote sensing techniques are mostly qualitative in nature. It has been observed that effect of complex nature of environmental parameters are difficult to be taken care of on a global monitoring of soil behavior and properties. Several researchers have got encouraging responses in their attempts to evaluate soil properties using remote sensing techniques. Some of the works are discussed below:

In their separate work on different types of soil in the Indo-Gangetic plains (near to kanpur), Kant Akshay and Singh S.B.B. (1993) as well as Sirohi Anand (1993)

have observed, with multiband ground truth radiometer, that, as the moisture content in the silty soil increases, its reflectance decreases. They have also worked on other soil types like clayey, silty clay, sand, red soil and sandy silt and found the similar results.

In order to make the most efficient use of multi-spectral data it is essential to identify the best possible band combination that could provide the desired information on the salinity status. For the selection of appropriate bands to characterize salinity status of soils, Csillag, F et. al. (1993) have used a modified stepwise principal component analysis (MSPCA) approach to statistically analyze reflectance data set. Discriminant function analysis (DFA) is used to test above described classification. Its results can be applied for weighing spectral bands according to their sensitivity to the chosen classification as well as in defining broad, but still potentially sufficient bands. Recognition accuracy of salinity status was observed to be 91, 90, and 88 percent with 10 nm, 20 nm, and 40 nm bands respectively for the data set used. Key spectral ranges are identified in the visible (550-770 nm), near infrared (900-1030 nm, 1270-1520 nm) and middle infrared (1940-2150 nm, 2150-2310 nm, 2330-2400 nm) portion of the spectrum at 20 nm, 40 nm, and 80 nm spectral resolution. Two of these (1270-1520 nm and 1940-2150 nm) can not be used with satellite data due to water vapor absorption in the atmosphere.

This study led to identification of highly correlated key narrow bands to study particular soil properties. Emphasis is given to reduction of data set, and data dimensionality without decreasing the proportion of information which can be extracted from original data set. Author has observed that salinity status is a complex phenomena, therefore, variation in the reflectance spectra of soil can not be attributed to a single soil property. Key soil properties such as pH, salt content, electrical conductivity and exchangeable sodium percentage, determine the salinity status of soils and this is reflected in the spectra of surface samples interacting with organic matter and clay content.

The efforts were made earlier to study the influence of organic matter (Sinha,1987), clay contents (Gerberman, 1979), and surface conditions (Sinha, 1986) on

the soil reflectance properties. In the visible part of the spectrum, the high reflectance of salt covered areas is prominent. Bands in the middle infrared give information on moisture content, which is often associated with salt content difference and some information on type of salts (Mougenot B. et.al.,1993).

For visual interpretation, a standard false color composite (FCC) image is used. Standard FCC image is usually made from data of green, red, and near infrared bands. Dwivedi R.S. and Rao B.R.M.,(1992), in a study have tried to identify the best possible three band combination. This is generally quite difficult, subjective and time consuming without using digital techniques. Authors have used parameter such as Optimum Index Factor (OIF) and selective principal component analysis of a highly correlated sub-set or band pairs. They ranked various three band combinations by estimating the OIF value that ranks the multispectral data in terms of scene variance and by accuracy estimation of visually interpreted maps derived from three band combinations. The band combination 1, 3, and 5 of the reflective TM bands (that is, 450 - 520 nm, 650-690 nm and 1550 - 1750 nm) is found to be the best for delineating salt affected soils. This combination ranked first in terms of OIF values as well as the accuracy of mapping salt affected soils. The normally used band combination 2, 3, and 4 ranked relatively low.

Rao et. al. (1991) have dealt with mapping the magnitude of sodicity in part of the Indo-Gangetic plains of Uttar Pradesh through systematic visual interpretation of Landsat TM data. They used standard false color composite (FCC) print made from bands 2, 3 and 4 of Landsat-TM data at 1:50,000 scale. Based on image elements and their correlation with the ground features, two categories, namely moderately and strongly sodic soils could be delineated. Soils with pH above 8.5 have been rated as alkali or sodic soil and further subdivisions into alkali classes, namely class 0,1,2, and 3 is made on the basis of aerial distribution. On these prints, strongly sodic soils, with pH above 10, appear as bright white patches with fine texture, while moderately sodic soils, with pH about 9.5, are manifested as dull white to strong brown. Slightly sodic soils was observed to support

crops with varying vigor and was found to have similar spectral response as of normal soils. The study has demonstrated the utility of large scale Landsat-TM data for delineating sodic soils categories. Data acquired during March-April was found to be ideal for mapping salt-affected soils supplemented by post-monsoon season data.

Reflectance of salt surface increases with increasing wavelength upto about 1 μm on many soil surfaces, but salt induces a relative higher reflectance in blue band by

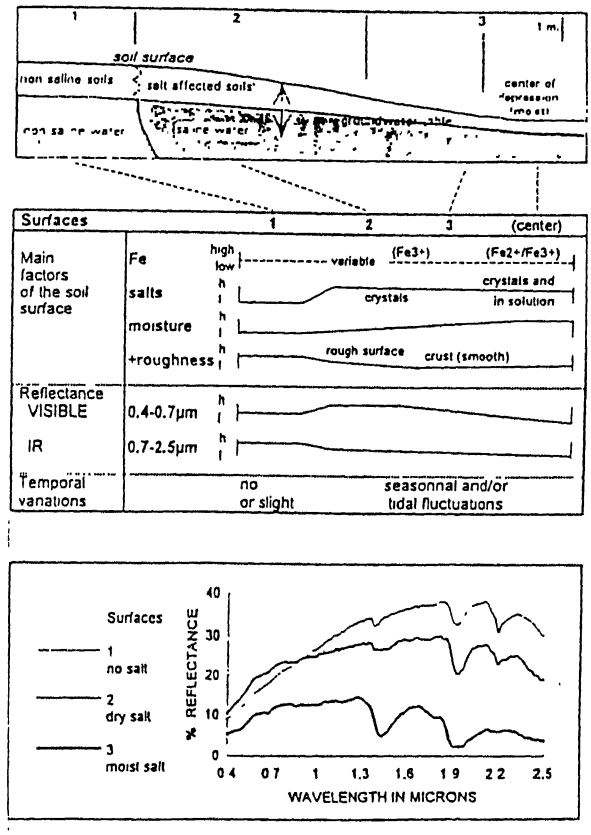

Figure 2.3: Example of relationship between bare surfaces of saline and non saline soils, groundwater, main factors influencing reflectance in visible and infrared (0.4-2.5 μm) and temporal variations (arid or semiarid land). Source: Mougenot et.al. 1993

masking ferric oxides. Often, salts have a low reflectance in the middle infrared bands. This is due to presence of water and hygroscopic characteristics of many salts, or to high moisture content of fresh salts (Mougenot et. al., 1993, Saha et.al., 1990). In the visible part of the spectrum the high reflectance of salt covered areas is prominent. Bands in middle infrared give information on moisture content, which is often associated with salt content differences, and some information on type of salts. Effect, on the spectral response of soil surface, by some factors such as salt, moisture roughness is presented in Fig. 2.3.

Mougenot et. al. (1993) have also dealt with spectral properties of different salts consisting of chlorides and sulfates. They used spectra of pure salts acquired with a laboratory spectrophotometer measuring in visible to middle infrared (0.4 to 2.5 μm) and compared characteristics absorption bands of salts as present on soil surface. The study concentrated on the presence of chlorides, carbonates, and sulfates. The author has also stressed that reflectance in visible and middle infrared bands reveal information of the Ist millimeters of the top horizon of the bare soils. Often, the characteristics of the surface is different from that of the layers below.

Mougenot et. al. (1993) have observed that salt efflorescence occurs from more rapid evaporation in the margin than in the center of depressions with vertical and lateral salts variations. High spatial variability of salt quantity is a characteristics of salt affected soils. On bare soils, satellite observations permit to detect salts on the surface, but the direct and precise estimation of quantity of ion of salts is not possible due to:

(i) Lack of specific absorption bands and spectral confusions (H_2O from free water, OH from clays),

(ii) Low spectral resolution of satellite bands,

(iii) Vertical, spatial and temporal variability of the saline profile.

Some authors have cautioned the use of photographic tone to identify soil properties. Tonal patterns can be good indicators of different soils, but the correlations of photo tone with organic matter content, moisture content, calcium carbonate content and

siltness of the soils are poor especially over large areas. In many cases, photographic tones are found to have little meaning and could be resulted from such transient features as surface waterlogging, stubble remaining on the surface after ploughing or different datesof cultivation. Although the predictability of soil types based on photographic tones is poor, field experience and landform analysis can adequately supplement the use of aerial photographs in soil mapping (Lo, C.P., 1986).

Many authors have used vegetation index to differentiate between healthy green vegetation and scant / diseased vegetation. It has been observed that reflectance from single leaves depends on their chemical composition (salt) and morphology. The use of these index can be easily extended to soil salinity study. The observation by Hardisky et. al., (1983), Mougenot et. al., (1993) is as follows:-

(i) Visible reflectance of leaves from plants growing on salt affected soils is lower than reflectance of non salt affected leaves before plant maturation and higher after,

(ii) Near infrared reflectance increases with leaf maturity,

(iii) Middle infrared reflectance decreases without water stress due to a succulent effect and increases in other cases. Cell thickening induces thicker leaves(as succulent vegetation) and hence transmittance decreases much more than general reflectance increases.

Clevers et. al.(1993) have dealt with the estimation of leaf area index (LAI) by means of weighed difference vegetation index (WDVI). Their observation shows that application of remote sensing techniques has the potential to provide quantitative, non destructive, and instantaneous information about agricultural crops. It can be applied with regard to the estimation of crop characteristics such as soil cover and (LAI). LAI is defined as the total one sided green leaf area per unit soil area and it is regarded as a very important plant characteristics because photosynthesis takes place in the green organs. LAI is generally estimated as (NIR / R). Among the ratio based vegetation indices, the normalized difference vegetation index [(NIR - R) / (NIR + R)] is the most common and

useful index. Hardisky et. al. (1983) have proposed an infrared vegetation index [(IR - NIR) / (IR + NIR)] to detect canopy moisture influenced by salinity and found it sometimes superior to NDVI. Typical spectral reflectance characteristics for healthy green.vegetation, senescent vegetation, and dry soil varies appreciably with wavelengths. Most vegetation indices are based on the fact that there are significant differences in the shape of these three curves. The authors have also tried to study the sensitivity of LAI on various factors like soil reflectance, solar zenith angle, diffused and total radiation, leaf inclination angle, chlorophyll content, mesophyll structure etc.

Often in the near infrared, an inverse relationship is observed between reflectance and salinity, since salt content induces less plant cover (decreasing of density, LAI, and height), and sometimes slight deposits associated with vegetation have similar effects. For the same reasons, saline stressed vegetation induces a reddish or dark red shift on standard color composite data. Contrasted associations of vegetation and bare soils can be more useful for salinity detection than individual surface types. It can emphasize potential evolution of the salinity which begins with small and irregular bare soil patches (Richardson et. al.,1976, Everitt et. al., 1977, Sharma et. al., 1988).

Good correlations between soil distribution and geomorphological shapes were observed by Manchanda et. al.(1983), Manchanda (1984). Relative elevation is one of the most evident landscape feature in relation to salinity and moisture provided by saline and shallow ground water table.

Mothikumar et. al.(1989) have tried to identify and map salt affected lands at village level, using Landsat TM data at 1:50,000 scale. Visual image interpretation techniques were based upon the photo elements such as tone, pattern, location, association, shape, and texture. The natural salt affected soils having surface salt encrustation showed highest reflectance value followed by the sodic soils (formed due to high residual sodium carbonate in irrigation water), natural saline soils and saline soils due to saline water irrigation. Soil chemical analysis was also undertaken to correlate the

interpreted satellite data. The author has observed that soil texture, pH, $CaCO_3$ and organic matter together accounted for 29.6 percent variation in the maximum reflectance percentage value out of which only pH accounted for more than half (14.2 percent variation).

Dwivedi (1991) have carried out an study to assess the effect of image scale on the delineation of soils. He used standard FCC prints using Landsat data for visual interpretation at 1: 250,000 and 1:50,000 scale. In a way, spatial resolution is analogous to the scale of observation. Experience with Landsat MSS shows that it can withstand an optical enlargement upto 1:100,000. Beyond this, the blurring effect becomes perceptible. Enlargement of Landsat TM data through the digital cum optical approach has been found helpful not only in refining the boundaries of salt affected soils but also in identifying patches with relatively very smaller dimensions and ultimately led to the improvement in mapping accuracy.

Joshi et. al. (1993) have used ground truth data and standard FCC print generated using Landsat satellite data to map the salt affected land in Saurashtra coast on various scales.

CHAPTER 3

SCOPE OF THE STUDY

The area, chosen for the present study, belongs to Indo-Gangetic plains of northern India, and is near Kanpur city. This area has a dense drainage network. It includes, apart from many distributaries and minors, a stretch of river Ganga, Non and Pandu and in the central part, lower Ganga canal . The seepage from canal network and rivers has led to the increase in the soil moisture, which is actually a major cause of soil salinity in this area. The problem of soil moisture and thus soil salinity is quiet high as observed during field visits. This offers a good scope to study salinity in the soil because it is harmful to civil engineering structures as well as to crop production. Large amount of qualitative work has been undertaken to identify saline zones in other regions but no standard literature is available on the study area. Hence, the present work is oriented to identification and monitoring of soil salinity in this area.

It is understood that chemical and mineral composition of material affects the spectral response. Thus, this study incorporates advance methods such as scanning electron microscopy (SEM), X-ray diffraction and conventional chemical analysis to determine mineral and chemical composition of the soil.

In most of the earlier works, very little effort has been made towards quantification of salt concentration in the soil. From the preceding discussion as presented in Chapter 2, it is evident that remote sensing techniques using spaceborne and airborne sensors can be effectively used for acquiring data to study soil properties at global level. It is also cost and time effective. However, to study minor details of the area and to know response of various ground features, it is necessary to have ground truth information. Again, to analyze digital data from satellites, accurate knowledge of the response of various Earth cover features is required.

The present work is aimed to utilize both satellite and ground truth data to model variation in the spectral response of soil with respect to moisture content and salinity. This model will help in global estimation of soil moisture and salinity quantitatively. Digital processing of satellite data is undertaken based on all the information available from laboratory tests and MGTR analysis. Data of IRS-1B is obtained for two periods, namely November,1992 and April,1993 to demarcate changes in efflorescence of salts. For better identification of the salt affected zones, the satellite data needs to be enhanced. A set of digital image processing techniques are to be applied like contrast stretching, filtering, arithmetic operations, principal component analysis and color composites.

Based on the results of empirical models using satellite data and confirming the information from digitally enhanced images, a photo map depicting salt affected zones can be prepared. This will provide a global information on the concentration of salt present in different zones of the region.

The techniques developed in present work will be useful to the field engineers working for land hazard management by providing them data base regarding soil condition in the area. Since remote sensing data is repetitive in nature, It would be of great use to monitor frequently the changes taking place in salinity level of the soil.

CHAPTER 4

DATA ACQUISITION AND LABORATORY ANALYSIS

4.1 Introduction

Spectral reflectance of soil is dependent on many factors. Without having an idea about some of these, it is very difficult to predict the nature and behavior of the response of various soil types. Some of the major factors are mineralogy, soil texture, moisture content, quantity and chemical compositions of salt, if present. The effect of all these factors is generally interdependent. Again, spectral response is not same during different seasons. In the present work, stress is given to obtain information on the factors like, moisture content, chemical and mineralogical composition of soil and their effect on spectral reflectance.

4.2 Area of the study

4.2.1 Location

Having a broad idea about the nature and appearance of saline land on the imagery, an area consisting of large number of saline patches is chosen using Landsat imagery of path no. 145 and row no. 42 on a scale 1 : 250,000. The approximate location of the area is determined from topographic sheet of the corresponding areas obtained from Survey of India. The chosen area, with an aerial extent about 340 sq. km is bound between 26°32' N to 26° 43' N and 80°. 2' E to 80° 18' E and forms part of the vast Indo-Gangetic alluvial plains covering part of Kanpur district of Uttar Pradesh, India (Fig. 4.1).

The study area, comprising part of the Indo-Gangetic alluvium of Pleistocene age (Dwivedi et. al. 1992), physiographically is a plain with local variations

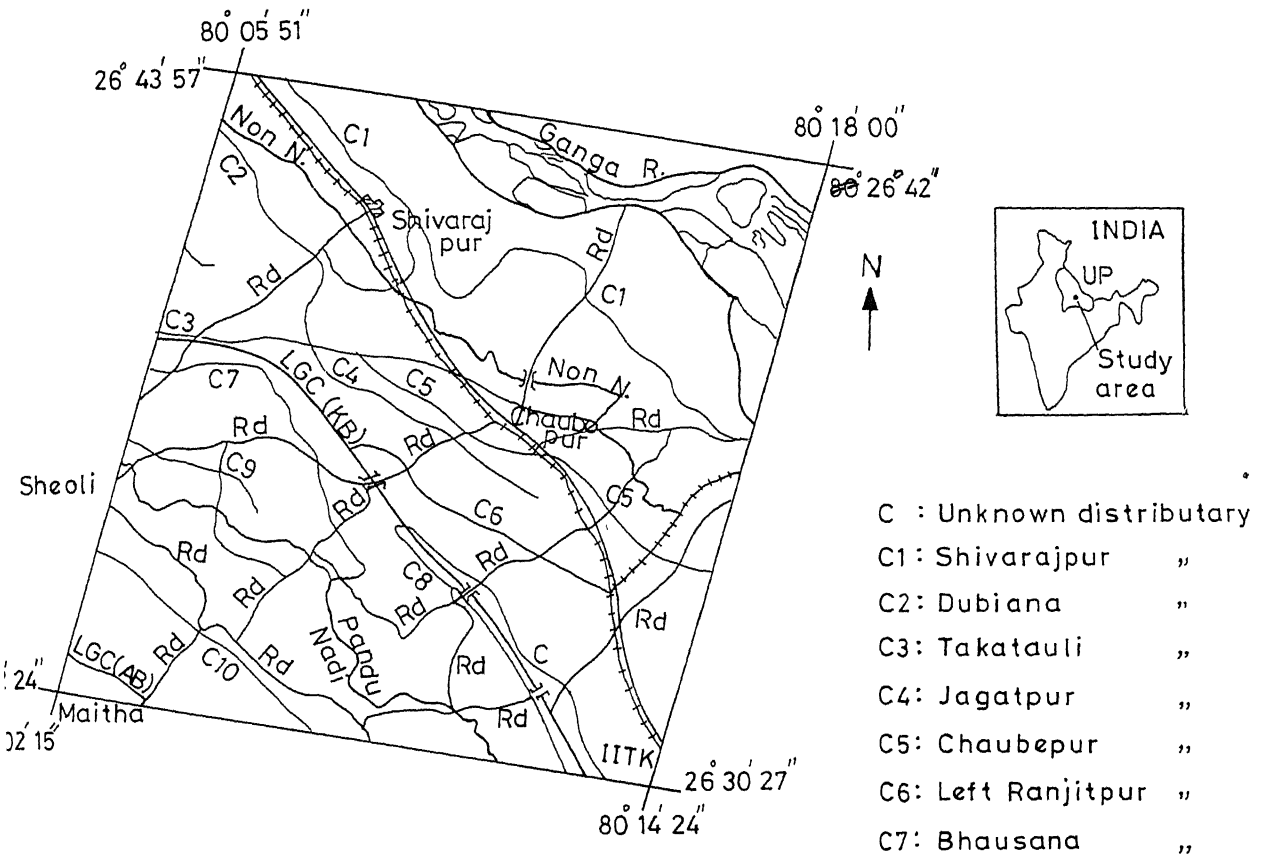

C : Unknown distributary
C1 : Shivarajpur „
C2 : Dubiana „
C3 : Takatauli „
C4 : Jagatpur „
C5 : Chaubepur „
C6 : Left Ranjitpur „
C7 : Bhausana „
C8 : Right Rampur „
C9 : Right Maddupur „
C10 : Sheoli distributary

+++++	Railway Track
Rd	Road
C	Canal /minor
LGC(KB)	Lower ganga canal (Kanpur branch)
LGC(AB)	Lower ganga canal (Allahabad branch)
	SCALE : 1: 250,000
	SOURCE: SHEET 63 B SOI INDIA

FIG. 4.1 LOCATION MAP OF STUDY AREA

such as paleochannels, oxbow lakes, minor depressions and sand dunes along the rivers and streams. Topography of the area is flat with gentle slope. The river Ganga drains the north-eastern periphery of the area, Non nadi traverses central to eastern part on both sides of the Lower Ganga Canal (Kanpur Branch). The area is irrigated by this canal and many other distributaries and minor channels as shown in Fig. 4.1. Ground water table in general is high and water quality is good. The climate of the area is semi-arid; sub-tropical and monsoonal type. Water in abundance is available for irrigation in this region.

A detailed description of Landuse / landcover of the area is shown in Fig. 4.2. This map clearly shows the dense network of drains and distributaries in the region. Metalled or unmetalled roads are generally present along these channels. Vast stretches of salt affected soils and frequent occurrence of saline areas along the ponds and canals are common feature. The extent and magnitude of salt is varying on different sites. At some places salt has spread on the ground as a white layer. The lack of vegetation or scattered vegetation on affected soil surface make it possible to directly detect presence of salt in the soil.

4.2.2 Topographic sheets

To know various details of the area regarding topography, villages and other features, topographic map obtained from Survey of India are used. Topographic map No. 63 B on a scale 1:250,000 is used for identification of prominent features of the region. For further details, a topographic map No.63 B/2 on a scale 1:50,000 is utilized. Sampling sites are chosen based on the extensive field visits and verifying exetnt of salinity.

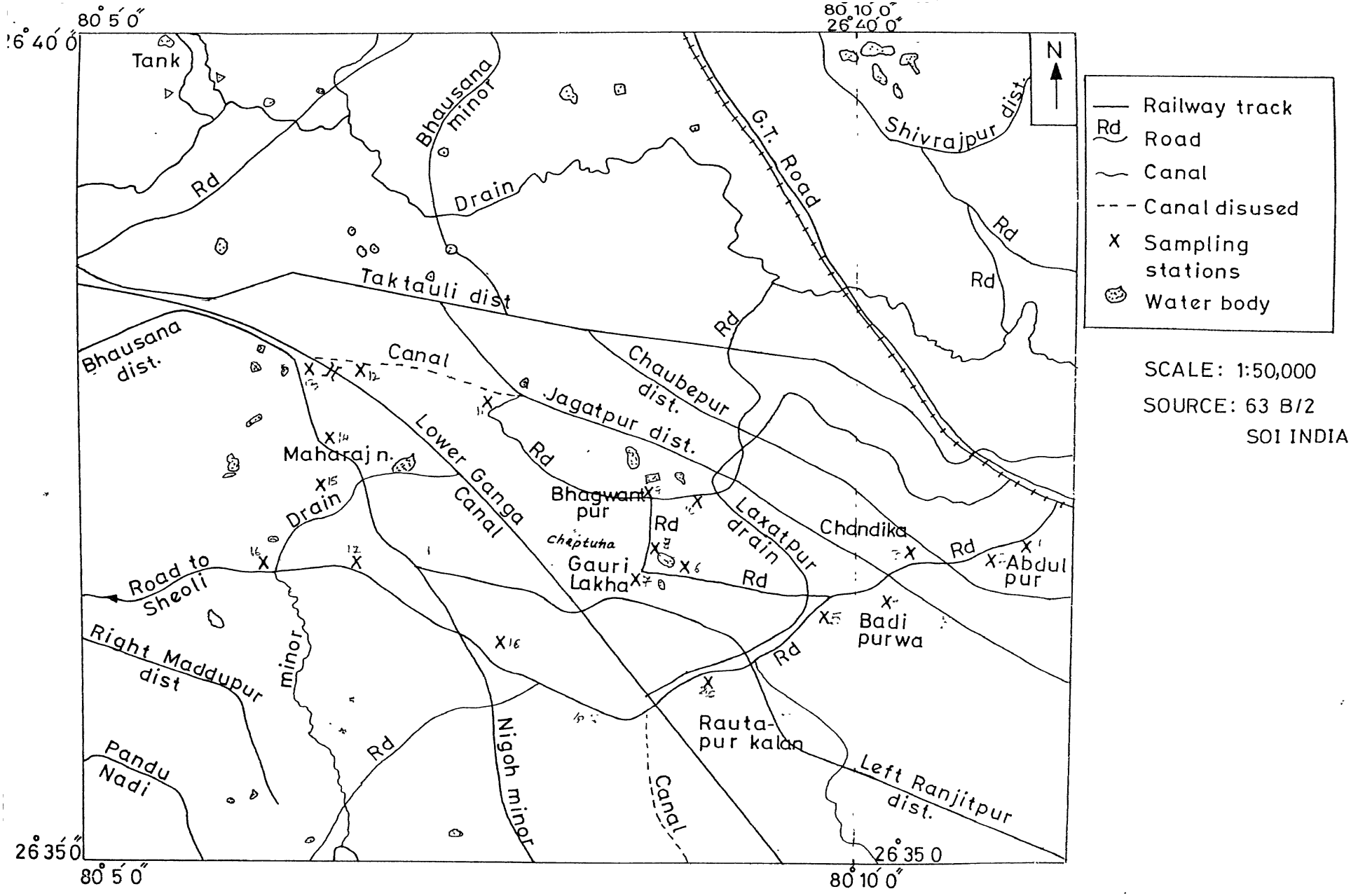

FIG. 4.2 LAND USE/ LAND COVER MAP AND SAMPLING SITES IN STUDY AREA

4.3 Probable Cause of Salinity in the region

Deposition of a layer of salt on top of soil surface is termed as Salinization. It is found on soils in arid, semi-arid, semi-humid, and even humid regions. The increase in the concentration of salts depends on many factors, Such as

(i) intrusion of sea water in coastal zones,

(ii) evaporation in depressions in arid or semiarid lands,

(iii) presence of various contributing elements in sedimentary deposits,

(iv) in hydrothermal alteration zones, and

(v) over irrigation coupled with bad drainage and subsequent evaporation

The last one seems to be the major cause for the presence of salts in the area of study. The area being in the Indo-Gangetic plains and having alluvial soil, various ions like chloride, carbonate, and sulfates can be present in the salt. It depends on the deposit in the area itself and the minerals present in the soil and rocks through which water has interacted.

Salinization is a continuous process. Presence of the salt on the surface is dependent on the season. As summer approaches, vegetation on saline areas changes from green to senescent. It looses its vigor and with time, becomes dead. Moisture of the soil reduces significantly. Moisture in top soil is negiligble but it increases as we go deeper and deeper. After some time, ground surface changes from brown to whitish color and becomes grassless. Still, some adjacent regions may have good vegetation cover. This is because, deposition and outcropping of salt on the surface is dependent on many factors like porosity and permeability of soil and the previous concentration of salts.

Plates 4.1, 4.2, and 4.3 clearly describes these phenomenon in detail. Plate 4.1 is taken near the canal side of village Bhagvantpur. Road along the canal is clearly visible in this. Plate 4.2 shows a region in village Gauri Lakha. A pond having

Plate 4.1 and 4.2: Efflorescence of salt on the surface (Bhagvantpur, Gauri Lakera)

Plate 4.3: A severely affected saline zone (Gauri Lakha).

water alongwith saline zones all around it are clearly visible in this plate. Plate 4.3 shows how a severely affected saline zone look like. This plate also presents a nearby greenland and some patches on the far side. Multiband Ground truth Radiometer alongwith Barium Sulfate plate used in the present study, is kept in the region and soil sample is being collected.

Due to over irrigation, frequent water logging, and high evaporation in the region, salt is transported through capillary action on the top of soil surface and deposited. This is a continuous phenomenon in a water logged area and in a long period of time, this accumulation leads to high concentration of these deposits and so the problem of salinity.

The study area affected by salinity is spread on both sides of lower Ganga canal. It also extends to far stretches due to large number of distributaries in the

region. It has a very dense drainage network as amply clear from Fig. 4.2. The amount of water available to the farmers through these drains is quite substantial. The soil in the area is sandy silt which is significantly porous and permeable in some regions. The percolation and infiltration of water to the ground is high because of the presence of these drains, most of which are generally unlined. Ground water table is quite high near the canal and decreases as we move away. The general level of ground water table is high and lies at a small depth from the surface. A large number of small channels dug in unplanned way by farmers has only multiplied the problem because of seepage and other losses. Thus the water, which is thought to be used for better crop yield is, in reality, creating and contributing to a serious problem of land degradation due to salinity. Plates 4.4 and 4.5 distinctly show the area on the two sides of Lower Ganga Canal . White patches and barren land can be easily observed in these plates. Green patches comprising grassland, agricultural fields and trees are also present in the area.

4.4 Sampling Sites

The sampling sites are marked in Fig. 4.2. Details about these are given in Table 4.1. These are selected such as to cover sites having well developed salts, affected but not visible on the surface, and normal soils. Samples are collected from ground surface as well as from certain depths. Proper care is taken in collecting and packing samples in order to preserve the in-situ moisture. They are collected from some depths, as the top layer of the soil has negiligible moisture.

Soil samples collected from the field are tested for moisture content in the laboratory, the presence of various elements, and minerals in soil is determined using SEM and X-ray analysis. Chemical tests are done to find pH, alkalinity, electrical conductivity and chloride concentration. A brief discussion on

Plate 4.4 and 4.5: The region on the two sides of lower Ganga canal. Salt patches are spread in vast areas around it (Jagatpur)

Table 4.1: Description of the sampling zones

Locations	Description of the site
1,2,6,19,20	Normal soils, These areas are in general have no significant effect of salt on the soil.
3,4,5,8,9,14,18	Soil moderately affected with salt, but the salt has not come above the ground at the time of sample collection.
7,10,11,12,13,15, 17	The soil is severely affected by salt, salt can be easily seen on the ground.

the methods used is given in following paragraphs.

4.5 Moisture content determination

Salt samples collected at the ground surface have very negligible amount of moisture while those collected from certain depth have significant moisture. To preserve this moisture, samples are collected and kept properly such as no loss of moisture can take place. These samples are tested, immediately after coming back from field, in laboratory. For determining moisture content small amount of soil sample is taken in a properly cleaned can and its weight (M_1) is noted. All the samples are weighed and then, kept in an oven for 24 hours to evaporate the moisture completely. Oven dried samples are weighed after 24 hours (M_2). Weight of can (M_3) is taken after removing dry soil from it. Moisture content in the soil is determined using equation:

$$w = \frac{M1-M3}{M2-M3} X\ 100\ \% \qquad (4.1)$$

where *M1*, *M2*, and *M3* are as described earlier.

Results of moisture content determination is given in Table 4.2.. The moisture content in the samples taken at certain depth varies from 6 to 20 percent. This clearly indicates that soil of the region has significant *in-situ* moisture.The moisture content increases as we go deeper. In the regions where salt has come on the ground, moisture content is low. Thus it clearly indicates that large moisture coupled with high evaporation rate is a prominent cause of salinization in the region. The moisture content for moderately saline areas is little bit higher than highly saline soils but lower than those of normal soils regions. The variation of moisture content in the region also justifies the variation in the spatial spread of saline zones.

4.6 Chemical Analysis

Having a broad idea about the presence of various ions in salt from earlier works on Indo-Gangetic plains and other areas (Mougenot et. al.,1993, Rao et. al.,1991, Kalra et. al.,1994), chemical lab analysis is performed in the laboratory to determine pH, Electrical conductivity, Alkalinity and chloride ions. Chemical analysis, generally requires a solution to test with for required parameters of the present study. Thus, It is decided to use extract of the samples collected from the field. Extract of soil samples is prepared by taking 1 gm of soil in 250 ml of distilled water and the solution is filtered. Similar type of extract is prepared for all the chemical tests. To determine chloride concentration and alkalinity, standard methods (Desceri et. al.) are used, which are discussed here briefly. Tests for concentration of SO_4^{-2} and hardness is performed but in our samples, negligible value is observed for these.

4.6.1 pH and Electrical Conductivity Determination

pH and electrical conductivity (EC) determination is done by pH

meter and electrical conductivity meter respectively. For pH determination, pH meter is first calibrated with standard buffer solution having a pH of 7.00. About 50 ml of sample is taken into a beaker and sensor tube of pH meter, which is always cleaned before and after the test with distilled water and dried using tissue paper, is dipped into it. The reading of digital meter is noted only after stabilization.

To measure electrical conductivity in the lab, electrical conductivity meter is used. First the unit is calibrated with standard solution and then its sensor is dipped into the beaker having about 50 ml of sample extract. The reading is taken corresponding to maximum position in the meter. The results are listed in Table 4.2.

4.6.2 Alkalinity Determination

The carbonates (CO_3^{-2}) and bicarbonates (HCO_3^{-1}) present in water mainly contribute to the alkalinity. The alkalinity is determined by titrating the water extract with N/50 H_2SO_4 acid. For titration, few drops of phenolphthalein indicator is added to 100 ml of samples. Sample color changes to pink in case of pH value being above 8.3 which is generally a case with salt samples, it is titrated till the color is discharged (first end point). Now a few drops of methyl orange is added and it is titrated with acid till color changes (2nd end point). Alkalinity is calculated as

$$\text{Alkalinity, (mg/l) as } CaCO_3 = \frac{A \; X \; N \; X \; 50000}{V} \qquad (4.2)$$

where

A = Volume of standard acid consumed (ml),

N = Normality of standard acid, and

V = Volume of sample taken (ml).

Alkalinity upto first end point is called bicarbonate

alkalinity while total alkalinity upto second end point is called carbonate alkalinity. The results are detailed in Table 4.2.

4.6.3 Chloride Determination

In a neutral or alkaline solution, chloride can be determined by titrating the solution with silver nitrate solution using potassium chromate as indicator for titration. In a 100 ml sample, 1 ml of K_2CrO_4 indicator solution is added. This solution is titrated with standard silver nitrate titrant to a pinkish yellow end point. The distilled water is titrated to get the reagent blank value. Chloride content is determined as follows:

$$\text{Chloride Concentration (mg/l)} = \frac{(A-B)\ X\ N\ X\ 35450}{V} \qquad (4.4)$$

where

V = volume of sample taken (ml),

A = volume of $AgNO_3$ solution used in titration for sample (ml),

B = volume of $AgNO_3$ solution used in titration for distilled water (ml),

N = normality of $AgNO_3$ solution.

The results are noted in Table 4.2.

4.6.4 Results and Discussion

The results of the chemical tests and moisture content determination are presented together in Table 4.2. The chemical analysis of the samples shows a typical trend. The salt samples generally shows higher values for various characteristics which decreases with the decrease in the effect and presence of salt in the soil. The chemical analysis of the saline samples has helped in identifying the presence of particular ions.

Table 4.2: Physical and Chemical properties of Soil Samples

Site No.	Moisture Content (percent)	pH	Electrical Conductivity ($\times 10^{-4}$) Siemens / cm	Alkalinity (mg/l as $CaCO_3$)	Chlorides Concentration(mg/l)
1	15.60	9.00	2	190	Nil
2	19.40	8.60	1.8	115	Nil
3	17.00	9.50	20	550	3
4	12.20	9.70	19	910	3.6
5	19.80	8.50	1.1	90	Nil
6	9.40	10.95	28	1090	5.3
7	7.80	10.90	34	1300	6.0
8	11.00	10.40	32	1220	5.9
9	5.85	10.50	33	1120	6.1
10	20.10	9.40	16	300	2.5
11	14.67	9.40	15	250	2.2
12	6.54	11.00	35	1390	6.4
13	18.20	9.40	20	490	4.0
14	13.33	9.20	21	930	3.7
15	13.54	9.60	23	780	3.5
16	10.50	10.80	34	1310	5.8
17	13.00	9.50	20	930	3.6
18	13.73	9.10	19	770	3.2
19	16.41	8.50	2	150	Nil
20	17.5	8.20	1.5	130	Nil

4.7 Scanning Electron Microscopy

4.7.1 Scanning Electron Microscope

The basic machine is composed of an electronic gun which provides a beam of electrons with energies from 1 to 50 keV. The electrons are accelerated past two or more condensing lenses that demagnify the beam into a small diameter probe, which is then scanned over the specimen. Deflection coils are placed to deflect the beam in a rectangular pattern over the sample. A detector that is sensitive to the chosen output signal from the specimen is connected through a video amplifier to the grid of cathode ray tube which is scanned in synchronism with the beam on the specimen. Thus an image of the specimen surface is built up on the cathode ray tube screen point by point.

The SEM produces images by scanning the surface of a specimen with a small electron probe (a beam of electrons) synchronously with an electron beam in in a cathode ray tube. A narrow beam of electrons is produced by successive electromagnetic condenser lenses which places a small spot of electrons on the specimen (~ 500 to 50 °A in dia.). The primary beam (also called electron probe) penetrates the surface and produces a variety of signals as discussed above, any of which can be used to generate image. Generally, in surface SEM, secondary electrons are collected to form the image. The contrast is due to topographical variations and atomic number differences in the specimen. The signals produced by the probe - specimen interactions are used to modify the intensity of the beam in the cathode ray tube.

Scanning Electron Microscope (Model JEOL JSM-840) is used in this study. This unit has a fully automatic vacuum control system. the operating vacuum is achieved through a pumping system controlled by a key. Specimen replacement is

accomplished with a compressive system of air locks. The equipment is fitted with excellent photographic recording facility along with a computer which analyses the composition and also enables detailed mapping of the individual locations.

4.7.2 Analysis Procedure

The SEM unit has an in-built computer with a software package to analyze various elements in the specimen and other study. It uses Chi-square interpolation technique to analyze various elements through pulse height analyzer. Electron beam can be focused at any position on the sample. Beam diameter used is about 0.05 μm, so at a time, study or analysis of only that area is done and it is not anyway representative of presence or absence of elements in the sample. Therefore, it is necessary to scan several positions on the specimen and check the presence of elements. Varying composition is observed in the analysis on the different spots of a sample in case of heterogeneous specimens. Based on it, a general presence of elements can be made.

Qualitative spectral scans involve displaying the X-ray rate meter output as a function of Bragg's angle or wavelength. It is based on the ability of a spectrometer system to measure characteristics line energies and relate these energies to the presence of specific elements. Once peaks are detected, their identity can quickly be established from standard chart like X-ray energy spectrometer chart. Quantitative analysis involves accurately measuring the intensity of spectral lines corresponding to preselected elements for both samples and standards under identical operating conditions, calculating intensity ratios, and then converting them into chemical concentration. Point analysis offer the greatest precision of measurement of composition. Here, in the present study, the aim is only to identify the presence of various minerals so that the results of spectral analysis can be extended to areas having

similar mineral composition. Electrons diffusing into the specimen from a static probe excite X-rays in very limited volume of material and it is the composition of this volume that is determined in a point analysis.

4.7.3 Sample Preparation

For scanning purposes, the preparation of sample requires extreme care. Application of a conductive coating is mostly used to allow continuous electrical conduction. For this, a thin layer of a conducting element is applied to the specimen. The layer is made as thin as possible under the constraint that it be continuous in order to provide a conducting path to ground. Thicker layer may interfere with the analysis of specimen as the depth to which electron beams penetrate is considerably small. For the analysis, soil samples are powdered finely and a small amount of it is mixed in the acetone. This solution is put in the vibrator and vibrated for three minutes. This way a fine suspension of soil in the acetone is ready. Few drops of this suspension is dropped on the stub and allowed to dry. Thus a fine layer of it is deposited on the stub. For silver coating on the specimen, stub is kept in the sputtering unit and a fine layer of silver is coated on the specimen. Now the sample is ready for testing in the SEM. Similarly, other samples are also prepared.

4.7.4 Analysis of Samples

Various portions of the samples are scanned to have a look of the composition of the specimen. Analysis is carried out with the help of an in-built computer and plot of the intensity for various energy levels is also taken. Photographs of the magnified portion of some specimen micrograph is taken to show the shape and nature of various crystals. The composition as observed for various samples comes

more or less same. For the general analysis of samples, a predefined set of elements are checked for their relative percentage. The elements are predefined on the basis of earlier work related to soil salinity study. Thus some major elements, like Na, K, Ca, Al, and Fe are selected because these are present in significant amount. To analyze the composition corresponding to various crystal shapes, a detailed analysis is undertaken for some samples. The common shapes like round, polygon and needle shape corresponds to silica, calcium, and sodium respectively. The crystal shape for potassium is also a polygonal. It requires a detailed study and enhancement to distinguish and identify various elements, but point analysis gives an idea about the presence of various elements. Results are presented in both, photographic form and tabular analysis for some of the specimens. These photographs were taken at different magnification. Specimen were viewed under magnification upto 3000. Electron beams are accelerated through a voltage of 15 kV.

4.7.5 Results and Discussions

Soil samples were collected from various locations in the study area. Some samples were of the salt only which has come above the ground while in others, salt is not so predominant at the surface. The analysis of the two type of samples varied significantly. The one, of salt, shows higher percentage of alkali and alkaline earth elements like sodium, potassium, calcium and aluminum while others shows less amount of these and major amount of silicon which is due to soil being sandy silt. This study, thus, has helped in identifying the presence of major elements in the salt. The result of SEM analysis shows similar composition for various samples of saline soils collected at different sites. Samples from severely affected zones as well as from moderately saline areas have typical elements like Na, Ca, K, Al, and Si in abundance. Samples of normal soils are lacking or shows traces of these, but higher concentration

of Si, a typical element of sandy silt soil. The presence of elements in saline soils is more or less common, though different points on the specimen may show different ratio for their presence. Hence the origin of salt in the soil, in this particular part of the Indo-Gangetic plains, can be attributed to same cause.

Photographic facility of SEM is effectively applied to have photographs of several samples. The more general and distinguishing shapes like needle, polygonal and round one are easily identified in these photographs. This gives an idea about the presence of elements like Na, K, Ca, and Si etc. The presence of these and other elements whose crystal shape is not so easily distinguishable, are confirmed by point analysis of various portions of specimen.

Plate 4.6, shows the analysis of a normal soil sample, with a magnification of 2000. It describes presence of the crystal of polygonal shapes in abundance. Other shapes are not so clearly visible. The analysis of this specimen in terms of preselected set of elements shows that Si is a major constituent, while K and Fe are also in significant amount. Na and Al are in small amount. A plot of intensity vs energy levels is shown in Fig. 4.3. In this plot, on the x-axis we have energy levels and on the y-axis, intensity corresponding to various elements. This plot shows some additional peaks, not named here, due to the stub material (Brass i.e. Cu and Zn) and coating material (Ag). Various Peaks are identified using X-ray energy spectrometer chart. Soil in this region is mainly sandy silt so presence of silica in the soil is very well justified. Similar composition is observed at various other positions on the specimen.

Plate 4.7 is concerned with the analysis of saline samples, taken at a magnification of 1500. It shows presence of crystals of needle and polygonal shapes in abundance. Crystals of round shapes are not so clearly distinguishable. Analysis of this specimen emphasizes that sodium, potassium, and silicon are major ones while iron, calcium, and aluminum are in minor quantities. Intensity peaks of this sample are plotted with respect to various energy levels as shown in Fig 4.4.

Plate 4.8 presents analysis of a sample collected from highly saline areas,

Plate 4.6: Micrograph of a Normal Soil Sample

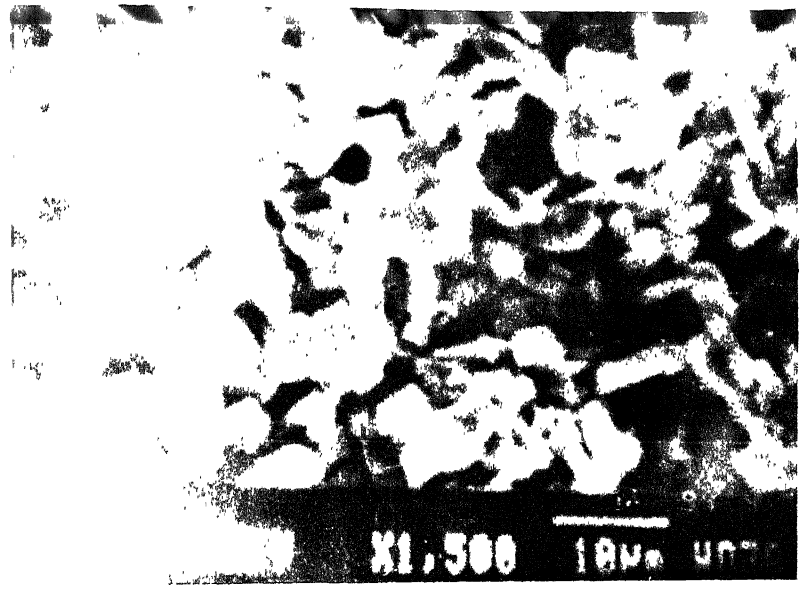

Plate 4.7: Micrograph of a Saline Soil Sample

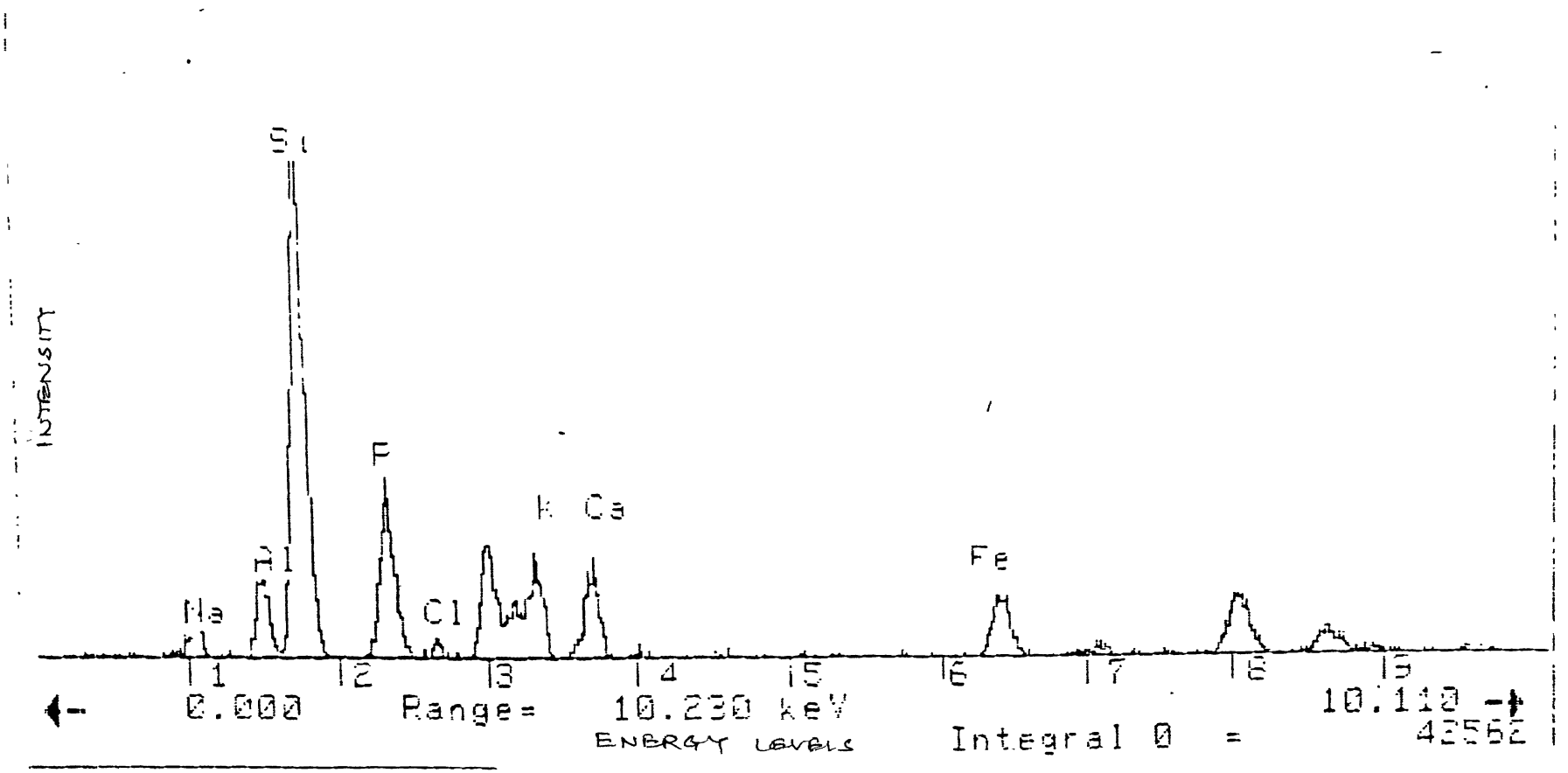

Fig. 4.3: Intesity Vs. Energy Levels for a sample

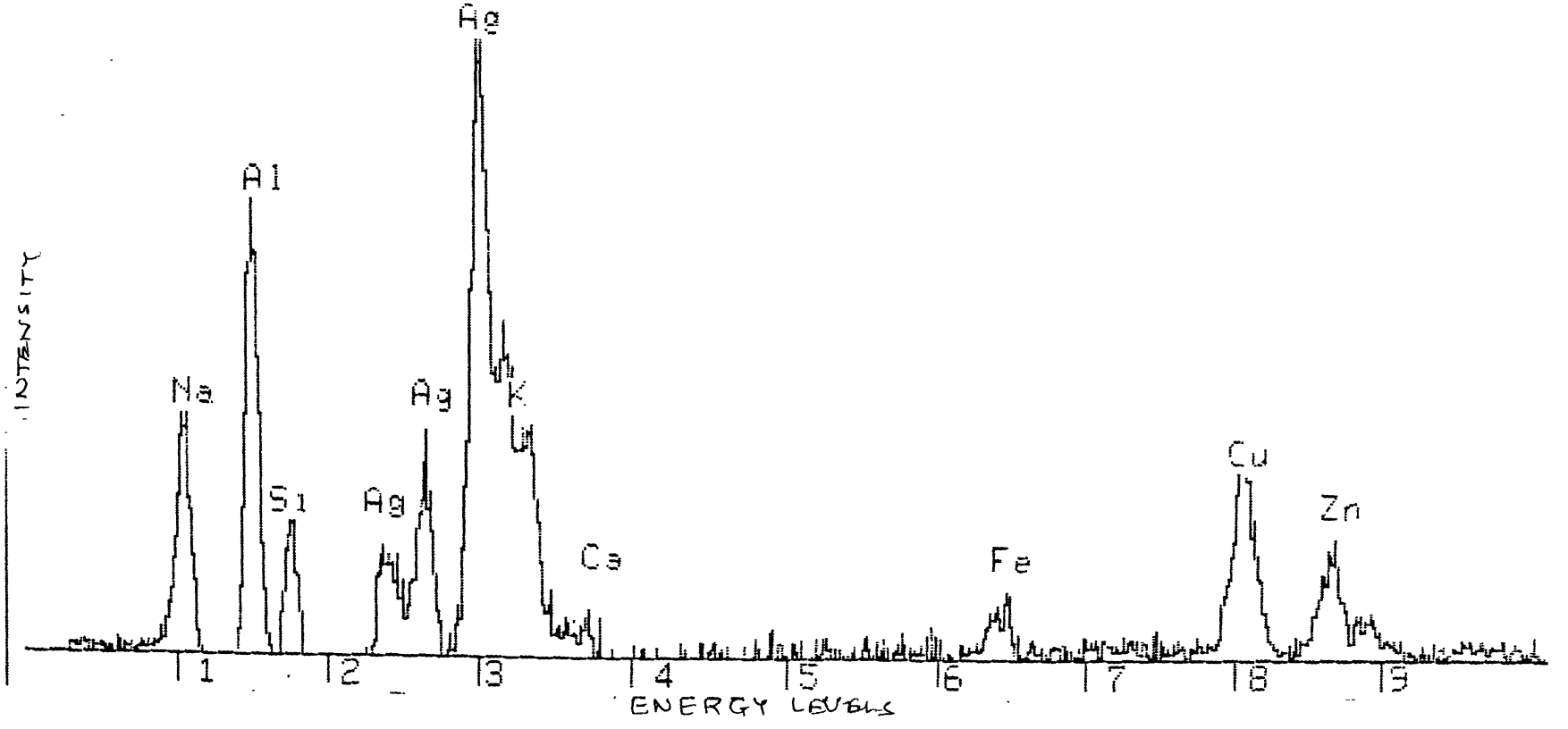

Fig. 4.4: Intesity Vs. Energy Levels for a sample

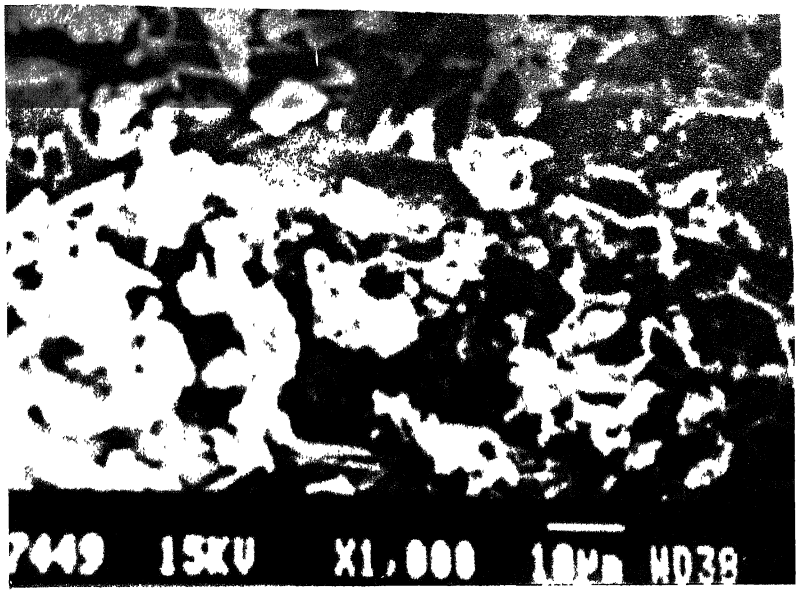

Plate 4.8: Micrograph of a Highly Saline Soil Sample

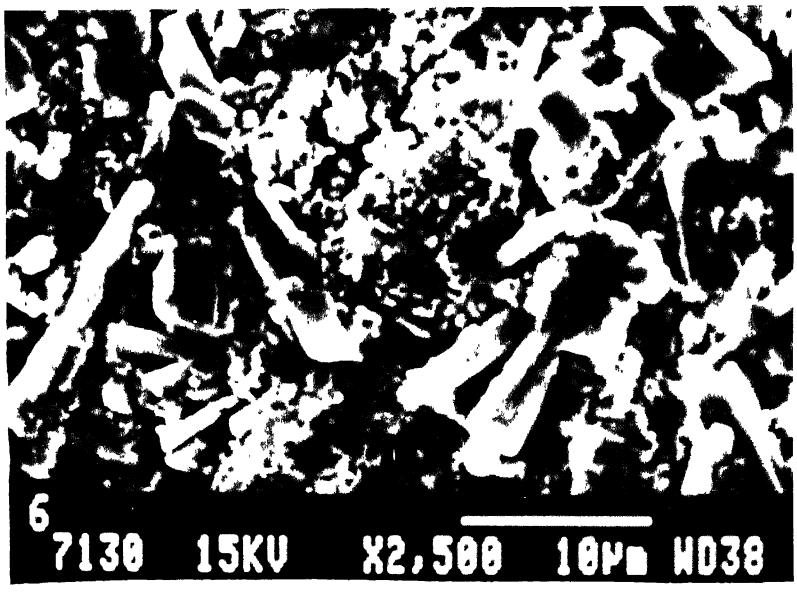

Plate 4.9: Micrograph of a Saline Soil Sample

with a magnification of 1000. It shows the presence of needle shaped crystals in abundance. Distinguishing other shape in this particular piece is not easy. The analysis of this specimen shows higher percentage of sodium.

Plate 4.9 is related to a saline soil sample, taken at a magnification of 2,500. It shows presence of some needle shaped crystals. Shape of other crystals is not easily identifiable. Analysis of it shows major presence of calcium, sodium and aluminum while elements like silicon, iron and potassium are in minor amounts.

Plate 4.10 presents the composition of previous saline sample at dense clustered zone, with a magnification of 3,000. This part shows higher percentage of round shaped crystals hence a higher composition of calcium, potassium and silica.

Plate 4.11 is one of normal soil, very less affected by salinity, with a magnification of 2000. It clearly shows the presence of polygonal and somewhat round shaped crystals in abundance. Analysis of the specimen indicates the varying proportion of different elements. Here silicon is most predominant, while iron, potassium, calcium, sodium, and aluminum are in decreasing order. The similar composition is observed nearly at all other locations on the specimen. Thus it represents the general presence of various elements in this sample. This sample is of a region which is not severely affected by salts.

It was discussed earlier that various locations on a specimen can have altogether different composition. Plate 4.12 presents the description of same saline sample as presented in Plate 4.9, but at different position on the prepared specimen. This, taken at a magnification of 2500, clearly shows abundance of needle shaped crystals (hence higher percentage of sodium), in contrast to the previous one. Another position on the same specimen represents relatively different composition. In this, analysis on and near particular shape of the crystal (marked by the arrows A, B, and C) is undertaken. This is represented in the tabular form. This indicates that needle shaped crystals are mainly of sodium and potassium, round shapes are of calcium, and polygonal or some arbitrarily round shapes are mainly associated with silicon which is

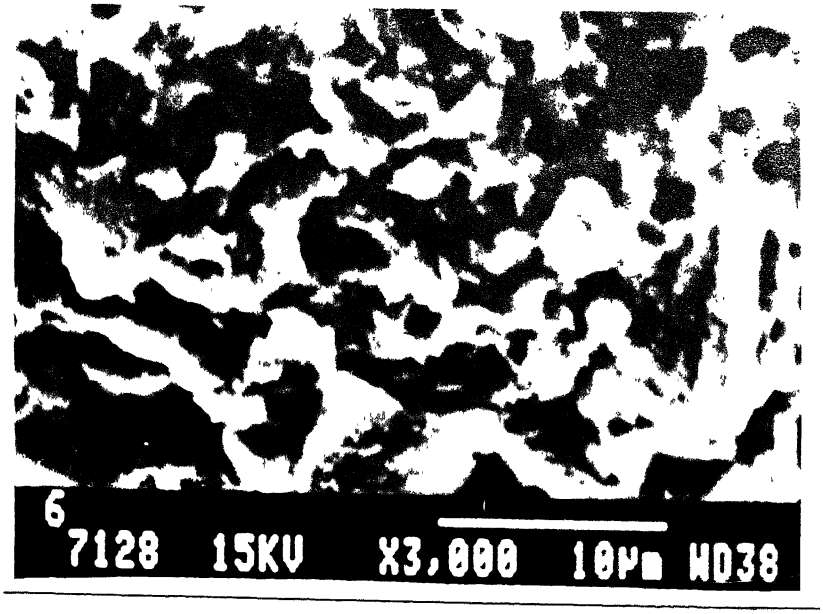

Plate 4.10: Micrograph of same Saline Soil Sample at Different Locations on the specimen

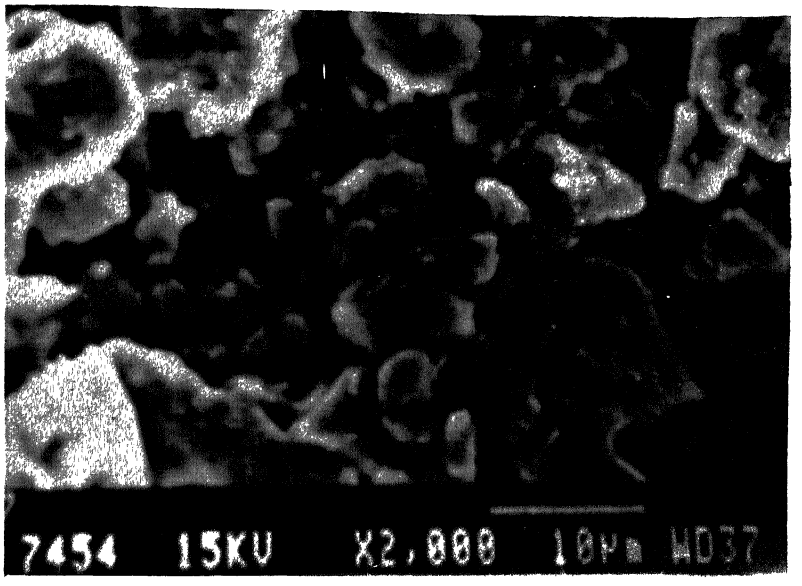

Plate 4.11: Micrograph of a Normal Soil Sample

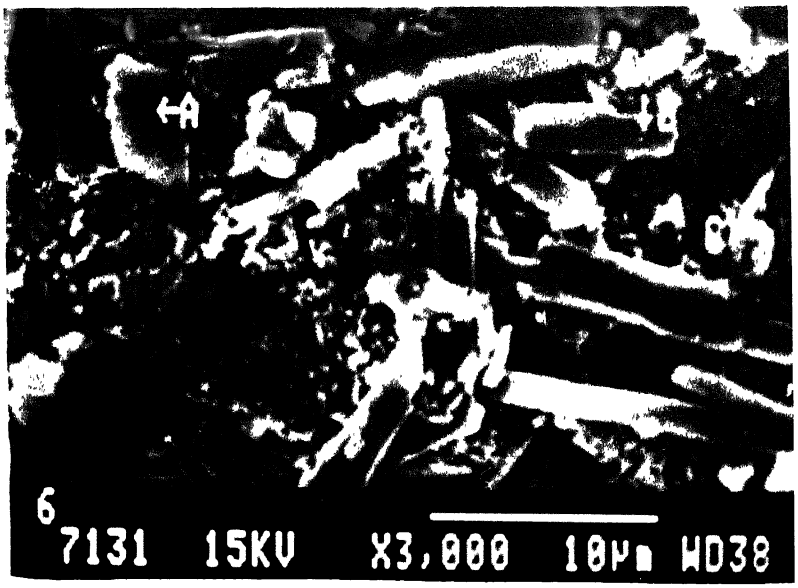

Plate 4.12: Micrograph showing Various regions on a Saline Soil Sample

really true as we know from other studies.

Comparative analysis of saline samples and normal soil samples is presented in Table 4.3. This also includes analysis of the specimen on particular positions marked in Plate 4.12.

Table 4.3: Typical Elemental Compositions of Soil Samples.
(Number corresponding to each element are weight percent.)

Element	Normal Soil	Saline Soil	Mark A	Mark B	Mark C
Na	9.16	40.63	7.90	70.48	15.02
K	13.21	32.95	2.63	19.07	32.98
Al	7.59	3.02	5.20	1.00	14.52
Ca	9.22	3.4	26.56	2.56	0.00
Fe	20.67	10.47	11.94	6.89	9.94
Si	40.15	9.53	20.26	0.00	27.39

4.8 X-ray Analysis

A given substance always produces a characteristic diffraction pattern, whether that substance is present in the free state or as one constituent of a mixture of substance. This fact is the basis of X-ray diffraction method. Chemical Analysis of sample shows only the presence of elements while the particular advantage of diffraction analysis is that it discloses the presence of a substance as that substance actually exists in the sample. Diffraction analysis is therefore useful whenever it is necessary to know the state of chemical combinations of the elements involved or the particular phases in which they are present. In the present study, mineralogical analysis is carried out to know the mineralogical composition using the powdered X-ray diffraction technique. The identification of different minerals present in the soil samples by this technique is done on the basis of their characteristics diffraction peaks

from interplanar spacings (d values) corresponding to particular 2θ angles for CuK∝ radiations. Thus the abundance of various mineral present in the soil is noted by seeing the intensity of peaks.

4.8.1 Principle

X-ray diffraction pattern analysis is based on Bragg's diffraction law, which is an essential condition for diffraction to take place. It is expressed as

$$2d \sin \theta = n\lambda \qquad (4.5)$$

where

d = spacing between crystal lattice planes,

θ = diffraction angle,

λ = wavelength of radiation used, and

n = order of reflection, its value is limited by the condition that sin θ should not exceed unity.

4.8.2 Experiment

X-ray diffraction analysis is carried out on General Electric unit of RICH SEIFERT (Model M2 111) using copper Kα (CuKα) radiation. For this, soil samples are powdered finely and placed in an experimental dish. The sample is mounted on the unit and allowed to rotate with constant speed. X-ray pattern between 2θ vs intensity are obtained for range of 2θ between 10° to 60°. Various intensity peaks can be identified using ASTM crystallographic standard cards for appropriate presence of materials. But this requires relation between d and intensity peaks. To obtain d for different θ, keeping λ and n constant, a computer program is written to

tabulate d Vs 2θ using Bragg's law.

This analysis is of approximate nature only because there is lot of scope for errors. These may be due either to errors in diffraction pattern of unknown constituents or to error in the standard card file itself.

4.8.3 Results and Discussions

Reflectance of the soil due to their mineralogical assemblages depend on the dispersion of these minerals and their relative abundance in the soils. The effect on the reflectance properties of a soil due to mineralogical compositions are determined largely by the integrated contribution from each surface grain. The reflectance properties of the soil obtained in the present investigations are dictated only by the surface soil conditions in the considered wavelength range, and do not depend on the depth parameters as such.

The normal soil in the region shows relative abundance of minerals like quartz, feldspar, Kaolinite, orthoclase and muscovite. The extent of their presence in different samples of normal soils is not same but this has given an idea about the general presence of different minerals in the normal soil of the area. The results are similar to the one obtained by Sirohi A. (1993) in the nearby areas.

The salt present in the saline zones shows relative abundance of carbonates, chlorides and silicates of sodium, calcium, and potassium etc. in different phases and with different relative magnitude. The samples from highly saline zones shows very high presence of these minerals and very small quantity of normal soil samples.

The objective of the test is to know the mineralogical composition qualitatively only and not quantitatively in any case and to report it so that when ground truth information is referenced in future works, one should also consider the

particular mineralogical compositions of the area. Effect of mineralogical compositions on the spectral response of soil is usually correlated in the infrared region (0.8 -1.5 μm) of the spectrum (Goetz et.al. 1985). In the present investigations, almost all the factors related to mineralogical compositions are changing hence it is not possible to study this particular aspect in detail.

4.9 Multiband Ground Truth Radiometer Analysis (MGTR)

The knowledge of spectral reflectance behavior of various feature is important in the development of remote sensing technology, and in the analysis and interpretation of remote sensing data. It becomes more important in case of small features because of limiting resolution capacity of common satellite sensors. Spectral response of a feature varies significantly with wavelengths. Thus for application of satellite remote sensing to the study of minute details, ground truth information helps greatly. In the present study, MGTR has been used to measure reflectance of soil at different locations and with different degree of salinity, in the prevailing field conditions.

4.9.1 Description of MGTR

Multiband Ground Truth Radiometer, commonly called MGTR, of model 041, is used in the present work, for measuring the satellite simulated in-situ spectral reflectance data of various objects. It is manufactured by Optomech Engineers Pvt. Ltd., Balanagar, Hyderabad in the technical collaboration with Space Application Center, ISRO, Ahmedabad. It is a rugged, portable and battery operated field instrument with flexibility in selecting/interchanging the spectral band in the visible and near infrared region. MGTR measure the reflected radiation in a series of discrete

spectral bands rather than over a continuous spectral range. It has got 11 spectral bands in the wavelength range from 0.45 μm to 0.9 μm, out of which first four (1 to 4) are compatible with Landsat-TM, next four (5 to 8) are compatible with IRS (Indian Remote Sensing Satellite), and next three (9 to 11) are compatible with SPOT. The specifications of MGTR and details of various filters supplied with MGTR are given in Table 4.4 and 4.5.

The optical head and digital display panel are the two sub-systems of the instrument. The optical head receives the incident radiations and its field of view is 15° ± 2°. The output corresponding to the input radiation level at the selected spectral band is observed on the $3\frac{1}{2}$ digit display panel unit. This output is in the units of W cm^{-2} -Sr^{-1} -μm^{-1} when it is multiplied, by a decade factor indicated on the Range Select Control. Range of the output recorded by the digital panel meter is from 0.01 x 10^{-5} W cm^{-2}-Sr^{-1}-μm^{-1} to 19.99 x 10^{-2} W $cm^{-2}Sr^{-1}$-μm^{-1}. The power supply to the optical head

Table 4.4: Specifications of MGTR*

1	Field of view	15° ±2°
2	Spectral band	11 bands in the range 400 to 900 nm
3	Output	On $3\frac{1}{2}$ digit digital panel meter, Measurements are in radiometric units of W/cm^2 - Sr - μm
4	Dynamic range	0.1 X 10^{-6} to 30 X 10^{-3} W/cm^2 - Sr - μm
5	Initial Stabilization	5 minutes
6	Absolute accuracy	± 5%
7	Total weight	3.4 kg
8	Ambient temperature	5° to 45° C
9	Humidity	30% to 90% RH at 40° C

Table 4.5: Details of filter supplied with MGTR*

MGTR Bands	Satellite	Central Wavelength	Band width	Range
1	Landsat TM	0.485	0.07	0.45 - 0.52
2	Landsat TM	0.560	0.08	0.52 - 0.60
3	Landsat TM	0.660	0.06	0.63 - 0.69
4	Landsat TM	0.830	0.14	0.76 - 0.90
5	IRS	0.485	0.07	0.45 - 0.52
6	IRS	0.555	0.07	0.52- 0.59
7	IRS	0.650	0.06	0.62 -0.68
8	IRS	0.815	0.09	0.77 - 0.86
9	SPOT	0.545	0.09	0.50 - 0.59
10	SPOT	0.645	0.07	0.61 - 0.68
11	SPOT	0.840	0.10	0.79 - 0.89

*Source: Instruction manual of Multiband Ground Truth Radiometer, Model 041 (1991), (Wavelength in μm)

is ± 18V at ± 5 mA under dark condition, and 9 V at 300 mA to the digital display unit. This instrument can work under ambient temperature from 5° C to 45° C and at relative humidity from 30% to 90% at 40° C (non-condensing).

4.9.2 Acquisition of Reflectance Data

The spectral reflectance measurement using a radiometer consists of a three-step process. First, the instrument is aimed at $BaSO_4$ plate of known stable reflectance. This is done to quantify the incoming radiation incident upon the measurement site. Next, the instrument is sighted at the target of interest and the radiation from the object is measured. Finally, the spectral reflectance of the object is

computed as follows:

$$\text{Reflectance } (\%) = \frac{\textit{Radiance from the object}}{\textit{Radiance from } BaSO4 \text{ plate}} X\ 100 \qquad (4.6)$$

Specially prepared barium sulfate powder and paints are used as standards for reflectance measured by radiometers (Duggin, 1985; and Slater, 1985). These materials are satisfactory for use in the wavelength range 0.20 - 2.00 μm. The absolute value of luminous reflectance of $BaSO_4$ powder is 0.995 ± 0.001, and that of the paint, when properly applied is 0.992 ± 0.001 (Grum and Luckey, 1968). The MGTR is calibrated with the uniformly coated barium sulfate plate is taken as 100% reflected radiation (for all purposes), and thus, quantifying the incoming radiation incident upon measurement site. Plate 4.13 shows MGTR and $BaSO_4$ calibration plate in the study area. This calibration plate is considered as an ideal and perfectly diffuse (Lambertian) surface. The secondary reflections falling on the measurement area, from the nearby objects have a profound effect on the spectral reflectance data of the area (Duggin, 1980; and Kimes et al ., 1983).

The readings have been taken within 5 minutes for a particular band as Sun angle changes by 1° in each 5 minute. The reflectance (to be more precise, reflectance factor) of the desired target at a particular wavelength is then calculated by the above mentioned procedure. In order to minimize the error in the measurement, we have taken following precautions:

1. The measurements have not been taken when Sun was directly above, to avoid the shadow of the radiometer, and
2. The measurements have not been taken when Sun was obstructed by the clouds, since the irradiance conditions change very fast in such conditions. During the experimental study on the field, It was a clear weather day and Sun angle is such as not to cause too much errors.

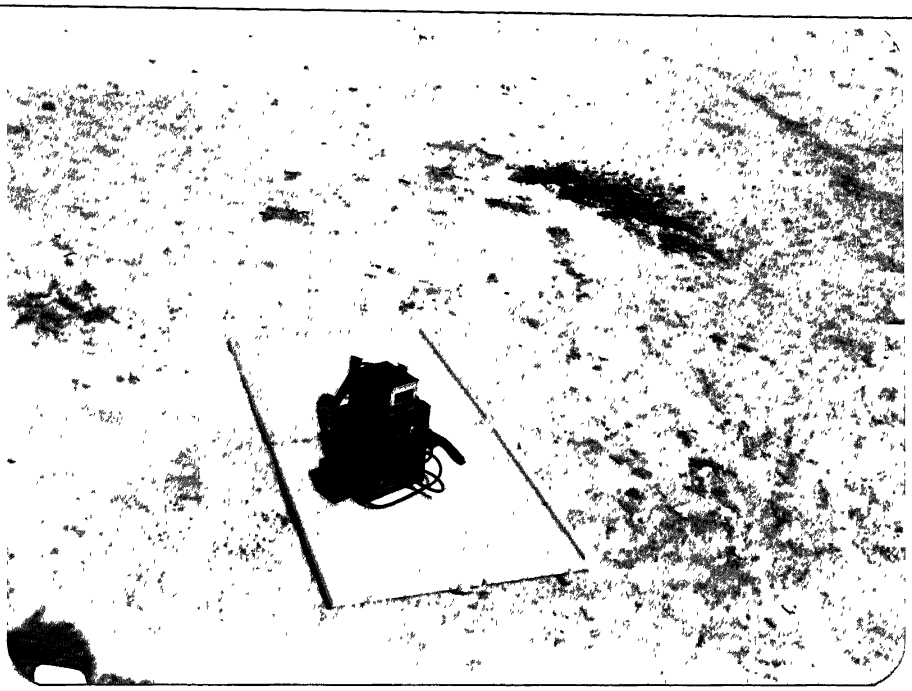

Plate 4.13: MGTR and $BaSO_4$ calibration plate in the field.

4.9.3 Results and Discussion

The Earth's surface is covered by the various types of soil. Soil in a region may be different due to effect of various factors and hence response of soil is not always same. Remote sensing has been widely used for mapping and classification of the soils on the basis of their diagnostic properties. The typical response of soil in different wavelength ranges is characteristic of various constituents present in it.

Spectral reflectance measurements are carried out on all the sites using MGTR. The response of various soil covers is quiet different from one another. The reflectance values as obtained is presented in Appendix A.1. Seeing the observed response of the soil covers thoroughly, it can be very well categorized into that of normal soils, moderately affected soils and that of highly affected saline zones. A typical curve showing the spectral response of these soils is drawn in Fig. 4.5. The

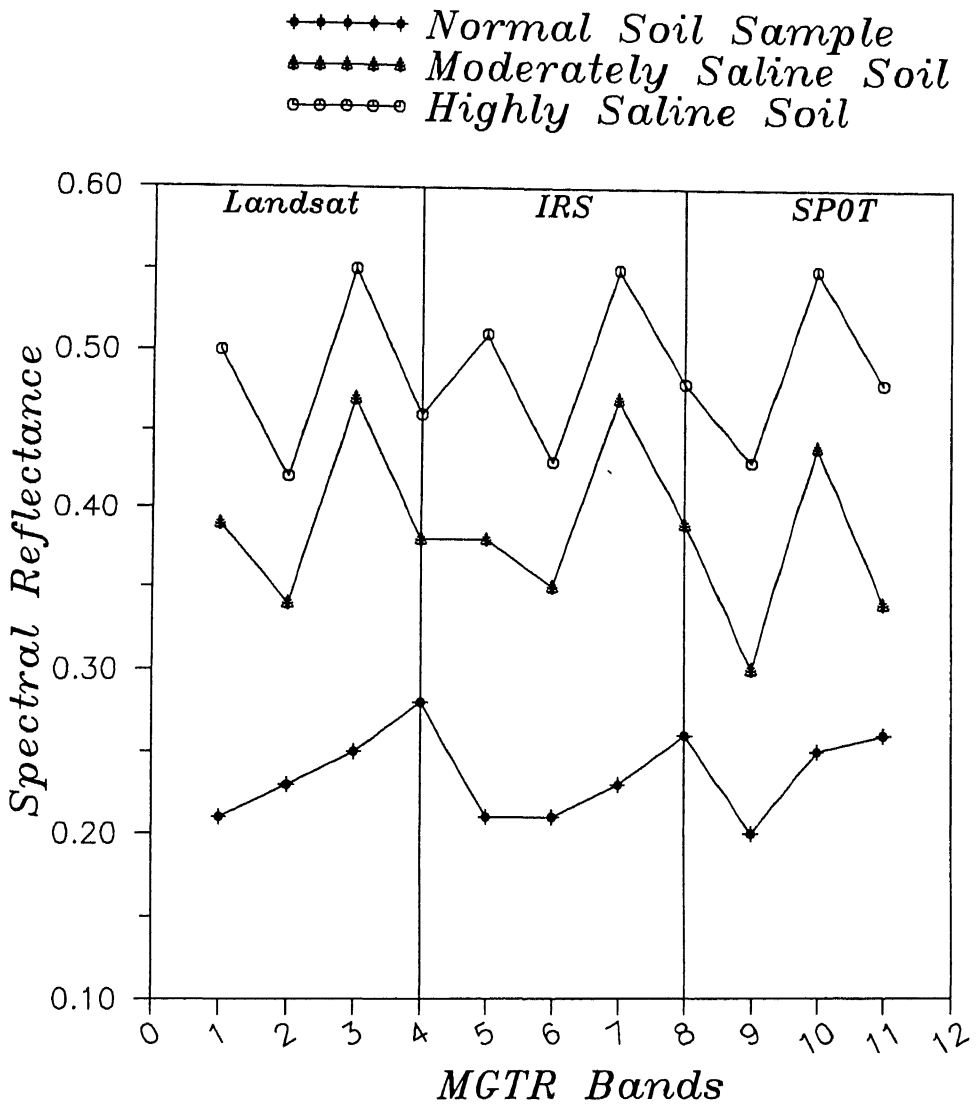

Fig. 4.5: Spectral Response of Different Soils

response of dry bare soils is as predicted and reported earlier (Jensen, 1986, Lillesand and Keifer, 1994). The response of saline soils is in accordance with the earlier work (Mougenot et.al.1993, Dwivedi and Rao,1991). The saline soil has a higher reflectance in the blue and red band and significantly low values in the green and near infrared band.

It has been earlier discussed that the spectral response of green vegetation is low in ~~blue~~ red wavelength and becomes higher in near infrared band. Response of dry soil follows a continuous positive trend in the visible to near infrared wavelengths. The spectral response of saline areas makes it easy to distinguish it from other uses of soil cover. In an agricultural area, band 3 and band 4 can be effectively used to discriminate between a green land and that of a barren land due to salinity. Keeping this in mind and that the area under study mainly comprises of agricultural lands, band 3 is considered best for the delineation of saline zones. The high spectral response of saline zones make it easy to demarcate and distinguish the barren land due to salinity and other effects.

CHAPTER 5

DIGITAL ENHANCEMENT OF SALINE ZONES

5.1 INTRODUCTION

A digital image is comprised of large number of individual picture elements, called pixels. Each one of it has an intensity value and an address in the two dimensional image space. Multispectral scanning makes use of different spectral bands of electromagnetic spectrum to record spectral response of various features. This helps in discriminating various objects and to determine the physical conditions of the objects based on the magnitude of reflectance in each band.

Remotely sensed image consists of a wealth of information. Due to various atmospheric effects, sometimes, the contrast of the image is not conductive for effective retrieval of information present. Digital image processing provides ample of scope to enhance the images to a particular level, where delineation of objects of interest becomes easier. In this chapter, several standard image processing operations are being utilized to get a set of enhanced images which may offer much better scope of delineating saline zones than raw multispectral imagery.

Two new indices namely salinity index (SI) and Normalized difference salinity index (NDSI) are proposed in the present study based on spectral behavior of saline soil, which may have great potential in the identification of saline zones in the soil. Several computer programs are written to analyze and perform various operations on the data. Help of standard image processing and GIS software packages like IDRISI and ILWIS is taken on several stages of the study.

5.2 DATA USED

From the Indian remote sensing satellite reference map, path and row

number of the study area are obtained as 26 and 49 respectively. IRS-1B LISS II A satellite data is chosen for the present study. To observe and monitor changes in the extent of saline zones and vegetation, digital data of two periods namely, November, 1992 and April, 1993 is obtained. These particular months are chosen because of their being best periods for studying soil salinity as concluded in earlier studies.

IRS-1B is a sun synchronous satellite having its orbital altitude about 904 km above Earth surface with equatorial crossing time at 10:08 AM. The sensor payload system consists of two pushbroom cameras (LISS II) of 36.25 m resolution and one camera (LISS I) of 72.5 m resolution. Each camera system images in four spectral bands in the visible and near infrared region (0.45 - 0.86 μm). The ground swath for the image obtained by the LISS I camera is 148.48 km whereas the LISS II cameras image adjacent swaths of 74.24 km width each, with an overlap of 1.5 km across track. The reflected energy sensed for each pixel by the detector is quantified into 128 grey levels.

Digital image is supplied on two floppies containing records of ground reflectance values sensed in four bands. It has 2048 bytes of header information followed by 512 X 512 bytes for each band in band interleaved by lines (BIL) format. Data storage in the BIL format is as follows: first 512 bytes corresponds to first line of 512 pixels of band 1, Next 512 bytes corresponds to first line of 512 pixels of second band, and so forth for band 3 and band 4. From fifth 512 bytes, this cycle is repeated in the same order. So, the whole data corresponding to four bands each having 512 X 512 bytes is stored. First and foremost task is to separate out data of all the bands in separate files. In order to retrieve maximum information about saline zones, a set of image processing operations have been used. They are being elaborated below.

5.3 DIGITAL SMOOTHING

Spatial frequency of remotely sensed digital image is defined as the number of changes in the grey levels per unit distance for any particular part of the image. Methods for selectively emphasizing or suppressing information at different spatial scales contained in image data is called spatial filtering. These techniques require that the image data be altered in a particular manner. The filters applied in the present work are: Moving average and Median filter.

In this operation, image smoothing operations are required so as to eradicate noisy pixels. These pixels having high grey levels similar to saline patches may cause misinterpretation. At the same time, the care has to be taken to preserve the boundaries of saline patches. More precisely, the aim of digital filtering here is to eradicate spurious noise and preserve edges.

5.3.1 Moving Average Filter

This technique of filtering de-emphasizes the high spatial frequency detail and allows low frequency information to dominate. This simple smoothing operation, however blurs the image, especially at the edges of the objects (Gonzalez and Wintz, 1977). It is excellent for random noise removal say due to backgrounds. A typical kernel used for this type of filtering is

$$1/9 \begin{vmatrix} 1 & 1 & 1 \\ 1 & 1 & 1 \\ 1 & 1 & 1 \end{vmatrix}$$

5.3.2 Median Filter

This is an advanced smoothing filter which utilizes the median value of

the neighborhood rather than the mean of the window. It is a nonlinear signal processing technique which has received attention lately due to its edge preserving nature. It is much less sensitive to errors or to extreme data values compared to a moving filter, thus it is superior to it. Within the chosen window, it search for median values of the included pixels and assigns it to the central pixel. The output image, thus received, is smoother than the original one.

5.4 CONTRAST STRETCHING

For any particular area being imaged, it is unlikely that the full dynamic range of the sensor is used. Reasons for this are many including sensitivity of the detectors. The corresponding image is dull and lacking in contrast. It is very difficult to identify details on an underexposed image. Contrast stretching is used to brighten up a dark image to make it more interpretable while maintaining the relative distribution of gray levels. Contrast stretching is based on the histogram of the original image. The following two approaches have been used in the present work:

5.4.1 Linear Stretching

This contrast stretching technique involves mapping of the pixel grey level values (GL) from observed range GL_{min} to GL_{max} to the full range of the display device, generally 0-255 on a 8-bit display device (Jensen, 1986). The overall effect of this simple technique is to brighten up an image which is underexposed (too dark) or to darken an otherwise overbright image. It does not take into consideration any character of the image data other than the maximum and minimum pixel values (Lillesand and Keifer, 1994). Graphically, it can be represented as shown in Fig. 5.1. This figure shows how the values of an underexposed image are stretched to the full

scale of the output device using a linear transfer function. Mathematically, the output brightness value are computed according to Equation 5.1 given below.

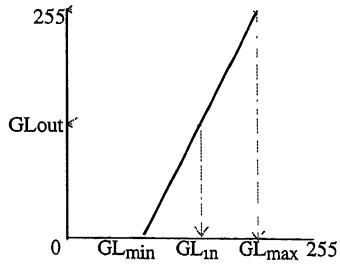

Figure 5.1 A linear transformation function (Jensen, 1986)

$$GL_{out} = \frac{GLin - GL\min}{GL\max - GL\min} X\ GLr \qquad (5.1)$$

where

GLin = grey level value of input pixel,

GLout = grey level value of corresponding output pixel,

GLmin = minimum grey level value in the image,

GLmax = maximum grey level value in the image, and

GLr = range of grey level values (256 in the present case)

5.4.2 Histogram Equalization

In this approach, display levels are assigned grey level values on the basis of their frequency of occurrence. After having the histogram of the image, number of output grey classes to redistribute the data set are assigned. Program then assigns an approximately equal number of pixels to each of the classes. Histogram equalization applies the greatest contrast enhancement to the most populated range of grey level values in the image (Mather,1986). It automatically reduces the contrast in

the very light or dark parts of the image associated with the tails of a normally distributed histogram. A typical histogram equalization process can be understood from the Fig. 5.2 (Jensen,1986). The transfer function corresponding to this tries to equalize the number of pixels in each group. But, if there are many pixels in a single group, it

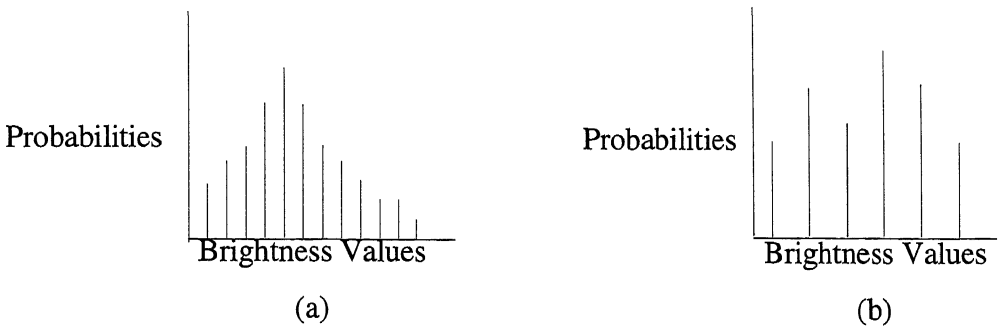

Figure 5.2: Histogram showing the probabilities for brightness value ranges (a) original (b) after histogram equalization

can not differentiate between these pixels and keep them in a single group. Therefore even after histogram equalization, each group do not have equal number of pixels as evidently clear from the figure.

5.5 ARITHMETIC OPERATIONS

Information extraction and identification of various features in a multispectral digital data can be made easier by applying certain arithmetic operations on it. It is commonly realized to use more than one band at a times to enhance understanding of the various features of the Earth cover. Some of these operations are addition, subtraction, multiplication and division. These operations are applied on pixel by pixel basis. Operations like subtraction and divisions are found to be of particular help in the present study. These are presented in the following paragraphs.

5.5.1 Image Subtraction

Image subtraction is often used to reveal differences which have come during the two periods of imaging. Spectral response of surface features is generally different in different bands as observed in the digital data. Considering this fact, It can be also applied to data of different bands to enhance the contrast between several features. This way, generally, information extraction about features of interest can be increased.

The response of salt patches and saline zones is generally higher in band 3 and significantly lower in band 4 while that of vegetation and other related objects is higher in band 4 and lower in band 3. In this study, it has been tried to enhance the saline land features by subtracting images of two bands namely, red and near infrared of the same area. Image differencing is performed on pixel by pixel basis. The resulting image tends to have a histogram that is normal in shape. This procedure assists in the interpretation and understanding of an image in a better way. The mathematical expression is given as

$$GL_{i,j,r} = GL_{i,j,l} - GL_{i,j,k} \quad (5.2)$$

where

$GL_{i,j,r}$ = resultant digital number at position i,j,

$GL_{i,j,l}$ = digital number at position i,j in band l, and

$GL_{i,j,k}$ = digital number at position i,j in band k

5.5.2 Image Ratioing

Spectral response of Similar surface materials can vary due to the effect of topographic conditions, shadows, or seasonal changes in sunlight illumination angle and intensity. Image division, also called ratio transformation, of the remotely sensed

data can, in certain instances, be applied to reduce the effects of such environmental conditions. It may also provide unique transformation, not available in any single band. The process of dividing the pixels in one image by corresponding pixels in a second image is known as band ratioing (Lllesand and Keifer, 1994).

Ratioing of two bands data enhances several features while suppresses some other features depending on the nature of the spectral reflectance curve of various features. A major advantage of the ratioed image is that it convey the spectral or color characteristics of image features, regardless of variations in scene illumination conditions. A ratioed image of scene effectively compensates for the grey level change caused by the varying topography and emphasizes the color content of the data (Mather 1982, Lillesand and keifer,1994). These clearly portray the variation in the slopes of spectral reflectance curve between two bands involved. The mathematical expression for the simple ratio is given as,

$$GL_{i,j,r} = GL_{i,j,l} / GL_{i,j,k} \quad (5.3)$$

where symbols have usual meanings as discussed above.

Another most common operation, and even better in most of the cases, is normalized ratio. This is given as,

$$GL_{i,j,r} = \frac{GL_{i,j,l} - GL_{i,j,k}}{GL_{i,j,l} + GL_{i,j,k}} \quad (5.4)$$

To enhance the salinity feature in the image, two new indices namely, Salinity Index (SI) and Normalized Difference Salinity Index (NDSI), are tried in the present study. Salinity Index is the ratio of red band to near infrared band (eq. 5.3) while NDSI is the Ratio of the difference of the red to NIR and ~~divided by the~~

summation of the same two (eq. 5.4). These are found particularly useful in the identification of the salinity zones on the displayed image. Here SI is found to be superior in discriminating the saline zones. The red to NIR ratio is typically very high in case of highly saline zones. NDSI has positive values for saline patches, high for highly saline and a low but, positive, for mildly affected patches. While in cases of vegetation, whether healthy and green to senescent, it is negative.

5.6 PRINCIPAL COMPONENT ANALYSIS

There is normally a high correlation between various spectral bands associated with a multispectral image scene. Adjacent bands in a multispectral remotely sensed image are generally correlated (Jensen, 1986). Principal component analysis (PCA) tries to maximize the variance and minimize the correlation. It is designed to remove such high correlations among original band set. It creates new images, each of which is achieved by adding different proportions of the input bands. A new pair of axes are defined by rotating original axes such that principal component one is along the direction of maximum variance of dataset (Kennie and Matthews,1985). The transformations of raw remote sensing data using PCA can result in new principal component images that are often more interpretable than the original data. It also helps in reducing data dimensionality i.e. the number of bands in the dataset that must be analyzed to produce usable results (Jensen,1986).

The application of the transformation to the correlated remote sensor data will result in an uncorrelated multispectral data set that has certain ordered variance properties. This can be better understood from Fig. 5.3 which shows a two dimensional distribution of pixel values for two bands. The spread or variance of the distribution of points is an indication of the correlation and quality of information associated with both bands. principal components on this scatter plot is obtained by

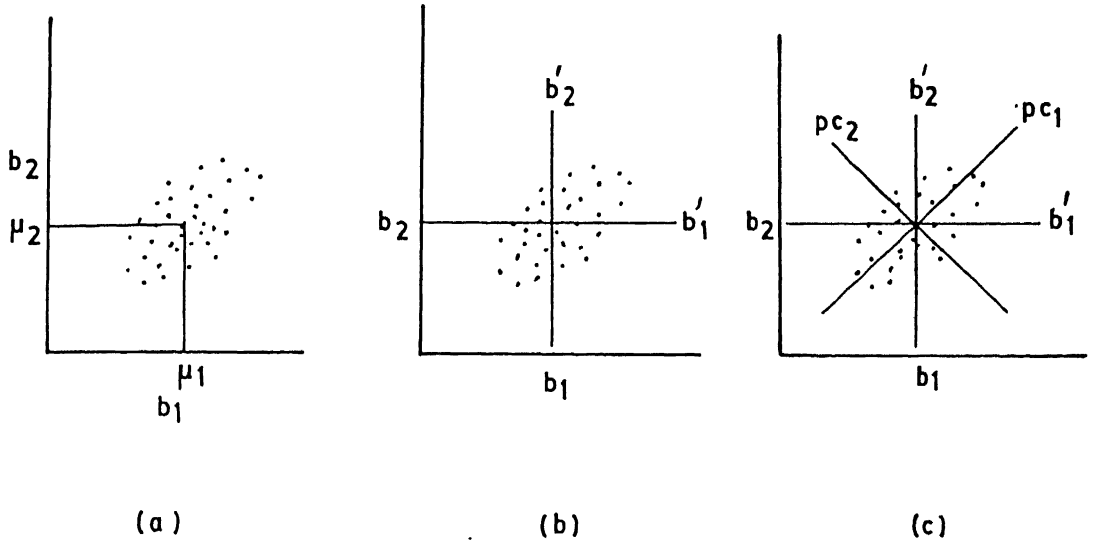

Fig. 5.3 Graphical illustration of data transformation using principal component analysis;
(a) Scatter plot of Band 1 and 2; (b) Linear translation of the origin and axes; (c) Rotation of axes to map the data in the direction of maximum variance.

Table 5.1: Percentage Information Content in Various Principal Components

Principal Component \ Period	April	November
1	88.48	74.49
2	8.02	22.31
3	3.02	2.60
4	0.48	0.60

transforming the axes along the maximum variance direction and thus along the principal components. It is obtained based on mean and standard deviation, variance and covariance matrix, correlation matrix of the dataset. Eigen values and eigen vectors are calculated. Table 5.1 gives the percentage information content in various principal components.

Multiband visible / near infrared images of the vegetated areas show negative correlations between the near infrared and visible red bands and positive correlations among the visible bands because the spectral characteristics of vegetation are such that as the vigor or greenness of vegetation increases the red reflectance diminishes and NIR reflectance increases (Dwivedi and Rao, 1992) Mather 1987)

The character of the saline soil is such that as salt increases, red reflectance increases while NIR reflectance decreases. Soil moisture show a reverse trend with wavelength.

5.7 COLOR COMPOSITE

Optimum index factor (OIF), which is indicative of the information (variance) content of the data, can be applied to evaluate the usefulness of different band combinations. The OIF value (Chavez et. al. 1982) is based on the variance and the correlation among the different bands. It weighs the variance of the individual bands by using their standard deviations and the correlation between the bands by their correlation coefficients. The OIF is computed for each of the band combination by dividing the sum of the standard deviations of each of three band components by the sum of the absolute value of the correlation coefficients computed for the same three bands taken two at a time. Expression is given as

$$OIF = \sum_{j=1 \text{ to } 3} Sd_i \; / \sum_{j=1 \text{ to } 3} |CC_j| \qquad (5.5)$$

where

Sd_i = Standard deviation for band i

$|CC_j|$ = Absolute value of the correlation coefficients between two of the three bands

The three band combination having the largest OIF is then selected for color composit because it should display the maximum information with the least amount of duplication. Often, three band combinations that are within two to three rankings of each other appear similar in color composite form because there is little difference in their information content.

False color composites (FCC)) can be used to read information easily knowing behavior of different features. FCC is obtained by assigning bands in a particular order. This is an important tool for visual interpretation of an area from remote sensing data. FCC incorporates responses in three band combinations. Generally the contrast of the image improves. In the present study, color composite are generated using three band combinations of original data in four bands as well as principal components obtained from original set of data. These composites are particularly helpful in differentiating the features. Even some minor features become clear in composite images.

5.8 RESULTS AND DISCUSSIONS

Remote sensing data obtained by satellite covers a large area at a time. If proper information base for the interpretation of various details on an imagery is available, one can very easily extract lot of information from the satellite data. Alongwith ground truth information, one should also be equipped with sufficient hardware and software tools to manipulate large volume of data. The raw image, as obtained from satellite, can not be interpreted to the level,one is interested in, if there is

lack of ground truth information and necessary facilities.

Red wavelength has great potential in identifying the saline zones. Highly saline zones can be easily identified on original image but to delineate moderate saline zones, one has to apply certain transformations on the original data to increase its usefulness for interpretation.

The images of the raw data, as recorded in red wavelength (band 3), are shown in Plates 5.1 to 5.2. Plates 5.1 is data of April, 1993, while plate 5.2 is of November, 1992 period. The differences in the spectral response of various features can be easily noted in these images. The original images of the area in other wavelength lack contrast and are of less use in identifying saline zones. The image of near infrared wavelength makes it very easy to identify water bodies and moist zones, but the saline patches have low response in this band. The images taken during two seasons are useful to show changes in the pattern of land cover of the study area.

The original images belonging to April period are showing some bright patches on similar positions in band 1 and 3 but in band 2 these patches are not so clear. Band 4 image is quiet different from other three bands. These bright features are of saline surfaces based on the observations of Mougenot et. al. 1993 and Rao et.al 1991.

Comparing the original images of the two periods difference in spatial extent of vegetation is clear to certain extent. April images are capable of providing more information about the presence of certain features compared to November one. Again, Having a look on the raw images, and from literature and the earlier works, it can be easily concluded that band 3 and band 4 images can be effectively used to delineate saline zones from normal soil and vegetations.

Moving average filtering of the image has effectively reduced the noise. However result of median filtering is quite superior than ~~others~~ it. The moving average

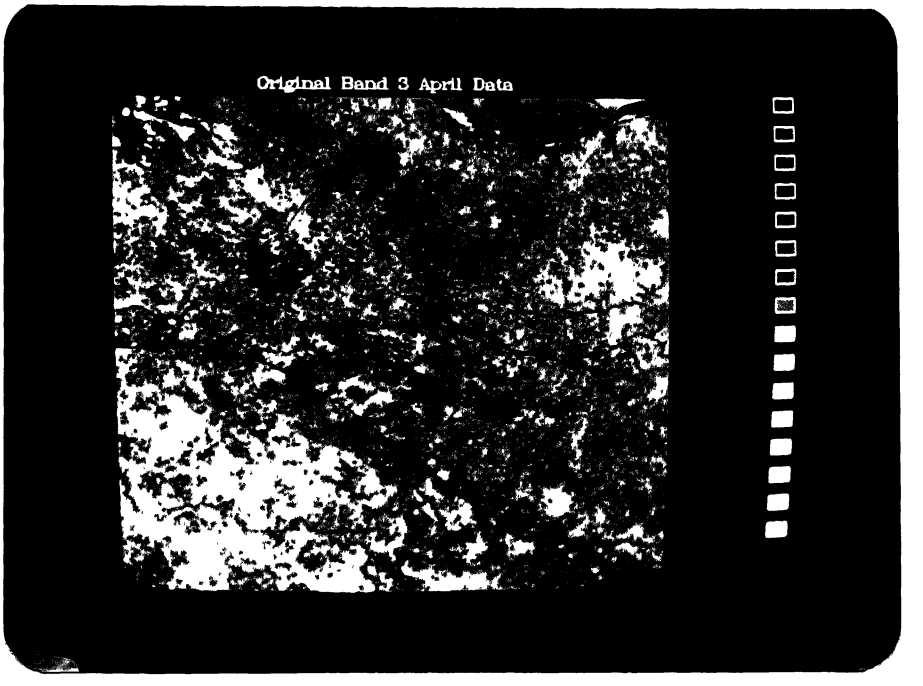

Plate 5.1: Original Red Band Imageof April period

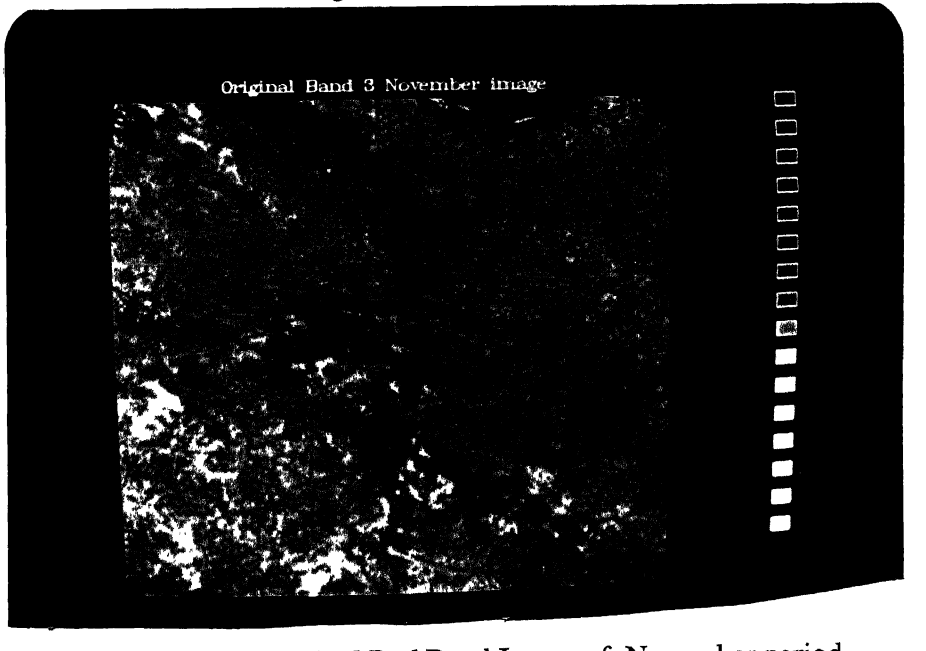

Plate 5.2: Original Red Band Image of November period

filtering has caused a general smoothing of the image and blurred the edges. Median filtered image is better in terms of noise removal and edges are preserved. The noise in the image is reduced significantly. The saline zones as well as vegetation zones are easy to distinguish in the median filtered image as can be seen in plate 5.3 and 5.4. The class variations within a group has become clear after filtering. The difference in the spread of saline zones and vegetation cover can be easily marked from the two plates. Even the order of salinity can be differentiated seeing the brightness level of these patches.

Though the range of grey level values available in IRS sensors is 0 to 127 i.e. 128 grey levels, raw images especially November one, have not utilized it fully and remain underexposed. Therefore corresponding images are dull, and have poor contrast amongst features. To increase the contrast of images, two techniques namely, linear stretching and histogram equalization stretching, is applied on the original images. The stretched image is quiet successful in providing information about some of the features.

Histogram equalized images show better contrast for some features of the images. Plate 5.5 and 5.6 show the stretched images of the band 3 using histogram equalization technique. A comparison with original images makes it clear that these are more informative.

Tonal variations in enhanced images have helped in recognizing the spatial extent of features during two periods. It can be easily seen that saline zones have less spatial extent during winter period which was as observed during field visit and informed by the local peoples. Enhancement has also helped in recognizing the probable presence of new saline zones, which was not clear in original image. In the region near Ganga river stretch and alongside lower Ganga canal, enhancement has shown a possible presence of saline zones.

The above discussed operations are performed on the data of single

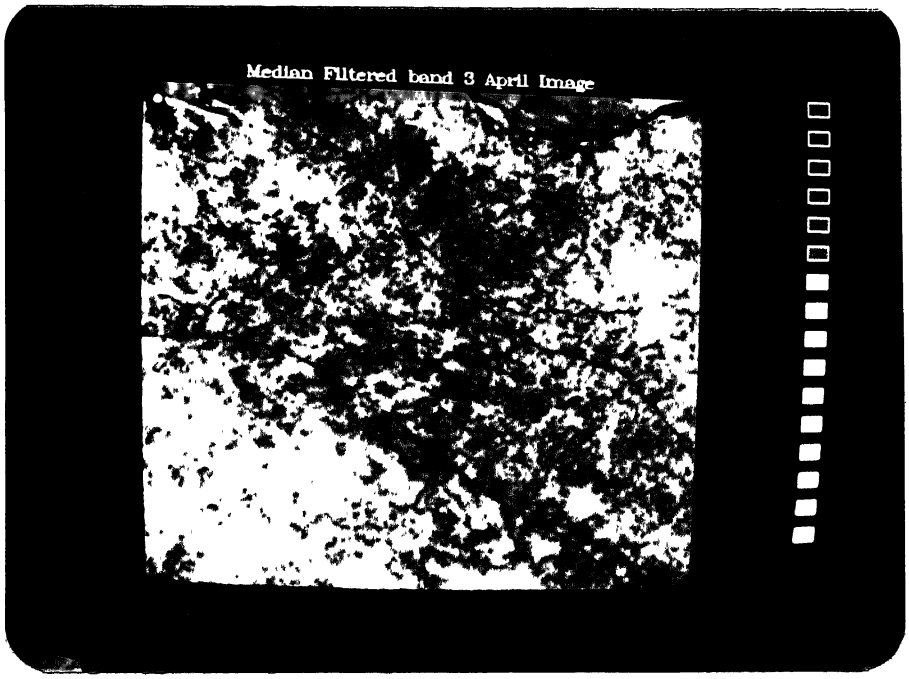

Plate 5.3: Median Filtered Red Band Image of April period

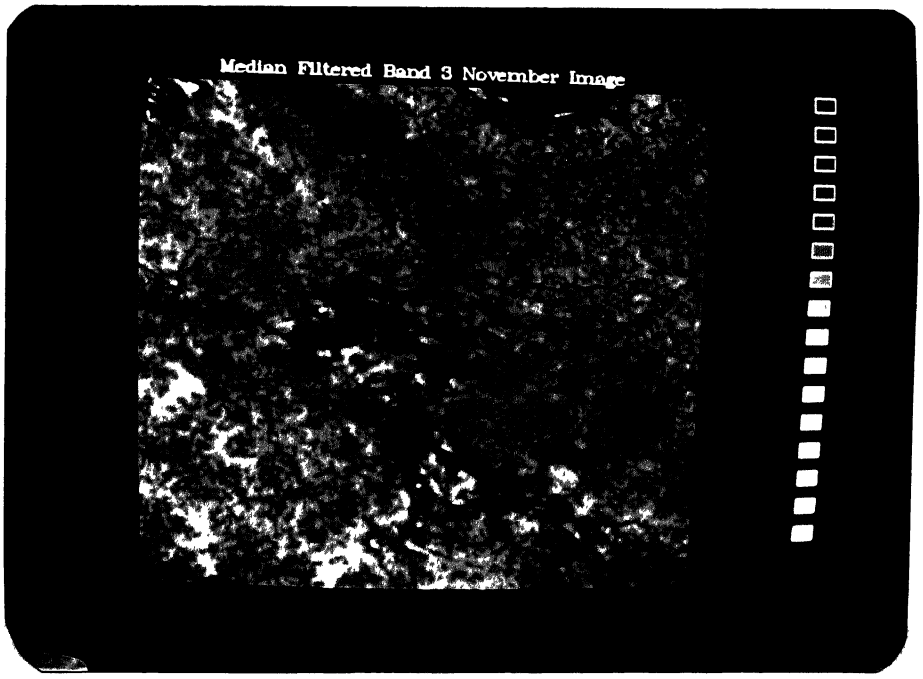

Plate 5.4: Median filtered Red Band Image of November period

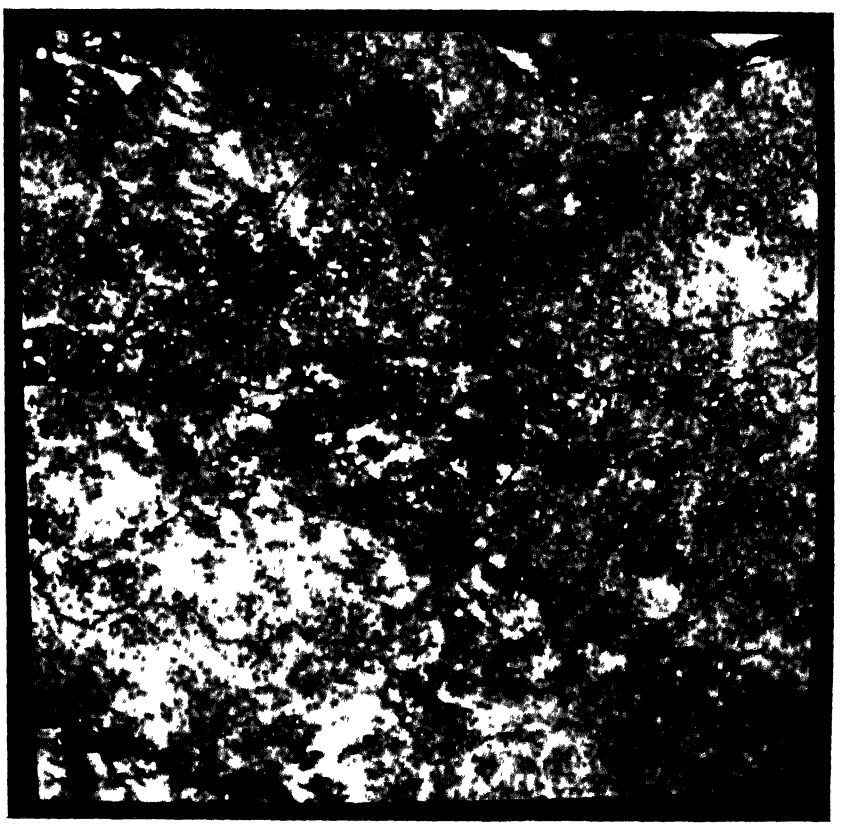

Plate 5.5: Histogram Stretched Red Band Imageof April period

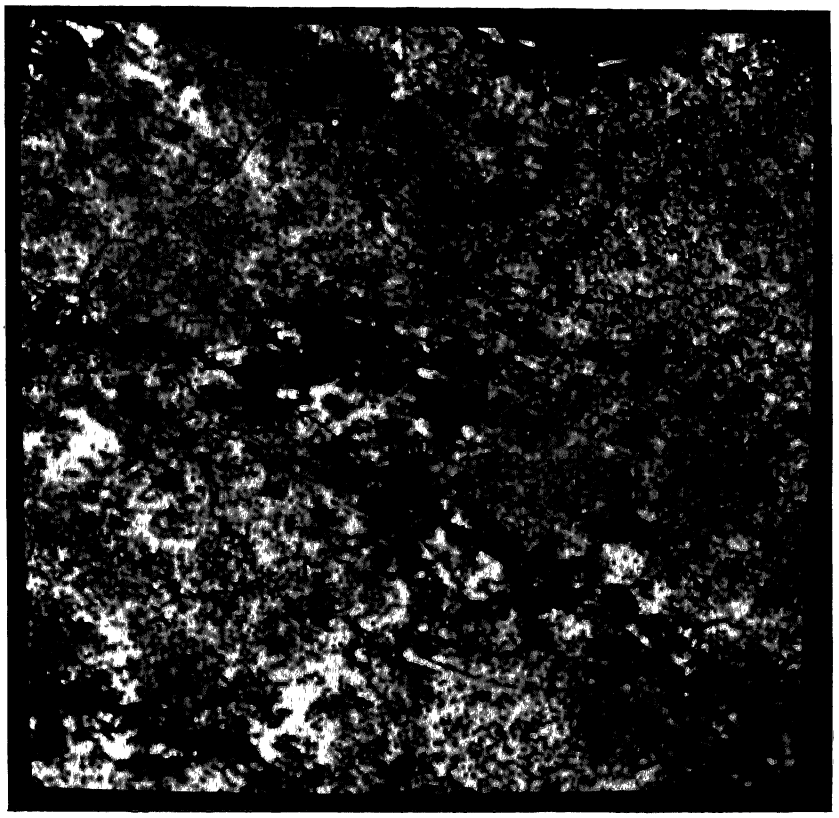

Plate 5.6: Histogram Stretched Red Band Imageof November period

bands. The multispectral remote sensing has provided an opportunity to study the response of various features in different wavelength ranges. Some transformations, like arithmetic operations, principal component analysis, and color composit image study are applied in the present study to improve the delineation of saline zones.

Various arithmetic operations, like image addition, image subtraction and image ratioing are tried in the present work. These operates at pixel levels in corresponding images. Addition of images of two bands does not produce any good result for the required information but subtraction of two images in pair, also called image differencing, either 1-2, 1-4, 3-2 or 3-4 resulted in quiet informative images. Among these, one for 3-4 produces very good results. The success of subtraction in the improvement of the readability of data is obvious because of the varying response of different feature in different bands. It was already discussed in Chapter 2 that the spectral response of dry soil, saline zones and vegetation is quiet different in different bands from visible to near infrared. The response of water bodies and thus moist soil is also different in visible and near infrared wavelengths. keeping these facts in mind the study of different features in the image has helped in describing the resultant image of subtraction.

The resultant pixel values in a subtracted image varies from positive to negative numbers. To make interpretation easier and better, and to identify boundaries of different features it is recommended to study subtracted image of reverse order also. For example, to obtain image subtraction from band 3 to band 4 and also from band 4 to band 3. Plate 5.7 and 5.8 presents band 3 - 4 images of April and November period while Plate 5.9 and 5.10 present images of band 4 - 3 of the two periods. Taking these two bands is particularly helpful because vegetation response in band 4 is highest compared to other features while in band 3, Salt and saline zones has highest response. Salt zones are enhanced and take important positions in the image when we consider image subtraction from band 3 to band 4 image. The high positive values in the output

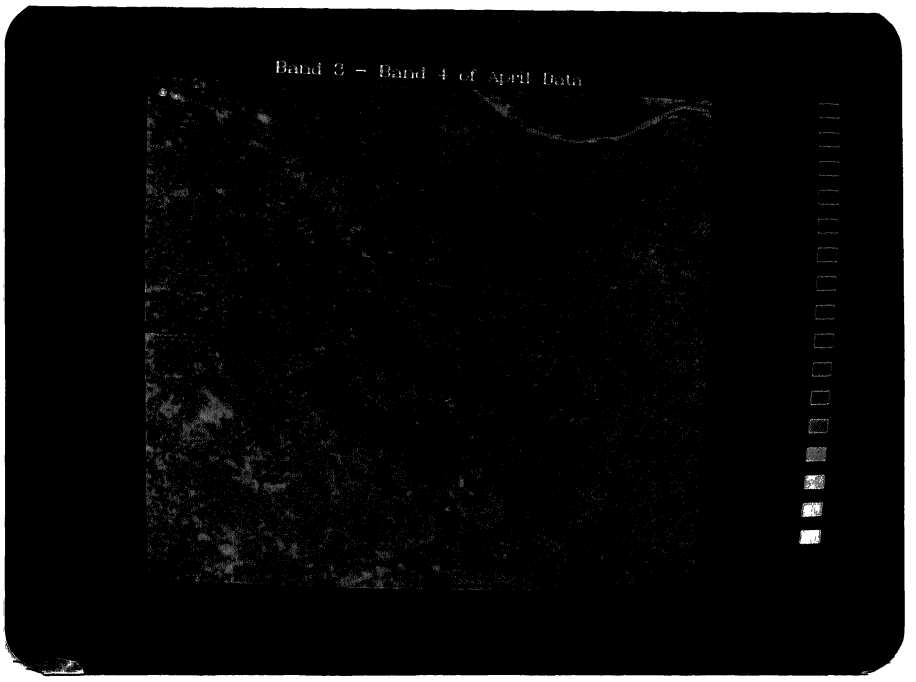

Plate 5.7: Subtracted Image (Band 3 - Band 4) of April period

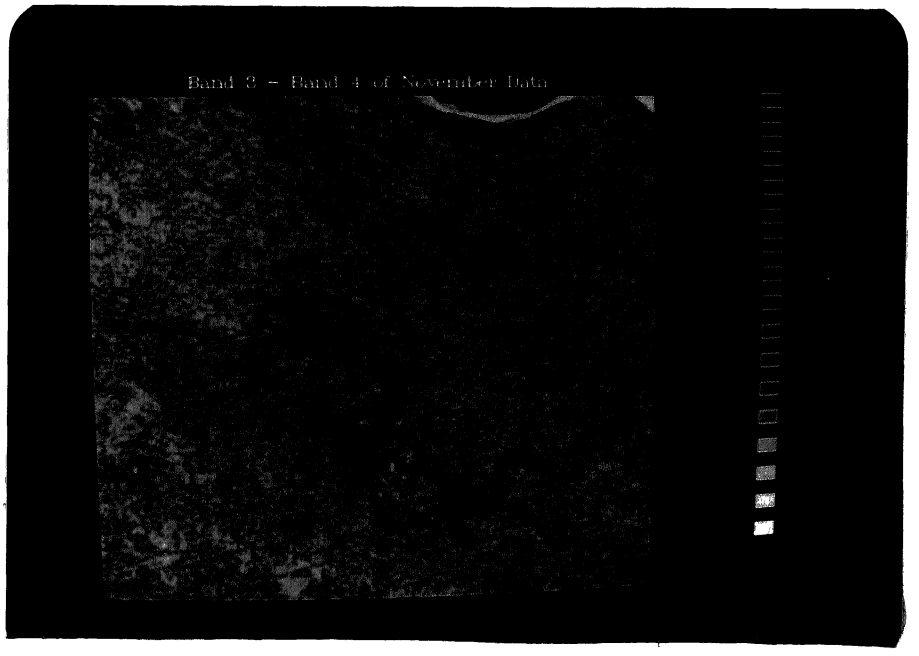

Plate 5.8: Subtracted Image (Band 3 - Band 4) of November period

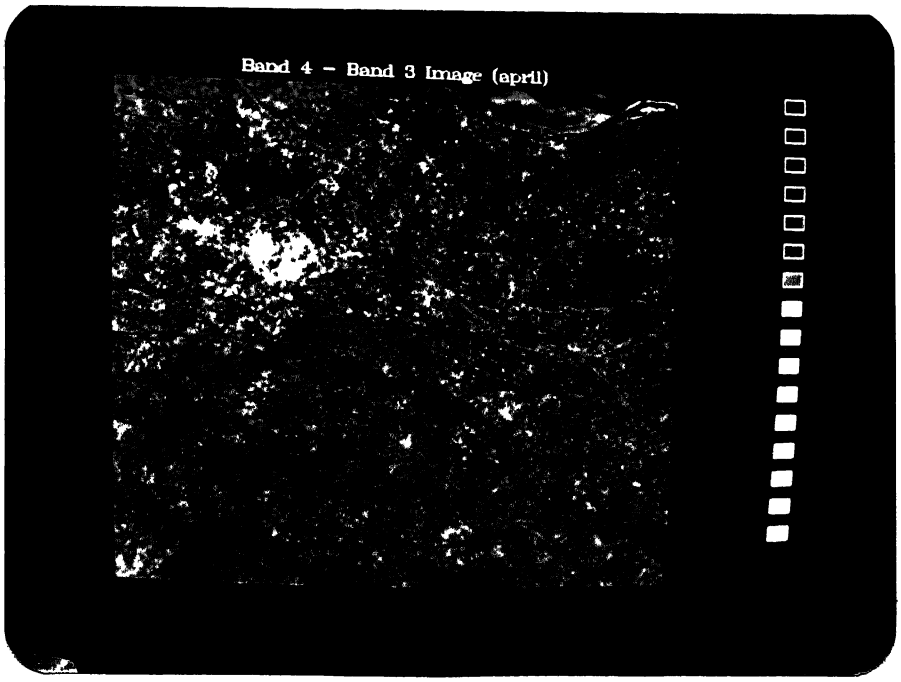

Plate 5.9: Subtracted Image (Band 4 - Band 3) of April period

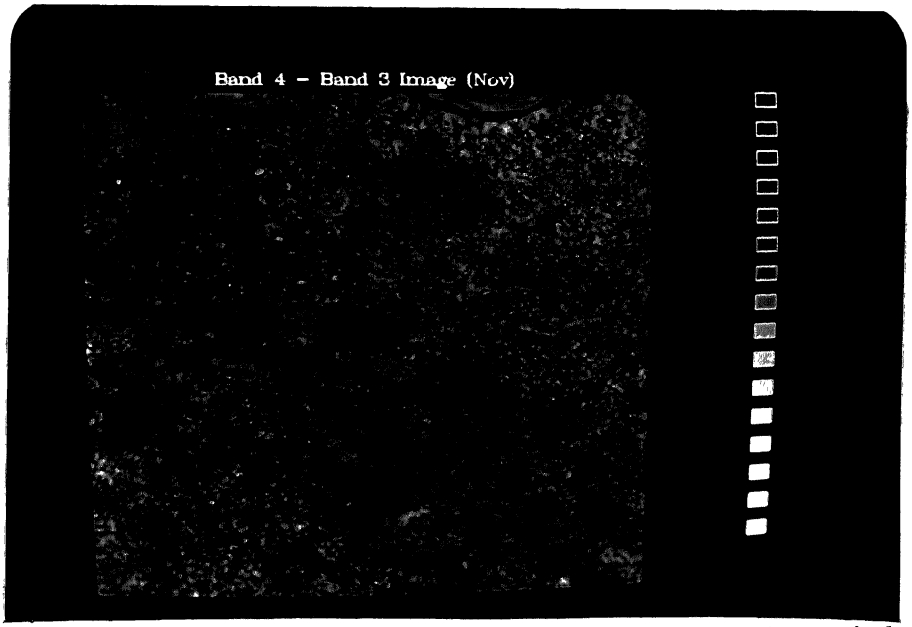

Plate 5.10: Subtracted Image (Band 4 - Band 3) of November period

indicates severely affected saline zones while high negative values are indicative of healthy green vegetation. Classifications amongst the groups can also be made by keeping track of tonal variation. Saline patches are quiet bright in a band 3-4 image and it is not easy to distinguish various levels within a class but in the reverse order i.e. band 4-3 image, though saline patches are in dark tone, it is easy to mark out different levels within these. Even tonal variations can help in identifying the extent of green vegetation.

Ratioed images are found more useful than the subtracted one. Leaf Area Index (LAI), which is ratio of band 4 to band 3, and Normalized Difference Vegetation Index (NDVI), which is ratio of band 4 - band 3 to band 4 + band 3, are very well used in the enhancement of vegetation. Here, considering the opposite behavior of ~~it~~ saline zones, new indices namely, Salinity index (SI) and Normalized difference salinity index (NDSI), defined earlier are attempted. The resultant image after applying SI operation enhances the saline zones but information about other features is lost. Plate 5.11 and 5.12 shows the SI image of two periods. Plate 5.13 presents LAI image, that is band 4 / band 3 image of April period. The difference between the two can be very easily noted as the two have enhanced features in reverse sense. The SI image clearly gives an idea about various saline zones because of high enhancement to these pixels.

The SI image of two periods, seen in default colors, has clearly shown the differe e in the spread and its extent during two seasons. The saline zones which are quiet prominent in the April period, have significantly shrinked during November.

The NDSI and NDVI image of the two periods are presented in plate 5.14, 5.15, 5.16, and 5.17 of April and November period. In NDSI image, the saline zones has become brighter while vegetation and moist zones have dark shades. Thus it helps in enhancing the saline zones of an image, still resultant image has poor contrast The same function, when applied to an stretched image, enhances saline patches in a

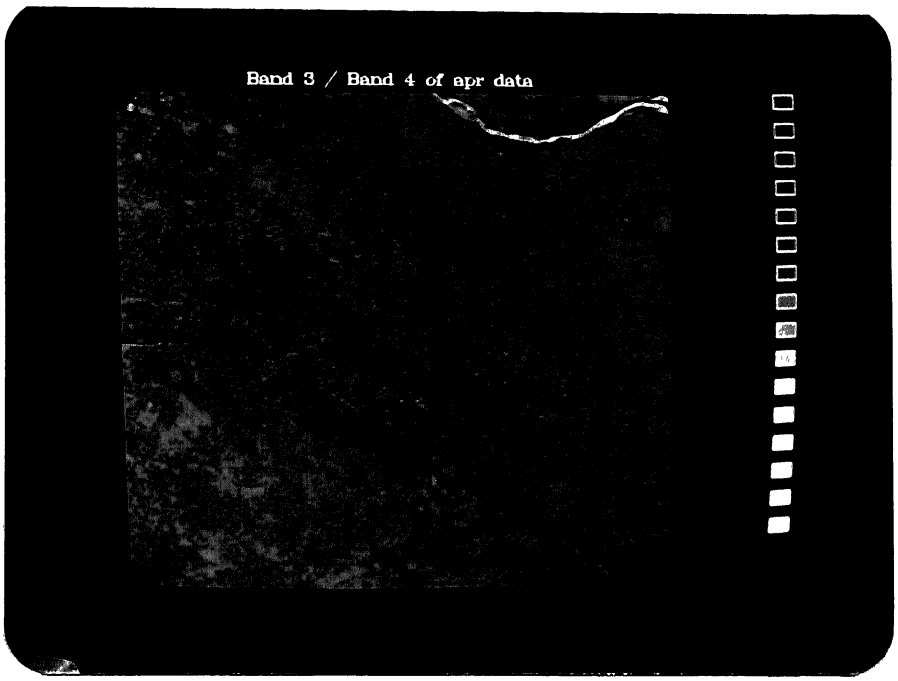

Plate 5.11: SI Image (Band 3 / Band 4) of April period

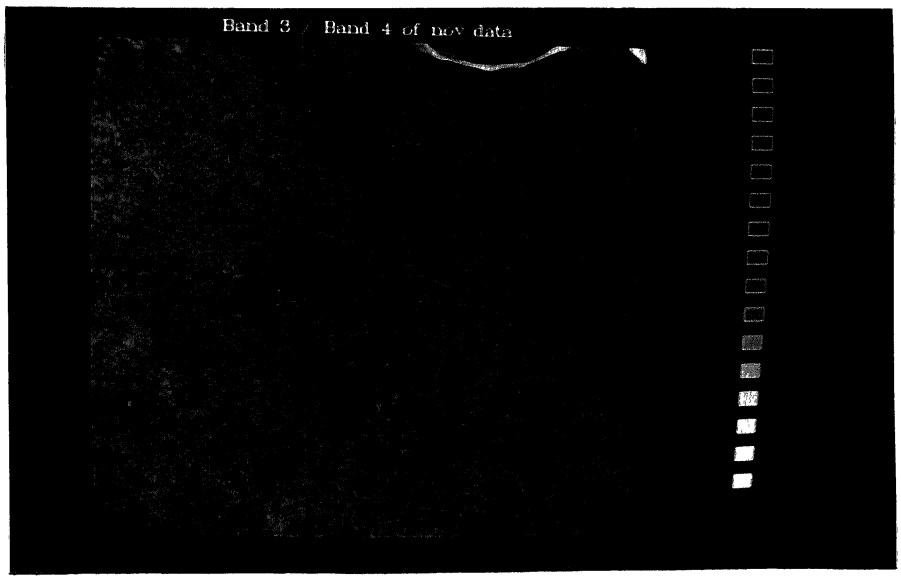

Plate 5.12: SI Image (Band 3 / Band 4) of November period

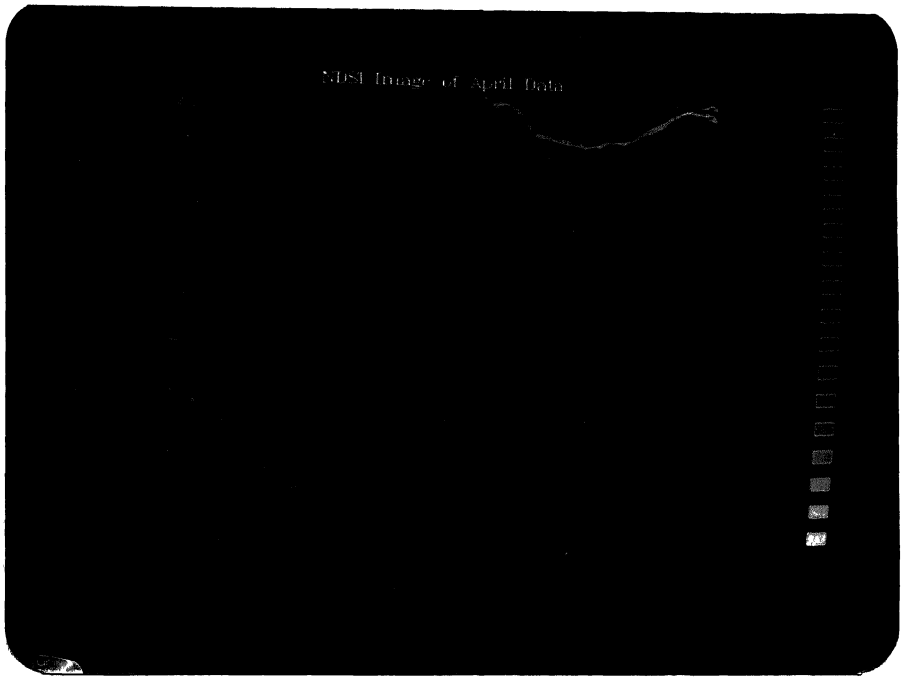

Plate 5.14: NDSI Image of April period

Plate 5.15: NDSI Image of November period

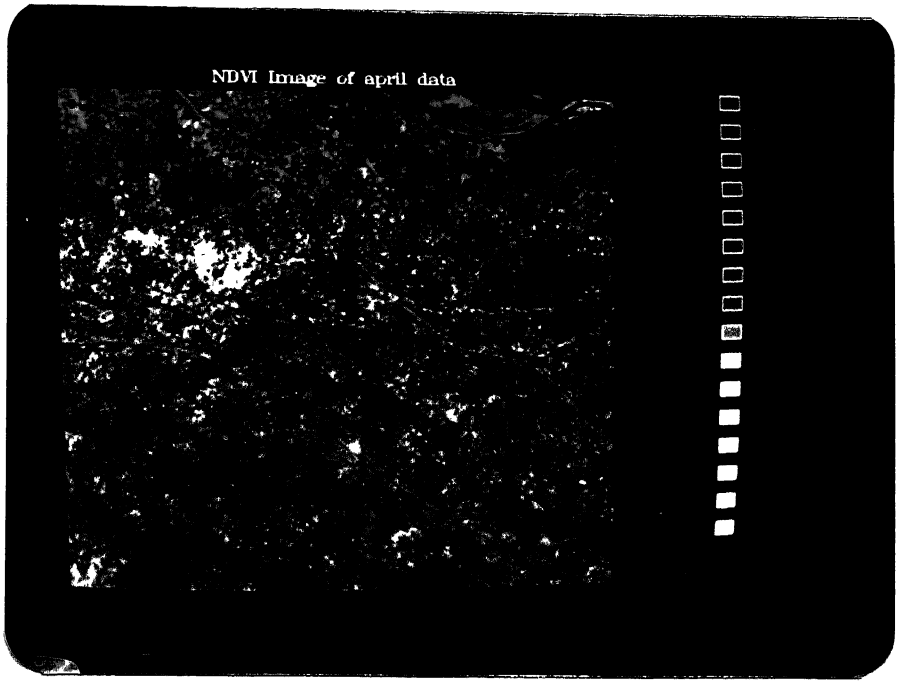

Plate 5.16: NDVI Image of April period

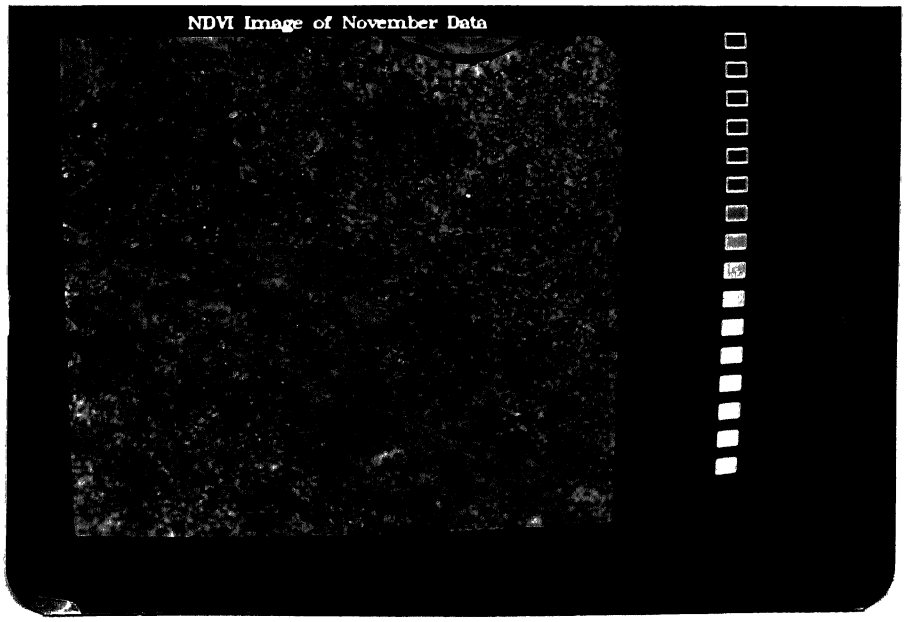

Plate 5.17: NDVI Image of November period

much better way. The NDVI image have vegetation in high tone while saline regions have become darker. Thus, the two indices are helpful in enhancing special features i.e. saline areas and vegetation respectively.

To obtain a color composite, data of minimum three wavelength is required. To choose best possible band combinations of the original data, an approach utilizing calculation of OIF, as discussed in the Chapter 2 earlier, is adopted. Various band combinations are ranked as shown in the table 5.1 on the basis of OIF values.

Table 5.1: Ranking of Different Band Combinations Based on OIF Value

Rank	Bands	OIF value April	OIF value November
1	1 3 4	13.708	10.292
2	2 3 4	12.414	9.058
3	1 2 4	11.252	7.802
4	1 2 3	10.914	4.851

This table shows that band 1, 3, and 4 combination has potential to provide maximum information. Accordingly, Color composite of the two periods are prepared and it has been certainly observed that features are more clear in the order as shown by the above table. Plate 5.18 and 5.19 presents the false color composite of the April and November period using band 1,3, and 4 combinations.

Principal component analysis of the original data is performed to reduce dimensionality. This resulted in two principal components having about 96 percent information, while principal component 3 has about 3.5 percent information. Now to extract information from these components, a color composite is prepared using three principal components. Plate 5.20 and 5.21 shows color composites of the two periods using principal components. These plate are very clear in the sense that they have

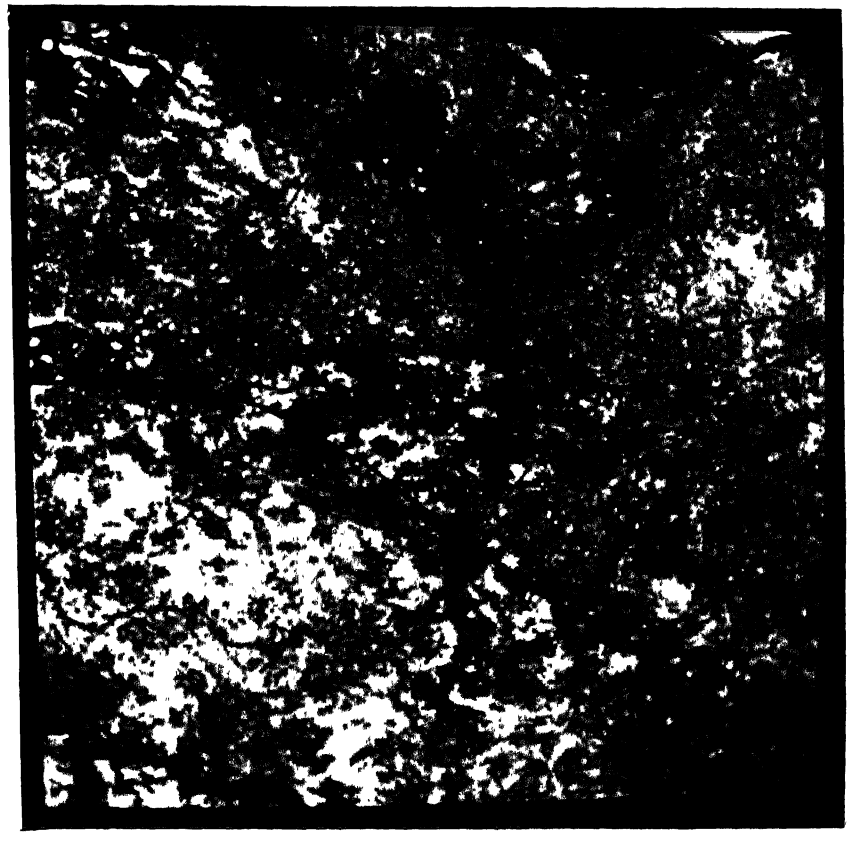

Plate 5.18: FCC of Original Bands 1,3, and 4 of April period

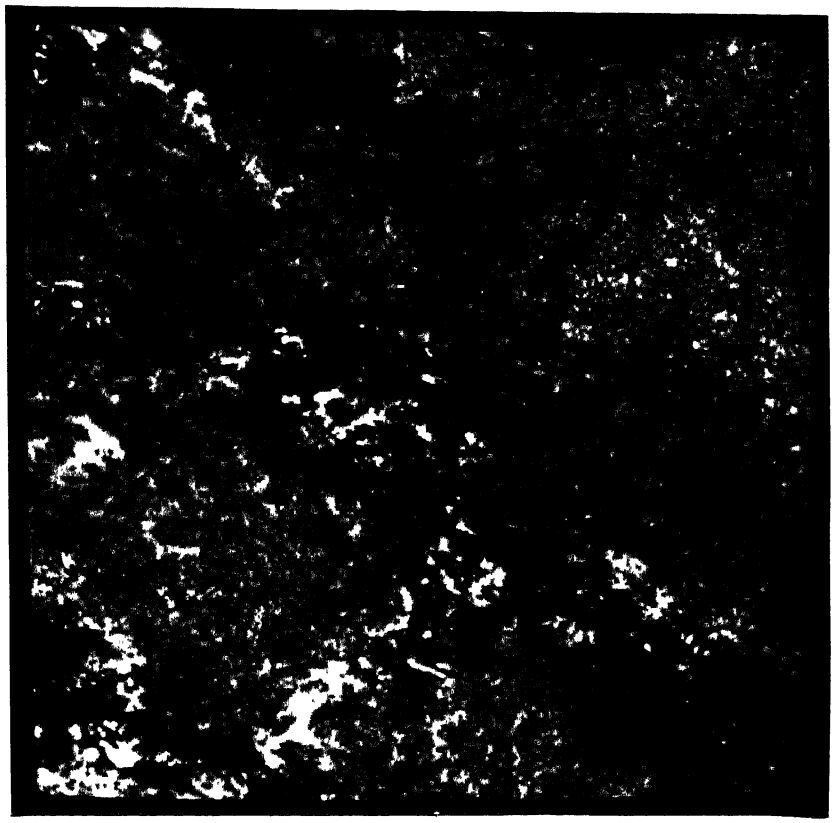

Plate 5.19: FCC of Original Bands 1,3, and 4 of November period

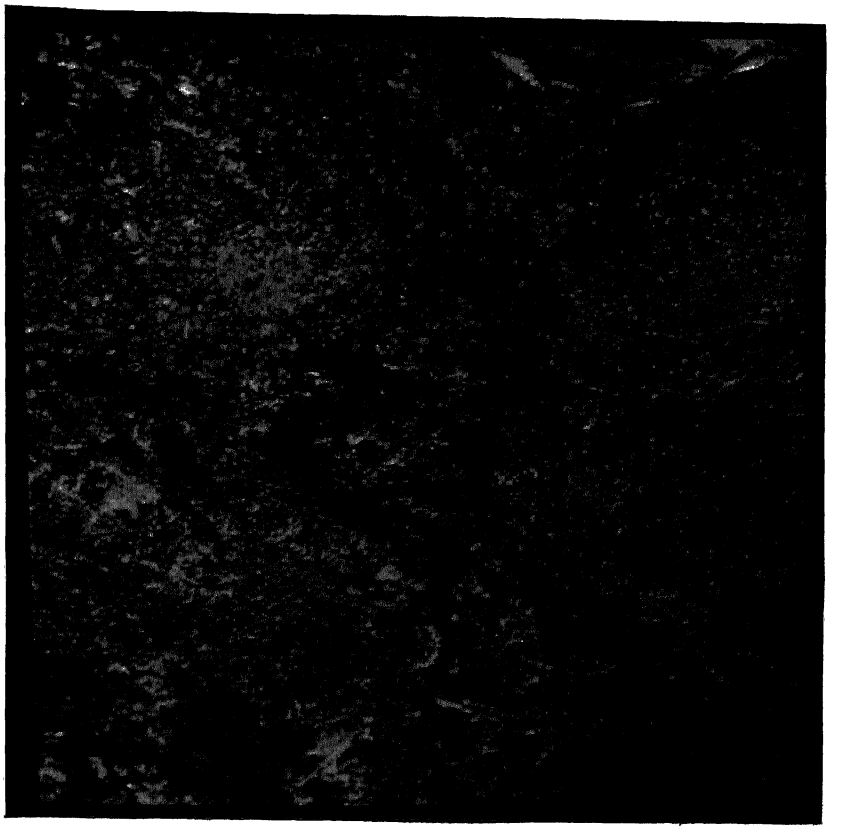

Plate 5.20: FCC using Principal Components of April period

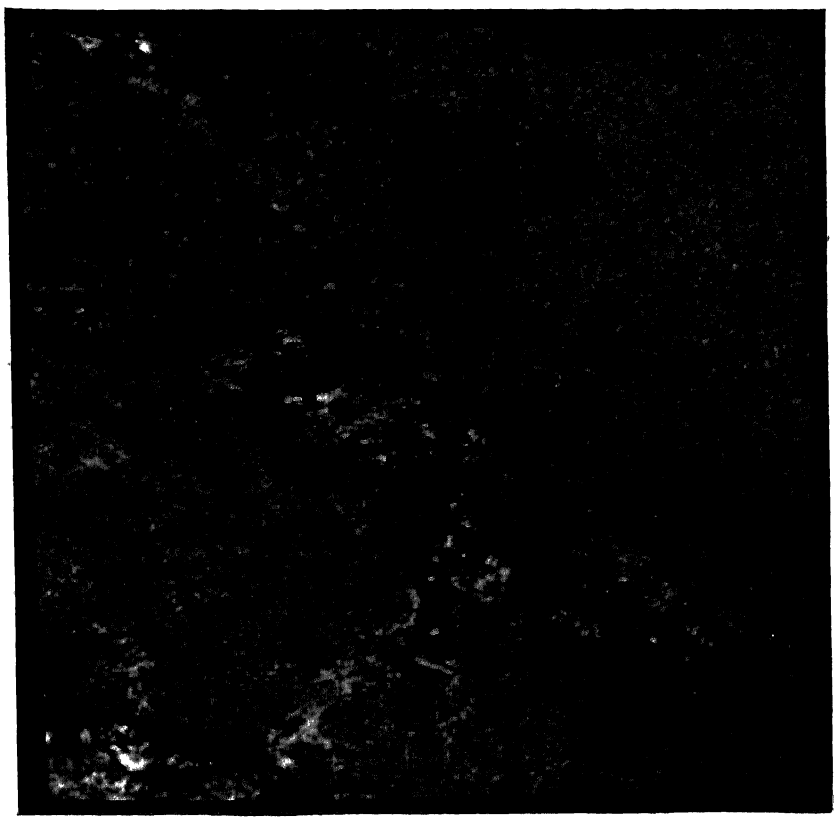

Plate 5.21: FCC using Principal Components of November period

defined and delineated certain features very clearly. Again, these color composites are also superior in the sense that in these features are better separated.

The color composites, whether prepared from original data or using principal components, the delineation of saline zones and identification of additional features is very prominent than other techniques.

Plate 5.22 presents false color composites using band 1, 3, and 4. Name of some prominent features is marked on it. The biggest saline zone of the area, between Pandu nadi and lower Ganga canal (Kanpur branch) is specially marked in it. The spread of this saline zone and similar other zones is very clearly visible in this. Plate 5.23 presents a density sliced image of the histogram equalized stretched band 3 image of April period. The spread of various saline zones is quiet clear from this.

Plate 5.24 presents salinity map of the area. In it, saline zones are divided in three broad categories namely highly saline zones, moderately saline zones, and low saline zones. Identification of other features is not attempted in it and these are marked as moist/ vegetation zones and other features. This map is particularly helpful for ready reference of a pratcising engineer interested in knowing salinity spread in the area.

Area estimation corresponding to different grey level value is attempted for the two seasons. Area corresponding to three saline categories is presented in the table 5.2. From this, it can be easily inferred that area corresponding to different saline zones is considerably different in November period. This table also shows how the saline zones have changed during two seasons. The overall extent and its division in different group is considerably different. Thus, satellite data can also be analyzed for spatial extent of saline patches.

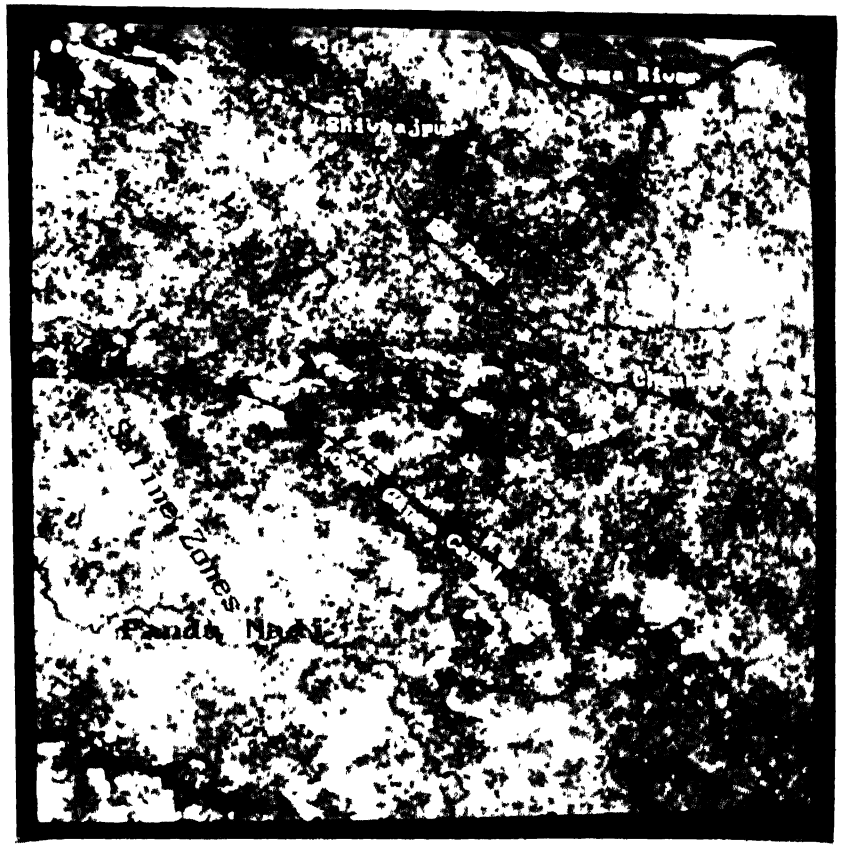

Plate 5.22: FCC using original 1,3, and 4 bands of April period with description of some features

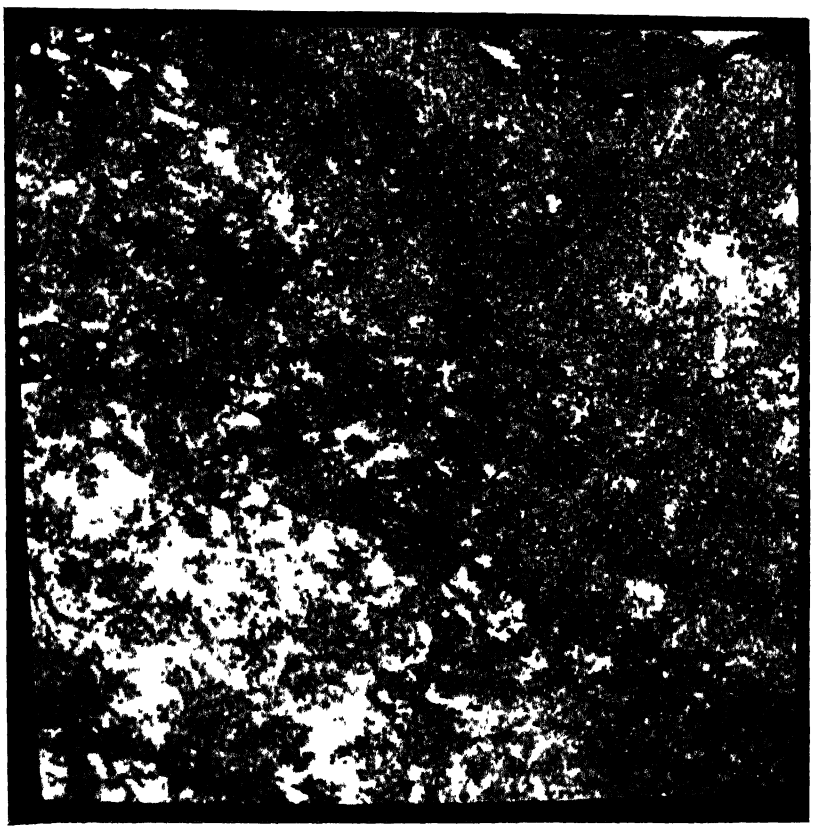

Plate 5.23: Photo map describing Soil Salinity in different zones

Density Sliced Image of Stretched (Histogram) Red band data

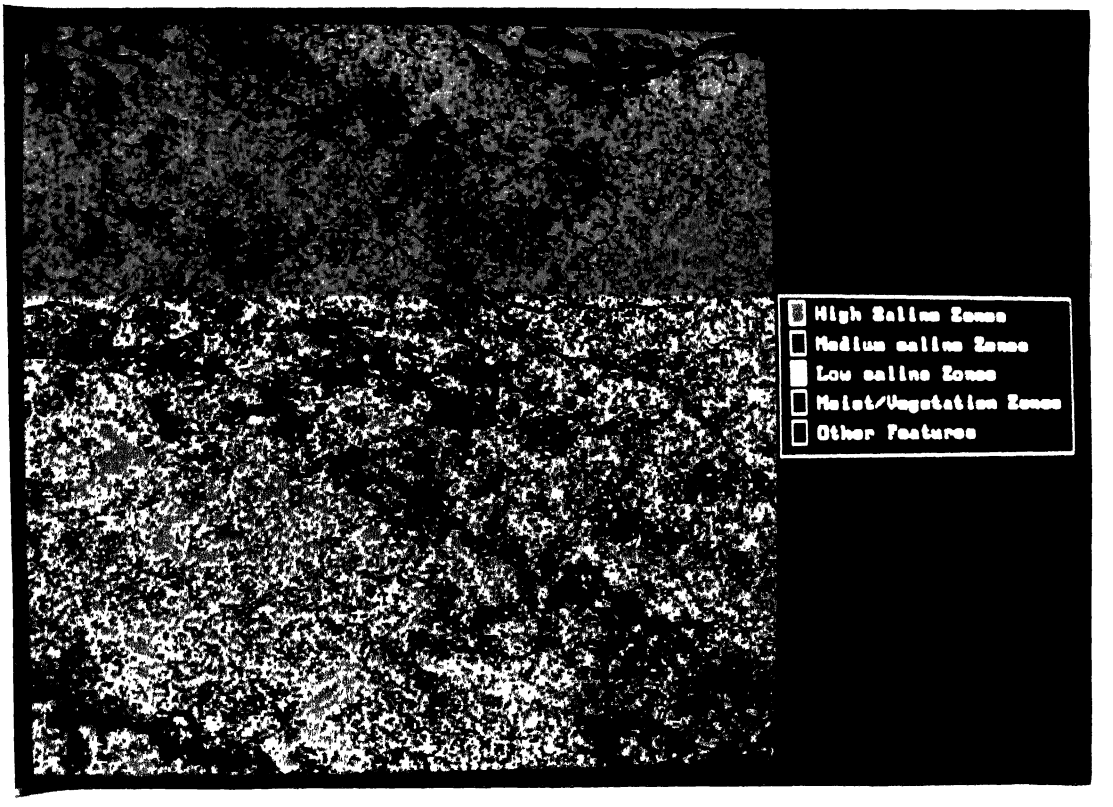

Plate 5.24: Photo map describing Soil Salinity in different zones

Density Sliced Image of original Red band data

Table 5.3: Area corresponding to saline zones during two seasons

Category	Area in April (ha)	Area in November (ha)
High saline Zones	1780	183
Moderately Saline Zones	4700	922
Low Saline Zones	8680	4870

CHAPTER 6

ESTIMATION OF SOIL SALINITY AND MOISTURE USING REMOTE SENSING

6.1 INTRODUCTION

The region affected by the salinity in the study area are well enhanced using the rich repertoire of digital image processing. As elaborated in chapter 5, Four zones of high, moderate, low concentration of salinity and unaffected by salinity, is effectively demarcated.

In present chapter, an attempt is made to estimate soil moisture content and salinity quantitatively. MGTR data in addition to IRS-1B has been used. Hand held radiometers have been extensively used whenever accurate spectral behavior of a cover type is to be determined (Mougenot et. al. 1993, Kant, 1993, Sirohi,1993). The main advantage in using MGTR lies in its fine resolution (0.25 X 0.25 m). The ground truth data, such as alkalinity and soil moisture content etc. are utilized in modeling the spectral reflectance with these parameters.

6.2 MODELING FROM DATA SET

In Chapter 4, the spectral reflectance collected using hand held MGTR are discussed. This has helped in determining the best band and band combination for investigating soil moisture and salinity. It has been concluded that band 3 and band 4 can be effectively used to discriminate between a green land and that of a barren land due to salinity. It is evident in Fig. 4.5, that band 3 is best suited for estimating salinity because of high magnitude of spectral reflectance in this band for saline soil than

normal soil and vegetation.

An attempt is made to model the band 3 with soil moisture and salinity. Empirical relationships as found suitable based on several trial with other form of equations is detailed below. The models have also been verified using Chi-square test.

6.2.1 Empirical Equation

Curve fitting of order two polynomial is found suitable as it has yielded best results compared to other relationships. The equation of curve for a order two polynomial is given as

$$y = a x^2 + b x + c \qquad (6.1)$$

where

y = the parameter considered like spectral reflectance (SR), salinity index (SI) or normalized difference salinity index (NDSI),

x = moisture content, ~~and~~ pH, and alkalinity, and

a,b,c = coefficient of regression

6.2.2 Chi-square test

Chi-square test is used for verification of models obtained by regression analysis. Those points of data set are used for testing which were not used for modeling of parameters. The Chi-square test equation is as follows:

$$\mathbb{X}^2_{comp} = (O_i - E_i)^2 / E_i \qquad (6.2)$$

where

$\mathbb{X}^2_{comp}$ is computed value of chi-square for considered degrees of freedom

E_i is estimated value, and

O_i is observed value

Now $\mathbb{X}^2_{comp} < \mathbb{X}^2_{critical}$ for model not to get rejected and its acceptability.

From Statistical tables, $\mathbb{X}^2_{critical} = 5.99$ for 5 percent degrees of freedom.

6.3 MGTR DATA ANALYSIS

Reflectance data for various soils is obtained using MGTR on the field. The spectral reflectance values are tabulated in appendix A1.An effort is made, here, to estimate the nature of different factors affecting soil response, and to model the dependence of reflectance on these factors. Important parameters affecting behavior of soils are moisture content, and presence of some ingredients like organic matter and various minerals. In the present study, moisture content and effect of salinity in terms of pH and alkalinity is considered. Here salinity is quantified in terms of alkalinity and pH. Salinity is considered moderate to high if pH is above 8.5. It was discussed earlier that red wavelength can be utilized as the best band for identification of saline zones. The same is utilized for modeling the parameters. It had also been proposed in Chapter 4 that SI and NDSI can be used to enhance the saline zones with respect to other features. These are also tried for modeling. Non linear model is attempted. The models are tested using Chi-square test as described above.

6.3.1 Relationship for Change in Moisture Content

Moisture content of the area affects its spectral behavior significantly. Reflectance of the soil decreases continuously as moisture content of the soil increases. SI and NDSI for the soil changes in quite ~~in~~ a different manner. Typical effects of

variation in the moisture content to the spectral response of soil, SI and NDSI is shown in Fig. 6.1. The particular trend followed in this figure for spectral reflectance (SR) is similar to that reported by Kant and Singh (1993), Sirohi (1993) and in other literature. SI and NDSI are new proposed indices hence no earlier work is available on it. The details of modeling are presented in the Table 6.1.

Table 6.1: Parameters of the fitted Model for variation in moisture

Parameter	a	b	c	Coefficient of Correlation	Chi-Square test results
SR	- 0.0013	0.013	0.512	99	0.5
SI	0.005	- 0.075	1.47	89	1.8
NDSI	- 0.02	1.41	-1.57	83	2.2

When all the raw data is used in developing empirical equations, SR has offered most accurate results than SI and NDSI. When data of normal soil is not considered, result changes dramatically. Thus, the model fitting for the Salinity Index and Normalized Difference Salinity Index has shown that these values are very sensitive to the extreme values. The above reported accuracy is obtained when normal soil samples are discarded in the analysis of data for SI and NDSI, though spectral reflectance is not that much sensitive to these variations.

In Fig. 6.1, SI and NDSI shows a nonlinear relationship with moisture content but the model could not offer satisfactory results. The reason being that in addition to high saline regions, soil were also collected from normal soil regions. Due to this incompatibility in proposed indices could not yield better results than spectral reflectance. Although the salinity index and normalized difference salinity index images as shown in Chapter 5 offer better results for delineation of saline and nonsaline zones.

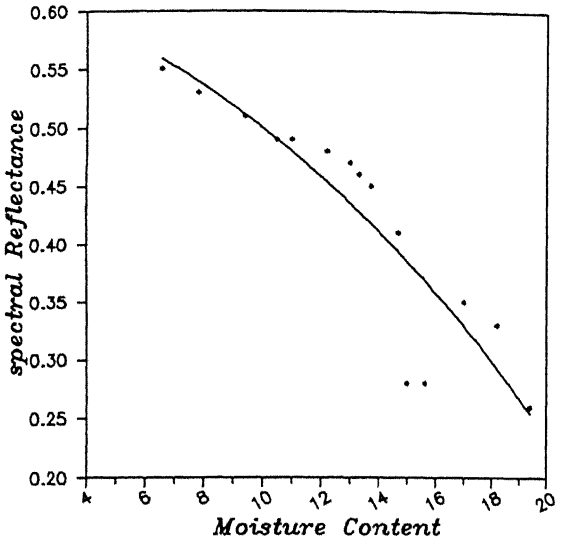

(a)

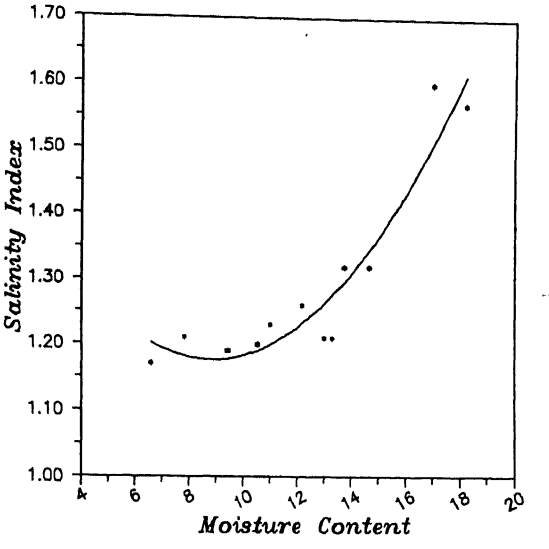

(b)

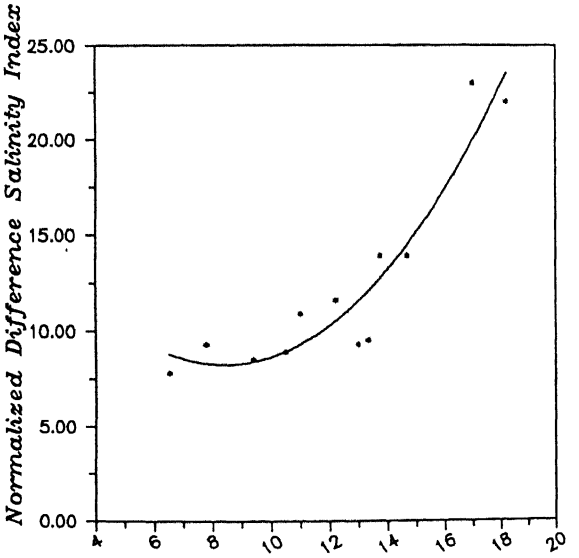

(c)

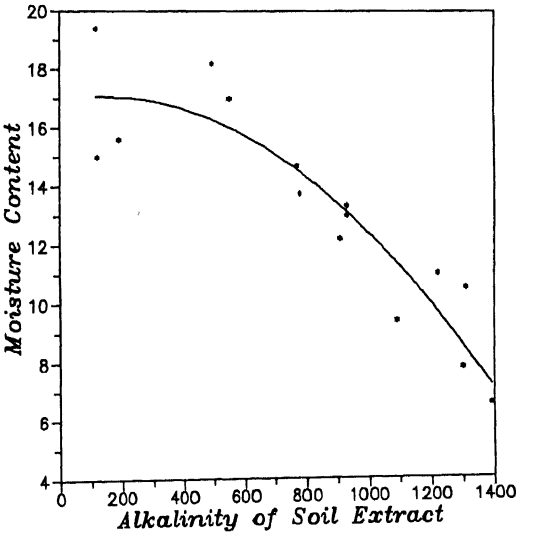

(d)

Fig. 6.1: Curve for Variation in Moisture Content

Moisture content and alkalinity are related as shown in Fig. 6.1 d. It is observed that nonlinear inverse relationship exists between the two.

6.3.2 Relationship for Change in pH of Soil Extract

pH of soil is an important parameter affecting many associated activities directly or indirectly. In the present study, soil salinity is quantified in terms of pH and alkalinity. Empirical relationship of SR Vs pH, SI Vs pH, and NDSI Vs. pH is developed. These relations are given in Table 6.2. The corresponding curves are shown in Fig. 6.2. The equation depicting relationships is a polynomial of order 2. Chi-square test results are also given in Table 6.2.

Table 6.2: Parameter of fitted Model for Variation in pH

Parameter	a	b	c	Coefficient of Correlation	Chi-square test result
SR	-0.014	0.37	-1.79	60	2.7
SI	-0.233	9.63	-21.55	53	3.9
NDSI	1.08	-25.7	159.7	33	4.91

The result in this empirical relationship are again similar to the previous one in the sense that sensitivity of the values of SI and NDSI is again observed here. But, the empirical relation fitted for spectral reflectance has offered good accuracy. This point is important because in further study, a relationship is required which is suitable for varying field conditions.

6.3.3 Relationship for Change in Alkalinity of Soil Extract

Salinity in the soil is mainly due to presence of carbonates and bicarbonates of alkali and alkaline Earth metals as discussed earlier. A polynomial of

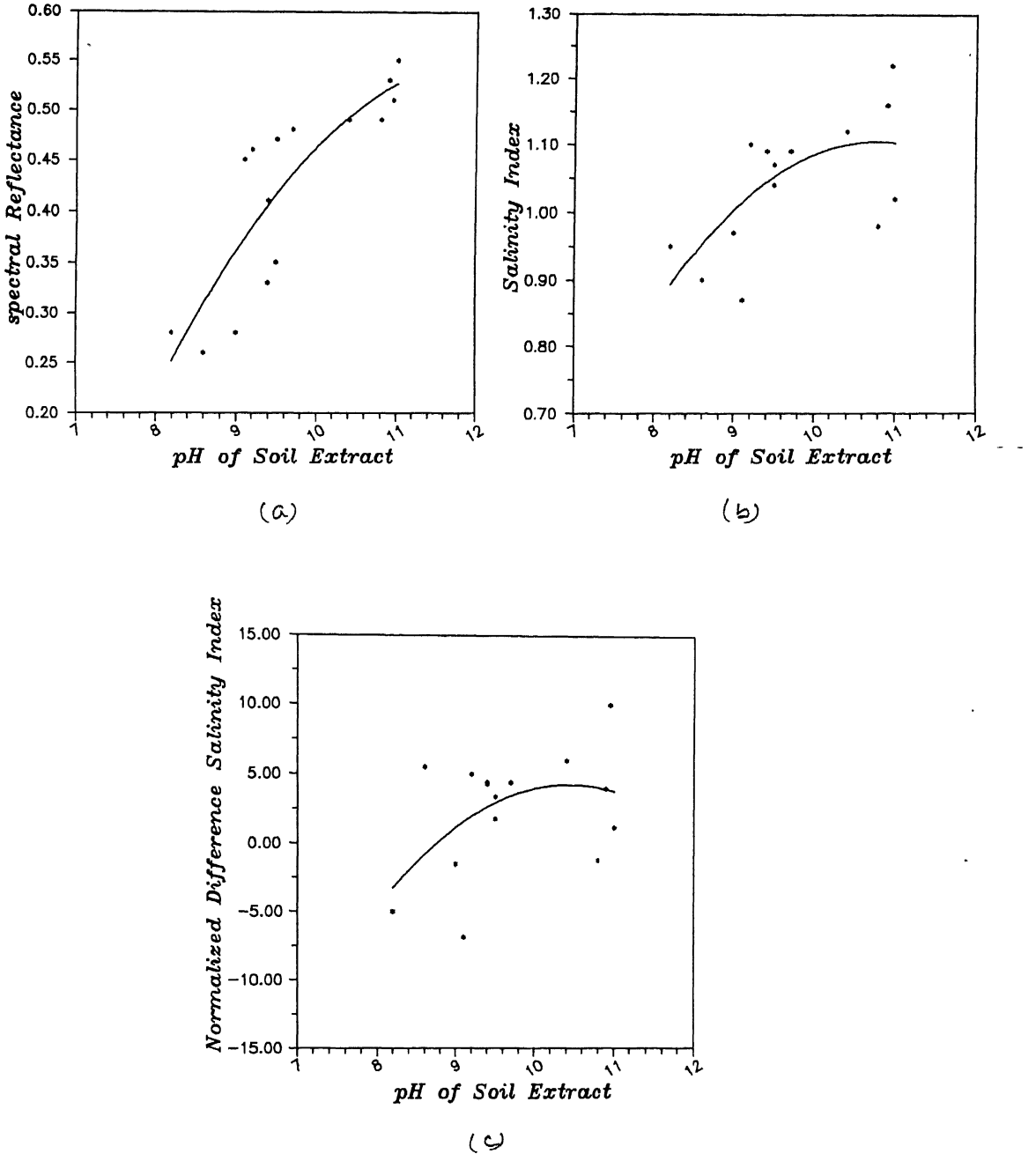

Fig. 6.2: Curve for Variation in pH

order 2 is found suitable. The equation for model fitting is given in Table 6.3. Corresponding relationships are shown in Fig. 6.3.

Table 6.3: Parameter of the Fitted Model for Variation in Alkalinity

Parameter	a	b	c	Coefficient of Correlation	Chi-square test value
SR	-5.56×10^{-8}	3×10^{-4}	0.23	96	1.0
SI	-1.65×10^{-7}	3.5×10^{-4}	0.9	33	4.9
NDSI	-4.7×10^{-6}	9.6	-1.48	10	5.9

From this table, it is very clear that curve fitting for spectral reflectance has yielded encouraging results. SI and NDSI can be related to alkalinity using an empirical polynomial of order two. Though accuracy of curve fitting increases as we increase the order of polynomial, yet it is not so good to accept the relationship.

6.4 IRS-1B SATELLITE DATA ANALYSIS

To extend the work done in the previous sections i.e. in MGTR analysis, grey level values are read from satellite image approximately near the sampling stations. these grey level values are presented in Table 6.4 along with other observations of laboratory tests.

The resultant equation obtained in MGTR data analysis are quiet good in case of spectral reflectance, but accuracy is considerably low in case of SI and NDSI parameter. It has also been pointed out that these indices are significantly sensitive to extreme and erroneous values. Considering all the above facts, empirical relationship

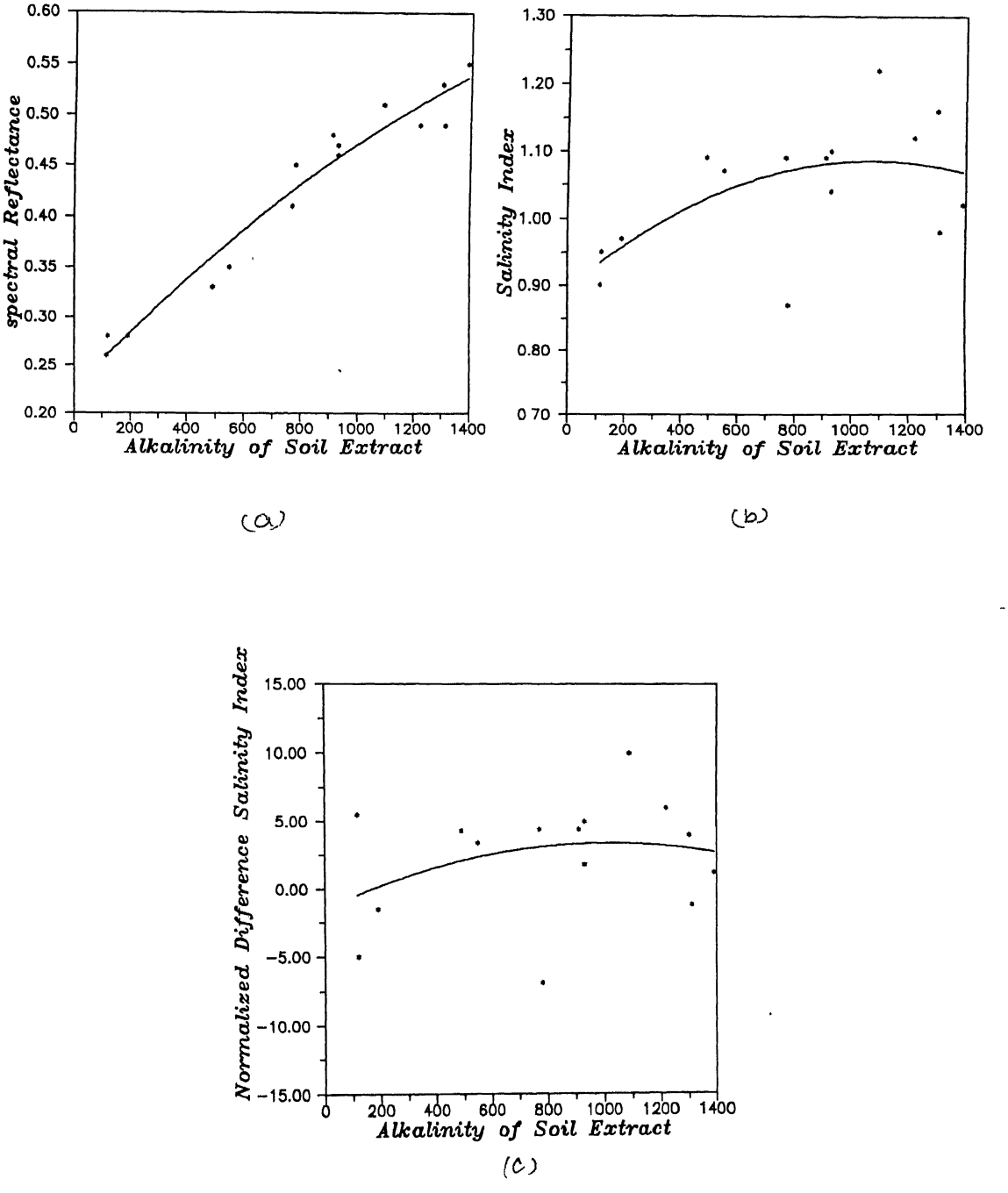

Fig. 6.3: Curve for Variation in Alkalinity

Table 6.4: Grey level values for sampling stations

Village	Row	Column	Grey level values	Moisture content	pH	Alkalinity
Abdulpur	245	341	65	15.60	9.0	190
Chandika	254	237	60	19.40	8.6	115
Badi Purwa 1	256	318	76	17.00	9.5	550
Badi Purwa 2	267	303	83	12.20	9.7	910
Champatpur	254	332	90	19.80	8.5	90
Gauri Lakha 1	269	212	100	9.40	10.9	1090
Gauri lakha 2	251	206	96	7.80	10.9	1300
Gauri Lakha 3	232	201	91	11.00	10.4	1220
Bhagvantpur	229	214	78	5.85	10.5	1120
Laxmanpur	225	167	98	20.10	9.4	300
Jagatpur 1	240	133	95	14.67	9.4	770
Jagatpur 2	249	129	86	6.54	11	1390
Maharaj Nagar	281	128	84	18.20	9.4	490
Manoh Bari	299	139	85	13.33	9.2	930
Manoh Choti	310	149	94	13.54	9.6	780
Bhausana	319	173	81	10.50	10.8	1310
Dileep Nagar	332	204	85	13.00	9.5	930
Rautapur Kalan 1	324	248	68	13.73	9.1	780
Rautapur Kalan 2	295	269	58	16.41	8.5	150
Near bridge on Sheoli Road	280	245	55	15.00	8.2	120

for only spectral reflectance or grey level values is attempted for satellite data. Here the band used is same as in MGTR study i.e. band 3 (red band). The same nonlinear model fitting as discussed earlier is tried. The results are presented in Table 6.5 and the corresponding curves are shown in Fig. 6.4.

Table 6.5: Parameters of Fitted Model for satellite data

Parameter	a	b	c	Coefficient of Correlation	Chi-square test result
Moisture Content	0.016	-3.2	123	68	3.9
pH	-5.32	117.38	-549	73	3.1
Alkalinity	-1.3×10^{-5}	0.05	55.6	80	2.8

The results in the case of moisture content are nearly 68 percent correct. When points corresponding to normal soils are not considered, accuracy increases significantly. The nature of curve for moisture content is somewhat a straight line and the points are quiet spread on both side of it. The curve for pH is non linear and continuously increasing, i.e. it is showing a positive relationship with grey level values. The curve for alkalinity is again similar to that of pH one. Coefficient of correlation for pH is 73 and for alkalinity, it is 80 percent. One thing is clear that for a highly saline zone, both pH and alkalinity is high but moisture content is low.

From the results of empirical relations, it is evident that equations for MGTR data have better accuracy nearly for all variables. The satellite data do not fit that perfectly with soil moisture. Reasons for it may be:

1. the high resolution of MGTR provides a scope to have reflectance values from a

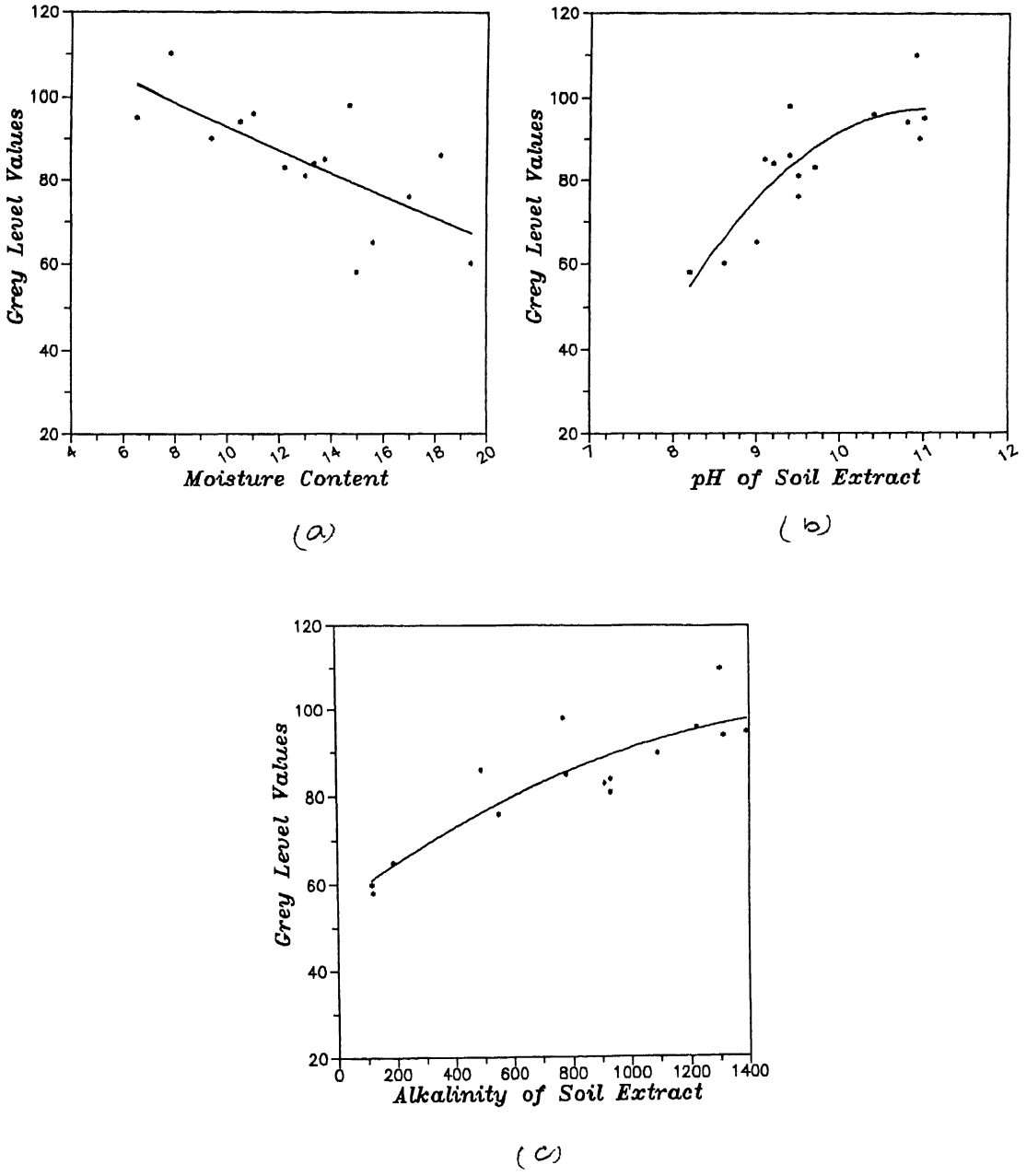

Fig. 6.4: Satellite Data Vs. Various Parameters

very small region of interest and hence there is greater accuracy and correlationpossible because of purity of data set. The resolution of satellite IRS 1B is quiet low compared to MGTR, and hence there may be impurity in the sample values itself.

2. the samples are collected from same sites as for MGTR observations, and so, they are true representative of ground situations in case of MGTR values. Grey level values are read from digital image for approximately same position so, it is not positioned accurately and hence ground observation is not exact representative for satellite data.
3. the effect of neárby areas on the response of a feature is prominent in case of high altitude observation of a satellite and hence poor correlations is observed.

The results of model concerning pH and alkalinity are highly encouraging and show great potential for quick and repetitive monitoring of soil alkalinity and pH.

CHAPTER 7

CONCLUSIONS AND FUTURE RECOMMENDATIONS

The possibility of utilizing remotely sensed data in delineation of saline and moist zones is investigated in this work. For this purpose, laboratory analysis of field data and digital image processing of satellite data is undertaken. Empirical relations are developed for soil salinity and moisture content with spectral reflectance. The results are verified using field checks and statistical analysis. Based on the results of the present work, following conclusions are made:

1. Spectral reflectance of soil is dependent on moisture content, salinity, chemical and mineral composition. From SEM analysis it is evident that shapes of crystal for saline soil is different than normal soil, which certainly influences the reflectance. This property provides a scope for differentiating saline and non saline soil. This is also supported by MGTR reflectance curve (Fig. 4.5).

2. Set of digital enhancement techniques on satellite data has yielded changes for accurate demarcation of salinity and its extent in the region. False color composites of principal components has yielded remarkably good results. New proposed indices SI and NDSI prove to be efficient in discriminating saline zones from non saline zones.

3. Salinity as reflected in digital images varies with season, In November, 1992 less zones of salinity are observed than April, 1993 image.

4. MGTR can be used effectively for estimation of in-situ soil salinity and moisture content using band 3 (0.62 - 0.68 μm). Models have been prepared for estimation of soil moisture and salinity using satellite data also. They have yielded encouraging

results and exhibit possibility for generating global database of salinity, pH and moisture of a vast region.

Future Recommendations

Though the present work has tried to cover various aspects related to soil salinity, yet there are number of points which need special attention . Some of these are:

1. The effect of mineral composition, texture, color, and presence of organic matter on the response of the soil is to be quantified.

2. The models generated could be strengthened involving other parameters such as diurnal, seasonal variation and soil roughness.

3. The database generated by the methodology proposed in the present study can be incorporated in geographic information system (GIS) environment for further analysis.

REFERENCES

- Al abbas, H.H., Srinivas, P.H., and Baumgardener, M.F. (1972). Relating organic matter and clay content to the multispectral radiance of the soil, *Soil sciences*, 14, pp. 322-327.
- Bertin, E.P. (1970). *Principles and practice of X-ray spectrometric Analysis*, plenum press, New York and London.
- Chavez, P.S. Jr., Berlin G.L., and Sowers L.B.(1982). Statistical methods for selecting Landsat MSS ratios, *Journal of Applied Photogrammetric Engineering*, No. 8, pp. 23-30.
- Clevers, J. G. P. W. and Verhoef, W.(1993). LAI Estimation by Means of the WDVI: A Sensitivity Analysis with a Combined PROSPECT-SAIL Model, *Remote Sensing Reviews*, Vol. 7, pp. 43-64.
- Csillag, Ferenc, Pasztor, Laszlo, and Biehl, Larry L. (1993). Spectral Band Selection for the Characterization of Salinity status of Soils, *Remote Sensing of Environment*, Vol. 43, pp. 231-242.
- Cullity, B.D. (1967). *Elements of X-ray Diffraction*, Addison and Wesley publishing company, inc., USA
- Curran, P. J. (1983). Estimating Green LAI from Multispectral Aerial Photography, *Photogrammetric Engineering and Remote Sensing*, Vol. 49, pp. 1709-1720,.
- Curran, P.J. (1985). *Principles of Remote Sensing*, English language book society, Longman.
- Desceri, Lenore S., Arnold E. Greenberg, R. Rhodes Trussell, (Editor). *Standard Methods for the examination of water and wastewater*, 17th ed.
- Duggin, M.J., 1980. The field measurement of reflectance factors, *Photogrammetric Engineering and Remote Sensing*, Vol. 46, pp. 643-647
- Duggin, M.J., and Cunia, T., 1983. Ground reflectance measurement techniques, a comparison, *Applied Optics*, Vol. 22,3771-3777.

- Dwivedi, R.S. (1992). Monitoring and the study of the effects of image scale on delineation of salt affected soils in the Indo-Gangetic plains, *International Journal of Remote Sensing*, Vol. 13, No. 8, 1527-1536.
- Dwivedi, R.S., and Rao, B.R.M. (1992), The Selection of best possible Landsat-TM band combination for delineating salt affected soils, *International Journal of Remote sensing*, Vol. 13, No. 11, pp. 2051-2058.
- Everitt, J.H., Escobar, D.E., Gebermann, A.H. and Alaniz, M.A.(1988). Detecting saline soil with vedio imagery. *Photogrammetric Engineering and Remote Sensing*, Vol. 54, pp.283-87.
- Everitt, J.H., Gerbermann, A.H and Cuellar, J.A.(1977). Distinguishing saline lands from nonsaline range lands with skylab imagery, *Photogrammetric Engineering and Remote Sensing*, Vol. 43, pp. 1041-47
- Gerberman, A.H. (1975). Reflectance of varying mixture of clay soil and sand, *Photogrammetric Engineering and Remote Sensing*, Vol. 45, pp.1145-1151
- Goldstein, J.I. and Yakowitz, H. (1975). *Practical Scanning Electron Microscopy*, Plenum press, New York, and London
- Gonzalez, R.C., and Wintz, P. 1977. *Digital Image Processing*, Addison Wesley Publishing Company, Inc. USA
- Grum, F. and Luckey, G.W. 1968. Optical sphere paint and a working standard of reflectance, *Applied Optics*, 7, pp. 2289-2294.
- Haddisky, M.A., Klemas, V. and Smart, R.M. (1983). The influence of soil salinity, growth form and leaf moisture on the spectral radiance of spentina alterniflora canoples, *Photogrammetric Engineering and Remote Sensing*, Vol. 49, pp. 77-83.
- Holt, D. B., Muir, M. D., Grant, P. R., Boswarva, I. M. (1974), *Quantitative Scanning Electron Microscopy*, Academic Press, London.
- Janza, F.J. (1975). Interaction mechanisms in reeves, R.G. ed., *Manual of Remote Sensing*, ch. 4, pp. 75-179, American Society of Photogrammetry, Falls Church Verginia.
- Jensen, J.R. (1986). *Introductory Digital Image Processing*, Prentice Hall, New Jersey, USA.

- Joshi, M.D., and Sahay, B. (1993). Mapping of salt affected land in Saurashtra coast using Landsat satellite data, *International Journal of Remote sensing*, Vol.14, No. 10, 1919-1929.
- Kant, Akshay, and Singh, S.B.B. (1993). Estimation of soil properties using remote Sensing Techniques, *B.Tech. Project*, Civil Engineering Department, I.I.T. Kanpur.
- Kennie, T.J.M. and Matthews, M.C. (1985). *Remote Sensing in Civil Engineering*, Surrey University Press.
- Kimes, D.S., Irons, J.R., Levine, E.R. and Horning, N.A. (1993), learning clas descriptions from a data base of spectral reflectance of soil samples, *Remote Sensing of Environment*, 43, pp. 161-169.
- Kumar, Manish (1993). Studies on monitoring of suspended solids in Pandu river system using MGTR, *M.Tech. Thesis*, Civil Engineering Department, I.I.T. Kanpur,
- Lillesand, T.M. and Kiefer, R.W. (1994). *Remote Sensing and Image Interpretation*, John Wiley & Sons, Inc.
- Lo, C.P. (1986). *Applied Remote Sensing,* Lomgman Scientific & Technical.
- Manchanda, M.L. (1984). Use of Remote Sensing techniques in the study of distribution of salt affected soil in north west India, *Journal of Indian society of soil sciences*, Vol. 32, pp. 701-706.
- Manchanda, M.L. and Iyer, H.S (1983). Use of Landsat imagery and aerial photograghs for delineation and categorization of salt affected soil of part of north west India, *Journal of Indian society of soil sciences*, Vol. 31, pp. 263-271.
- Mather, P.M. (1987). *Computer Processing of Remotely-Sensed Images*, John Wiley & Sons.
- Mothikumar, K.E., and Bhagwat, K.A. (1989)., Delineation and Mapping of salt affected lands in Pariej village of Kheda district(Gujarat) by Remote Sensing, *PHOTONIRVACHAK, Journal of the Indian Society of Remote Sensing*, Vol. 17, No. 4,
- Mougenot, B., Pouget, M., and Epema, G. F. (1993). Remote Sensing of Salt Affected Soils, *Remote Sensing Reviews*, Vol. 7, pp. 241-259.

- Rampal, K.K. (1982). *Textbook of Photogrammetry*, Oxford & IBH Publishers.
- Richardson, A.J., Gerbermann, A.H., Gansmann, H.W. and Cuellar J.A. (1976). Detection of saline soil with skylab multospectral scanner data. *Photogrammetric Engineering and Remote Sensing*, Vol. 42, pp. 679-684.
- Rao,B.R.M., Dwivedi, R.S., Venkataratnam, L., Ravishankar, T., Thammappa, S.S., Bhargawa, G.P., and Singh, A. N. (1991). Mapping the magnitude of Sodicity in part of the Indo-Gangetic plains of Uttar Pradesh, Northern India using Landsat-TM data, *International Journal of Remote Sensing*, Vol.12, No. 3, pp. 419-425.
- Saha, S. K., Kudrat, M. and Bhan, S. K. (1990). Digital processing of Landsat TM data for wasteland mapping in parts of Aligarh District Utter Pradesh, India, *International. Journal of Remote Sensing*, Vol. 11, pp. 485-492.
- Sharma, R. C. and Bhargava, G.P., 1988, Landsat Imageries for mapping saline soils and wetlands in north west India, *International. Journal of Remote Sensing*, Vol 9, pp.39-44.
- Sinha, A.K. (1986). Spectral reflectance characteristics of soils and its correlation with soil properties and surface conditions, *Indian Society of Remote Sensing*, Vol.14, pp. 1-9.
- Sinha, A.K.(1987). Variation in soil spectral reflectance related to soil moisture, organic matter and particle size, *Indian Society of Remote Sensing*, Vol. 15, pp. 7-11.
- Slater, P.N. 1985. Radiometric considerations in remote sensing, Proceedings of IEEE, 73, pp. 997-1011
- Thornton, P. R., . *Scanning Electron Microscopy - Applications to materials and device science.1968*, Chapman and Hall Ltd., London..
- Tripathi, N.K., Classifiers in Remote Sensing - A Comparative Study, *M. Tech. Thesis*, Civil Engineering Department, I.I.T. Kanpur, 1987
- Wells, O. C. (1974), *Scanning Electron Microscopy*, McGraw-Hill Book Company,

ADDITIONAL REFERENCES

- Balagurusamy E. (1992). *Programming in ANSI C*, McGraw Hill Publishing Company Pvt. ltd., New Delhi.
- Davis, J.C., 1986. *Statistics and Data Analysis in Geology*, John Wiley and Sons., USA. pp. 60 , 80-86
- Goetz, A.F.H., Wellman, J.B., and Barnes, W.L. (1985). Optical remote sensing of the Earth, *Proceedings of IEEE*, 73, 950-969.
- Kalra N.K. and Joshi D.C. (1994). Spectral reflectanec characterstics of salt affected arid soils of Rajasthan, *"Photonirvachak" Journal of Indian Society of Remote Sensing*, Vol. 22, No. 3, pp. 184-193.
- Kernighan, B.W. and Ritchie, D.M. (1991), *The "C" programming language*, Prentice Hall of India Pvt. ltd., New Delhi.
- Punmia B.C., (1988). *Soil Mechanics and Foundation Engineering*, A Saurabh and Co. Pvt. ltd., Madras.
- Sirohi, Anand (1993). Comparative study of different land covers using remote sensing techniques, *M. Tech. Thesis*, Indian Institute of Technology, Kanpur.
- Spiegel, M.R. (1982). *Theory and Problems of Probability and Statistics*, Schaum's outline series, McGraw Hill Book Company, Singapore.
- Wang Wally and Bibb Kenneth, 1991. *Illstrated Turbo C++*, BPB Publications, New Delhi.

APPENDIX

APPENDIX A.1

MGTR Observation of Reflectance Values on Different Stations

MGTRBands Station No.	1	2	3	4	5	6	7	8	9	10	11
1	.31	.33	.38	.26	.32	.33	.38	.26	.35	.38	.27
2	.21	.23	.25	.28	.21	.21	.23	.26	.28	.26	.26
3	.30	.23	.35	.21	.29	.23	.35	.22	.23	.34	.24
4	.41	.36	.49	.38	.41	.36	.48	.38	.35	.48	.38
5	.18	.21	.24	.28	.18	.21	.24	.26	.22	.23	.24
6	.44	.37	.51	.43	.45	.39	.51	.43	.39	.49	.43
7	.47	.40	.53	.42	.48	.40	.53	.44	.41	.53	.44
8	.42	.37	.50	.40	.42	.38	.49	.40	.36	.49	.40
9	.50	.42	.55	.46	.51	.43	.55	.48	.43	.55	.48
10	.16	.19	.26	.24	.17	.19	.25	.21	.20	.25	.21
11	.36	.28	.41	.31	.36	.27	.41	.31	.27	.41	.31
12	.48	.41	.56	.47	.48	.42	.55	.47	.42	.54	.46
13	.25	.28	.33	.19	.26	.28	.33	.21	.28	.30	.21
14	.40	.31	.46	.39	.39	.33	.46	.38	.33	.45	.38
15	.38	.35	.46	.38	.38	.34	.46	.37	.34	.46	.37
16	.43	.38	.49	.41	.44	.38	.49	.41	.30	.50	.41
17	.39	.34	.47	.38	.38	.35	.47	.39	.35	.47	.37
18	.39	.30	.45	.37	40	.30	.45	.34	.30	.44	.34
19	.27	.21	.38	.32	.27	.22	.39	.30	.22	.37	.29
20	.24	.20	.35	.29	.23	.20	.35	.28	.24	.36	.30